Elucidating the cellular targets of BoNT/X a potentially novel biopharmaceutical

Pollyanna Arlene Rouse

A thesis submitted in partial fulfilment of the requirements for the degree of

Doctor of Philosophy

The University of Sheffield

Faculty of Science

School of Biosciences

October 2024

Declaration

This thesis has been submitted in partial fulfilment of the requirements for the degree of Doctor of Philosophy. In accordance with the thesis format guidelines, this thesis is in a publication format, and includes two draft manuscript chapters. A declaration that specifies the contributions of Pollyanna A Rouse is provided prior to each manuscript.

I, the author, confirm that the Thesis is my own work. I am aware of the University's Guidance on the Use of Unfair Means (www.sheffield.ac.uk/ssid/unfair-means). This work has not previously been presented for an award at this, or any other, university.

Acknowledgements

Firstly, I want to thank my supervisor Professor Andrew Peden. Your knowledge and insight are inspiring. Working with you over the last 4 years has been instrumental in developing my confidence in my skills as a scientist and as a professional. Thank you for your support and guidance. To my industry supervisors, Mark Elliott, Matt Beard and Karen Bunting - I am extremely grateful for the constant support and encouragement you have given me over the years, thank you. To my advisors Jason King and Liz Seward, I want to thank you both for always being friendly faces to see around Florey. I have always appreciated your advice and encouragement; you made our advisory meetings something to look forward to. I would also like to thank Susan Clark at the Flow Cytometry Core Facility, and to Nick van Hateren and Darren Robinson at the Light Microscopy Facility, for providing fantastic training and support.

I want to thank the members of the Peden Lab for their friendship and help over the years, especially Ola, Dan, and Sam. To the Erdmann and King lab members, it has been wonderful sharing an office and lab with you - thank you for creating such a friendly and welcoming environment to work in.

My housemates and D&D crew - I don't know where to begin. Thank you for making our house feel like home. You helped to keep me sane during a very turbulent time in my life, I really appreciate you all.

My beloved pets, I am lucky to have had such wonderful companions who were always there for me when needed.

Finally, Mum and Dad. You inspire and motivate me every day. I'm convinced that no one in the world can feel as loved and supported as I am by you both. Life may not be simple for us, but with your help I have made it to where I am today, thank you.

This work was supported by the Biotechnology and Biological Sciences Research Council (BBSRC) and Ipsen Bioinnovation Ltd [Grant number: BB/T007222/1].

Abstract

Botulinum neurotoxins are produced by clostridia bacteria. A novel serotype named BoNT/X was recently discovered that targets a larger number of SNAREs than the other toxins. Previous work from the lab has shown that expression of the BoNT/X light chain leads to pleiotropic defects in intracellular trafficking, with loss of the TF-R from the cell surface, and impaired delivery of soluble and membrane anchored cargo to the plasma membrane. However, it was unclear whether these phenotypes are specific to SNARE cleavage. To address this, we have developed a novel reporter system for studying SNARE cleavage and used it to engineer SNAREs which are resistant to BoNT/X. Using the cleavage resistant SNAREs we have investigated their roles in both endocytic and biosynthetic trafficking. We have shown that cleavage resistant VAMP3 and Ykt6 are able to rescue TF-R trafficking, uncovering an unexpected role for Ykt6 in this process. We have extended these studies to examine the role of all R-SNAREs in the fusion of transport vesicles with the cell surface and investigated the impact of disease-causing mutations on R-SNARE function. Expression of cleavage resistant versions of VAMPs 1-3 and 8 partially rescue the fusion of cargo with the cell surface in the absence of Ykt6, and the insertion of a disease-causing proline substitution in VAMP3 disrupts its function. Prolonged expression of LC/X induces apoptosis in intoxicated cells which is due to SNARE cleavage as expression of cleavage resistant VAMP3 and Ykt6 restores cell viability. Intoxicated cells accumulate at G2/M, indicating there is a defect in cell division. Taken together, these results suggest that BoNT/X is not only a useful tool for studying SNARE function but also has the potential to be used as a novel agent to induce cell death.

List of Abbreviations

aa	Amino Acid
APC	Allophycocyanin
Arg	Arginine
ATP	Adenosine Triphosphate
BoNT	Botulinum Neurotoxin
BSA	Bovine Serum Albumin
CALM	Clathrin Assembly Lymphoid Myeloid Leukaemia
CD (e.g. CD63)	Cluster of Differentiation
COPI	Coat Protein Complex I
CO_2	Carbon Dioxide
DMEM	Dulbecco's Modified Eagle's Medium
DNA	Deoxyribonucleic Acid
Dox	Doxycycline
ECL	Enhanced Chemiluminescence
eGFP	Enhanced Green Fluorescent Protein
ELISA	Enzyme Linked Immunosorbent Assay
ER	Endoplasmic Reticulum
ERGIC	Endoplasmic Reticulum Golgi Intermediate Compartment
EtOH	Ethanol
FACS	Fluorescence-activated Cell Sorting
FBS	Fetal Bovine Serum
FKBP	FK-506 Binding Protein

FRET	Fluorescence Resonance Energy Transfer
GFP	Green Fluorescent Protein
HA	Hemagglutinin
HC	Heavy Chain
HEK	Human Embryonic Kidney cell line
HeLa	Human Cervical Cancer cell line
HRP	Horseradish Peroxidase
kDa	Kilodalton
K/O	Knock-out
LC	Light Chain
LC/X	Light Chain of BoNT/X
MAO	Monoamine Oxidase
MEM	Minimum Essential Medium
MS	Mass-spectrometry
NSF	N-ethylmaleimide Sensitive Fusion Protein
PBS	Phosphate Buffered Saline
PEI	Polyethylenimine
PFA	Paraformaldehyde
PI	Propidium Iodide
PVDF	Polyvinylidene Fluoride
Q-SNARE (Qa-, Qb-, Qc-)	Soluble N-ethylmaleimide-Sensitive Factor Attachment Protein Receptor - contains a Glutamine (Q) in the zero ionic layer

R-SNARE	Soluble N-ethylmaleimide-Sensitive Factor Attachment Protein Receptor - contains an Arginine (R) in the zero ionic layer
RFP	Red Fluorescent Protein
RNA	Ribonucleic Acid
RPMI	Roswell Park Memorial Institute (Cell Culture Medium)
SDS	Sodium Dodecyl Sulphate
SDS-PAGE	Sodium Dodecyl Sulphate Polyacrylamide Gel Electrophoresis
SEM	Standard Error Mean
SM	Sec1/Munc18-like protein
SNAP	Soluble N-ethylmaleimide-Sensitive Factor Attachment Protein
SNARE	Soluble N-ethylmaleimide-Sensitive Factor Attachment Protein Receptor
STX	Syntaxin
SV2	Synaptic Vesicle Protein 2
Syt	Synaptotagmin
TeNT	Tetanus Neurotoxin
TF	Transferrin
TF-R	Transferrin-receptor
TGN	Trans-Golgi Network
THP-1	Human Leukemia Monocytic cell line
Trx	Thioredoxin
TrxR	Thioredoxin Reductase
Tyr	Tyrosine

VAMP	Vesicle-associated Membrane Protein
VSV-G	Vesicular Stomatitis Virus G
WGA	Wheat Germ Agglutinin
WT	Wild Type

List of Tables

List of Figures

Table of Contents

Chapter 1

1. Introduction

The *Clostridium* genus contains over 100 different species of *clostridia*, several of which are human pathogens (Hatheway, 1990). They are rod-shaped spore-forming anaerobic bacteria that typically are found in low oxygen environments. *C. botulinum* and *C. tetani* produce potent neurotoxins which are among the most poisonous toxins known to humans, and as such have been identified as potential agents of bioterrorism (Arnon *et al.*, 2001).

Tetanus and botulism are conditions that cause spastic paralysis and flaccid paralysis respectively. Tetanus is the condition that arises from intoxication with TeNT, and botulism from BoNT intoxication (Dickson, 1918; Bizzini, 1979). There are three key routes of botulinum intoxication: foodborne, wound, and infant botulism (Hatheway, 1990). Presently, there is no known antidote for botulism, however there are antitoxins available to neutralise the action of the toxin. The antitoxin works if the BoNT molecule has not entered the presynaptic compartment in neurons, so it must be administered as soon as possible after intoxication (Winner, Bodt and McNutt, 2020). As BoNT works by causing flaccid paralysis, symptoms include breathing difficulties, constipation, and problems with swallowing (Thwaites, 2017). In severe cases respiratory failure could result in fatality.

1.1 Botulinum neurotoxins

BoNTs are classified into seven main serotypes (BoNT/A-G) (**Figure 1.1**) based on their reactivity to reference antisera and sequence homology. In addition to the main serotypes there are also mosaic toxins (e.g. BoNT/DC) and subtypes which show limited cross reactivity to the antisera (e.g. BoNT/A2) (Moriishi *et al.*, 1996; Nakamura *et al.*, 2010; Maslanka *et al.*, 2016).

There are newly discovered BoNT-like molecules that have been identified by bioinformatic analysis of environmental samples, such as BoNT/Wo, BoNT/En, PMP1 and BTNT (Zornetta *et al.*, 2016; Zhang *et al.*, 2018; Contreras *et al.*, 2019). BoNTs classically target different organisms, for example BoNT/A, B, E and F typically affect humans, whereas BoNT/C, D and E affect mammals, birds and fish (Lloyd *et al.*, 1976;

Ortolani *et al.*, 1997; Hyytiä, Hielm and Korkeala, 1998; Eleopra *et al.*, 2004), making understanding these toxins interesting not only for human biology and therapeutics, but also animal health and welfare.

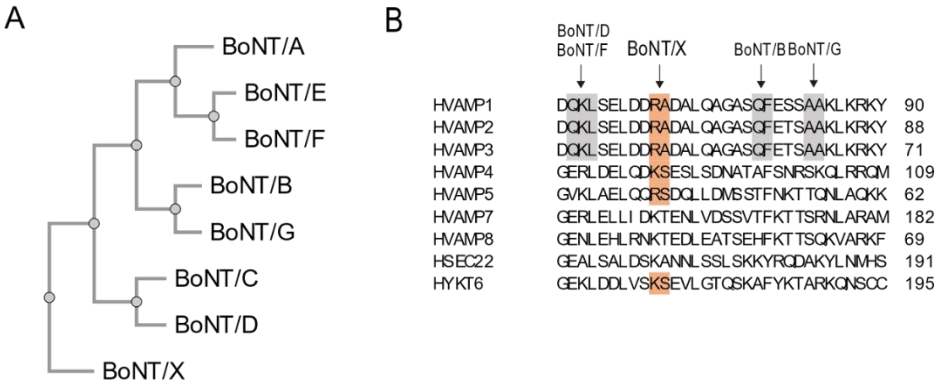

Figure 1.1 Phylogenetic tree of the BoNT family of proteins and SNARE cleavage sites

(**A**) Phylogenetic tree generated using ClustalOmega and the Simple Phylogeny tool (Madeira *et al.*, 2024) (**B**) Sequence alignment of R-SNARE family members and the cleavage site of different BoNTs, aligned using ClustalOmega (Madeira *et al.*, 2024).

Even though BoNT intoxication can be lethal, the potential to use BoNT therapeutically was investigated initially as an alternative non-surgical treatment for strabismus using BoNT/A (Scott, 1980). In recent years, BoNT/A has become a key treatment option for dystonic disorders, blepharospasm, hyperhidrosis, spasticity, chronic migraine as well as in aesthetics (Bushara and Park, 1994; Fonfria *et al.*, 2018). Currently the only commercially available BoNT serotypes are BoNT/A and BoNT/B, though BoNT/B is not as widely used (Fonfria *et al.*, 2018).

1.1.1 BoNT structure

The different serotypes all share the same general structure, comprising a ~50 kDa light chain (LC) and a ~100 kDa heavy chain (HC) connected by a disulphide bond (Pirazzini *et al.*, 2017). BoNTs are produced as ~150 kDa single-chain polypeptides, which are cleaved to form di-chain molecules (Turton, Chaddock and Acharya, 2002). The LC functions as a zinc-dependent endopeptidase and is known as the catalytic domain (Turton, Chaddock and Acharya, 2002). There is a His-Glu-x-x-His zinc-

binding motif in the LC that is highly conserved between the different serotypes of BoNTs (Schiavo *et al.*, 1994).

There are two ~50 kDa functional domains present in the HC, the N-terminal (H_N) and C-terminal (H_C) (Lacy *et al.*, 1998). The domains are arranged linearly, with the H_N separating the LC from the H_C (**Figure 1.2**). Binding of the toxin to the target cell membrane is facilitated by the ganglioside-binding domain (H_C), which allows the toxin to be internalised into neurons (Turton, Chaddock and Acharya, 2002). It has been proposed that the translocation domain (H_N) acts to form a pore in the endosomal lipid bilayer allowing the LC access to the cytoplasm (Turton, Chaddock and Acharya, 2002). The active site in the catalytic domain of the BoNT/A toxin is partially obstructed by a belt (N terminus of heavy chain), preventing catalytic activity until the LC is released in the cytosol. However, this appears not to be the case with other toxins such as BoNT/B (Lacy *et al.*, 1998; Swaminathan and Eswaramoorthy, 2000).

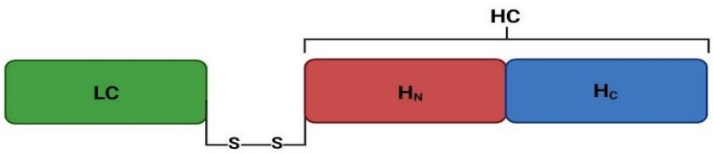

Figure 1.2. The domain structure of botulinum neurotoxins
Botulinum neurotoxins exist as a ~150 kDa protein, with a ~100kD Heavy chain and a ~50kD light chain. The heavy chain (HC) comprises the translocation domain (H_N) and the binding domain (H_C). The protease/catalytic domain is the light chain (LC). The HC and LC are connected by a disulphide bridge, and function as a di-chain molecule. Created with BioRender.com.

1.1.2 BoNT mechanism of action

BoNT intoxication works by interfering with vesicle fusion and therefore neurotransmitter release in neuronal cells (Pirazzini *et al.*, 2017). BoNTs have a high specificity for targeting neurons and recognise two receptors on the nerve terminal surface (Montecucco, 1986; Brunger and Rummel, 2009; Berntsson *et al.*, 2013). First the BoNT molecule binds to gangliosides on the neuronal cell membrane, then it binds to a protein receptor (Rummel *et al.*, 2009). There is a conserved ganglioside binding site in BoNT/A, B, E, F, G and TeNT which contains the core residues SXWY, these

residues however are not conserved in BoNT/C1 and BoNT/D (Rummel, Mahrhold, *et al.*, 2004; Fu *et al.*, 2009; Stenmark *et al.*, 2010). The two currently known protein receptors for BoNTs are synaptotagmin (Syt) and glycosylated SV2 (Pirazzini *et al.*, 2017). BoNT/A, E and F bind to SV2 (Dong *et al.*, 2006; Rummel *et al.*, 2009), BoNT/B and BoNT/G bind to synaptotagmin (Nishiki *et al.*, 1994; Dong *et al.*, 2003, 2007; Rummel, Karnath, *et al.*, 2004). Once bound, the toxin-receptor complex is then internalised into an intracellular vesicle (**Figure 1.3**) (Pirazzini *et al.*, 2017). The endosomal lumen acidifies due to the action of v-ATPase, which has been proposed to cause a conformational change of the toxin (Pirazzini *et al.*, 2016). It is in this acid conformation that the toxin inserts into the lipid bilayer, forming a channel and the LC can be translocated across the vesicular membrane into the cytosol (due to the H_N domain) (Montecucco and Schiavo, 1994). Variation in the speed of translocation of the LC has been observed between different serotypes (Keller, Cai and Neale, 2004; Sun *et al.*, 2012). With the LC in the cytosol, the disulphide bond can be reduced (Fischer and Montal, 2007). The reduction of the disulphide bond is thioredoxin reductase-mediated, which enables the LC to become active as a zinc-endopeptidase (Pirazzini *et al.*, 2014). The chaperone Hsp90 is also present on the cytosolic side of synaptic vesicle and works with thioredoxin reductase (TrxR) and thioredoxin (Trx) to reduce the disulphide bond (Azarnia Tehran *et al.*, 2017). The LC can then cleave SNAREs (soluble N-ethylmaleimide-sensitive factor attachment protein receptors) when it is free in the cytosol, the result of which prevents vesicles containing neurotransmitters from fusing with the plasma membrane during exocytosis (Montecucco, Schiavo and Pantano, 2005). This prevents neurotransmitter release.

The model outlined above is likely to be an oversimplification and several studies have challenged its dogma. For example, there have been unexplained observations where the speed of intoxication is not what one would expect (Ledda *et al.*, 2022) and that significant structural changes have not been observed in the HC and LC under acidic conditions (Galloux *et al.*, 2008), which has led to an alternative mechanism of action for BoNT/A being proposed (Yeo *et al.*, 2024). In genetically engineered neurons, it has been shown that the BoNT/A may traffic through the Golgi to the ER (via a retrograde trafficking pathway) and uses SEC61G to translocate into the cytosol. This demonstrates that there is much to be uncovered in BoNT mechanisms and cellular trafficking.

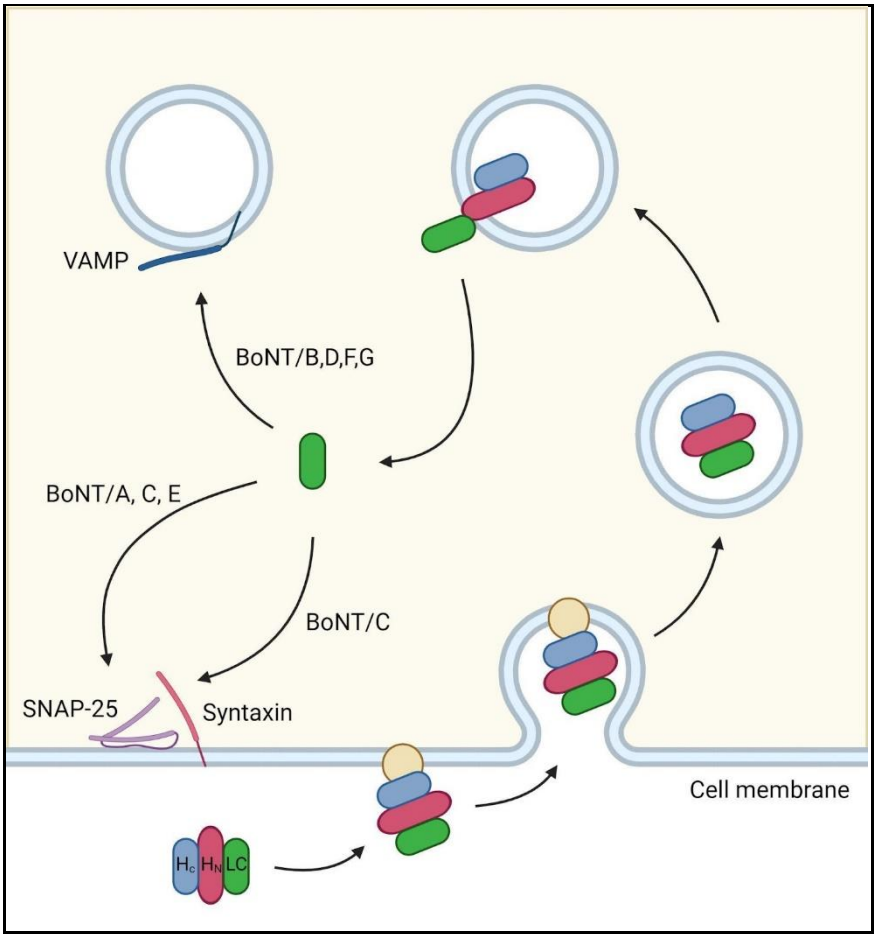

Figure 1.3. Summary of the classical BoNT mechanism of action

The BoNT molecule binds to its target receptor on the surface of a neuron and is internalised into the cell via endocytosis. It is then trafficked to endosomes, where acidification leads to the translocation of the light chain into the cytosol. The light chain is then able to cleave its target SNARE. Created with BioRender.com

1.1.3 BoNTs in neurotransmitter release

BoNT and TeNT both target neuronal SNAREs involved in neurotransmitter release. BoNT serotypes A, C and E have been shown to cleave SNAP-25 (**Table 1**) (Montecucco and Schiavo, 1995; Humeau *et al.*, 2000). TeNT and BoNT serotypes B, D, F and G can cleave VAMP1/2/3 (Humeau *et al.*, 2000). BoNT/C also cleaves syntaxin 1. The different members of the SNARE family have various roles within cellular trafficking, therefore BoNTs that cleave other SNAREs may have different effects on cellular trafficking and therefore potentially have new therapeutic utilities.

Table 1. The different binding and substrate targets of BoNT serotypes.

Serotype	Neuronal cell surface receptor	Substrate target	Cleavage site
A	SV2	SNAP-25	Q197-R198
B	Syt	VAMP1/2/3	Q77-F78
C/ CD		SNAP-25, Syntaxin 1	R198-A199(SNAP-25), K253-A254(STX1)
D/ DC	D- SV2, DC -Syt	VAMP1/2/3	K59-L60
E	SV2	SNAP-25	R180-I181
F	SV2	VAMP1/2/3	Q58-K59
FA	SV2	VAMP1/2/3	L54-E55
G	Syt	VAMP1/2/3	A81-A82

1.2 SNAREs

Soluble N-ethylmaleimide-sensitive factor attachment protein receptors (SNAREs) are a family of proteins that are essential for membrane fusion in the secretory pathway (Jahn and Südhof, 1999). Botulinum toxins are potent inhibitors of SNAREs and have therefore been used to study SNARE function (Schiavo *et al.*, 1992; Gaisano *et al.*, 1994; Steinhardt, Bi and Alderton, 1994; Regazzi *et al.*, 1995). In neurotransmitter release, vesicles containing neurotransmitters are generated at the Golgi and are then stored at the synapse beneath the plasma membrane. An influx of calcium in the presynaptic terminal triggers the fusion of synaptic vesicles with the cell membrane (Chen *et al.*, 1999). The synaptic vesicles contain VAMP2 (synaptobrevin) on the surface, the plasma membrane has SNAP-25 and syntaxin 1 (Söllner, Bennett, *et al.*, 1993; Söllner, Whiteheart, *et al.*, 1993). A four-helix complex (also known as the SNAREpin) forms a bridge between the vesicle membrane and the plasma membrane (**Figure 1.4**) (Hanson *et al.*, 1997). This coiled-coil bundle fuses the vesicle to the target membrane (Weis and Scheller, 1998). In the neuronal SNARE complex,

syntaxin and synaptobrevin contribute one α-helix each and SNAP-25 provides two (Sutton *et al.*, 1998). As SNARE proteins are required for membrane fusion, the cleavage of these SNARE proteins blocks the release of vesicular contents out of the cell.

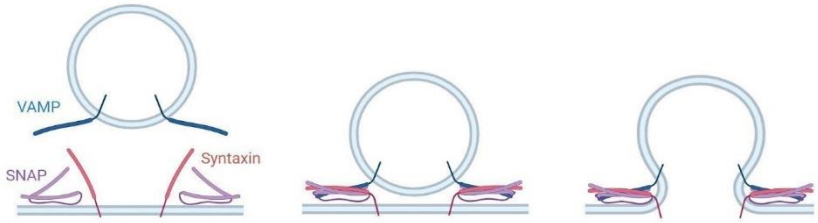

Figure 1.4. Neuronal SNARE complex formation
Q-SNAREs (SNAP and Syntaxin) on the plasma membrane form a SNARE complex with R-SNAREs (VAMPs) on vesicle membranes to facilitate membrane fusion. Created with BioRender.com.

In addition to the neuronal SNARE complex, which drives neurotransmitter release, there are many non-neuronal SNARE complexes that mediate fusion steps throughout the endomembrane system.

1.2.1 SNARE complex formation and disassembly

Within mammalian cells, most SNAREs have a C-terminal transmembrane domain which allows the SNARE to be inserted into the membrane at the ER. The SNARE protein is then trafficked to other membranes within the cells such as the plasma membrane, Golgi and endosomes. Membrane fusion not only requires SNARE proteins, but also additional chaperones and regulatory proteins to facilitate both the formation and disassembly of the SNARE complex. A key player in this process is N-ethylmaleimide Sensitive Factor (NSF). NSF hydrolyses ATP to drive the dissociation of SNARE complexes (Ryu *et al.*, 2015; Shah *et al.*, 2015; Choi *et al.*, 2018; Park *et al.*, 2023). NSF was initially believed to be involved in transport vesicle and Golgi fusion (Malhotra *et al.*, 1988), however it was later discovered that it is instead involved in SNARE disassembly and acts as a chaperone in SNARE recycling (Matveeva and Whiteheart, 1998). There are other proteins involved in SNARE complex disassembly,

known as Soluble NSF Attachment Proteins (SNAP), which exist in three forms in mammals, alpha, beta, and gamma (Clary, Griff and Rothman, 1990). α-SNAP in particular is required for NSF binding to SNARE complexes. The binding of NSF to the SNAP-SNARE complex forms a 20S supercomplex, which when hydrolysed causes a conformational change in the NSF N-terminal domain (Söllner, Bennett, *et al.*, 1993; Zhao *et al.*, 2015). This conformational change causes the SNARE complex to unwind.

For the regulation of SNARE activity, there are a number of proteins that interact with SNAREs and/or the SNARE complex. The Sec1/Munc18-like (SM) family of proteins are cytosolic proteins that are involved in the regulation of membrane fusion by interacting with SNAREs. An SM protein, Munc18, is involved in the regulation of syntaxin and SNARE complex formation (Hata, Slaughter and Südhof, 1993). It binds to syntaxin in a closed formation, regulating availability to form SNARE complexes, and is stabilised by the Habc domain of syntaxin (Dulubova *et al.*, 1999, 2007; Misura, Scheller and Weis, 2000). It has been suggested that Munc18 is involved in the transport of syntaxin to its target compartments (Rowe *et al.*, 2001; Han *et al.*, 2011), however a Munc18 knockout study did not find impaired trafficking of syntaxin to the target membrane (Toonen *et al.*, 2005).

Another key regulatory protein for membrane fusion is synaptotagmin 1, a calcium sensor (Zhou *et al.*, 2015). Synaptotagmins are a family of membrane-trafficking proteins that are involved in vesicle docking and regulate exocytosis. There are 16 synaptotagmin proteins, with synaptotagmin 1 (Syt-1), a calcium sensor, being involved in faster synchronous neurotransmitter release along with Syt-2 and Syt-9 (Xu, Mashimo and Südhof, 2007).

The exact number of SNARE complexes required to mediate exocytosis is not known, however BoNT has been used as a tool to estimate these numbers as they act on SNARE complex formation by targeting SNAREs (Montecucco, Schiavo and Pantano, 2005). As BoNT/A and BoNT/E both cleave SNAP-25 but have different rates of translocation and target different cleavage sites (Keller, Cai and Neale, 2004), comparing SNAP-25 cleavage and exocytosis in intoxicated cells can be helpful in estimating SNARE complex numbers.

Previously SNAREs were classified as either v-SNAREs (vesicle-localised) or t-SNAREs (target membrane-localised) (Rothman, 1994). However, when the crystallised structure of a SNARE complex was observed, SNARE proteins were reclassified as Q-SNAREs or R-SNAREs (Fasshauer *et al.*, 1998). Q-SNAREs provide complementary glutamines (Q) and R-SNAREs provide complementary arginine (R) to the zero ionic layer (the centre hydrophobic core of the SNARE complex) (Fasshauer *et al.*, 1998). All characterised SNARE complexes involved in membrane fusion consist of 3 Q-SNAREs (Qa, Qb, Qc) and 1 R-SNARE (Fasshauer *et al.*, 1998).

1.2.2 VAMPS/R-SNAREs

VAMPs (vesicle associated membrane proteins) are a family of SNARE proteins that are involved with vesicle fusion (Rothman, 1994). Using the Q-SNARE or R-SNARE classification system, VAMPs are classified as R-SNAREs, as they contain an arginine in the zero ionic layer. VAMP binding to syntaxin-SNAP-25 leads to the formation of a SNARE complex, which leads to membrane fusion (Hayashi *et al.*, 1994).

1.2.3 Q-SNAREs

Q-SNAREs can be divided into Qa-, Qb- and Qc-SNAREs, depending on the position of the SNARE motif. Qa-SNAREs are also known as syntaxins, Qb- and Qc- SNAREs are SNAP family proteins.

Syntaxins are membrane-integrated Q-SNAREs. They have a folded N-terminal H_{abc} domain, a single coiled-coil domain and are C-terminally anchored to membranes (Teng, Wang and Tang, 2001). There are 15 syntaxin family proteins in humans (Bennett *et al.*, 1993; Tang, Low, *et al.*, 1998; Tang, Tan, *et al.*, 1998). Syntaxin comprises a transmembrane domain, SNARE domain, linker region and a Habc domain. The exceptions are Syntaxin 11 and 19 which lack transmembrane domains and are anchored to membranes by palmitoylation (Prekeris, Klumperman and Scheller, 2000; Ampah *et al.*, 2018). The SNARE domain is the target for SNAP-25 and synaptobrevin. The Habc domain is an autoinhibitory domain, which folds and interacts with the SNARE domain in syntaxin to block SNARE motif formation (Lerman *et al.*, 2000; Teng, Wang and Tang, 2001).

Synaptosomal-associated Protein-25 kDa (SNAP-25) provides two of the a-helices in the SNARE complex and has both the Qb- and Qc- domains. There are several proteins that are closely related to SNAP-25 and exist within the SNAP-25 family of proteins, notably SNAP-23, SNAP-29 and SNAP-47 (Steegmaier *et al.*, 1998; Holt *et al.*, 2006).

1.2.4 Role of R-SNAREs in membrane fusion

Brevins

The brevins are small R-SNAREs that have a short N-terminal region, a SNARE motif and a C-terminal transmembrane domain (Trimble, Cowan and Scheller, 1988; Baumert *et al.*, 1989; Hazzard, Südhof and Rizo, 1999; Deák *et al.*, 2006). The brevin R-SNAREs are VAMPs1-5 and VAMP8. VAMP4 is also a brevin however is unusual in that it contains an extended N-terminal region that targets the TGN (Peden, Park and Scheller, 2001; Zeng *et al.*, 2003).

VAMPs 1-3

VAMP1 (synaptobrevin 1) and VAMP2 (synaptobrevin 2) are both synaptic vesicle proteins, with VAMP1 mediating neurotransmitter release in neurons (Nystuen *et al.*, 2007) and VAMP2 having a role in Ca^{2+} triggered neurotransmitter release in neurons (Schoch *et al.*, 2001). VAMP3 (also known as cellubrevin) is a ubiquitously expressed R-SNARE that is localised to early endosomes and recycling endosomes (McMahon *et al.*, 1993; Daro *et al.*, 1996; Bajno *et al.*, 2000). Studies have shown the inhibition of VAMP3 results in reduced trafficking of β1 integrin to the cell surface, without the reduction of total levels, suggesting there is a block in trafficking to the plasma membrane (Luftman *et al.*, 2009). The reduction of VAMP3 caused reduced cell adhesion to laminin but not to fibronectin or collagen, and did not impact cell proliferation (Luftman *et al.*, 2009). In neuroblastoma studies, it was shown that a reduction of VAMP3 resulted in worse neuroblastoma outcomes for patients (Zhang *et al.*, 2023). Interestingly, increased VAMP3 levels reduced cell proliferation and increased apoptosis, suggesting that VAMP3 may play a role in cell survival pathways (Zhang *et al.*, 2023). A recent study revealed the potential role of VAMP3 in Bax induced apoptosis, with VAMP3 showing anti-apoptotic properties (Akintade and Chaudhuri, 2021). Despite studies demonstrating co-localisation of VAMP3 with

transferrin (Kubo *et al.*, 2015) and evidence supporting the role of VAMP3 in key cellular processes such as transferrin recycling in CHO cells (Galli *et al.*, 1994), the loss of VAMP3 in mice knockout studies does not have an impact on viability (Galli *et al.*, 1994; Yang, Mora, *et al.*, 2001), and RNAi knock out did not impact transferrin recycling (Kubo *et al.*, 2015).

VAMPs 4, 5, and 8

VAMP4 is widely expressed and has been shown to likely mediate vesicle trafficking between trans-Golgi network (TGN) and late endosomes (Steegmaier *et al.*, 1999). VAMP4 was also identified as being a key SNARE involved in homotypic fusion of early endosomes (Brandhorst *et al.*, 2006). VAMP4 and VAMP7 appear to have a role in the release of lytic granules from NK-cells (Krzewski *et al.*, 2011). VAMP5 was discovered in muscle tissue where it was generally localised to the plasma membrane (Zeng *et al.*, 1998), however since its initial discovery it has also been found in other tissues such as liver and kidney (Takahashi *et al.*, 2013). Studies suggest that it may be involved in glucose uptake via GLUT4 trafficking in muscle (Rose *et al.*, 2009). The definitive role of VAMP5 is unclear, a VAMP5 KO mouse study revealed that by knocking out VAMP5 the resulting mice had a low birth rate and low body weight as well as abnormalities in the urinary and respiratory systems, suggesting that VAMP5 may be required for these systems to function (Ikezawa *et al.*, 2018). VAMP8 (endobrevin) is primarily localised to endosomes (Wong *et al.*, 1998) but is also found on the TGN and plasma membrane (Antonin *et al.*, 2000). It is known to be involved in homotypic fusion of endosomes (Antonin *et al.*, 2000) and co-localises with Syntaxin 7 so may be involved in endosome-lysosome fusion (Mullock *et al.*, 2000). VAMP8 may also be involved in exocytosis in exocrine systems as VAMP8 KO mice show abnormalities in salivary and lacrimal glands (Wang *et al.*, 2004, 2007). VAMP8 has also been linked to cytokinesis in cell division, where it is involved in abscission (Low *et al.*, 2003; Mukai *et al.*, 2008; Rannou *et al.*, 2012).

Longins

Like the brevins, longin SNAREs contain a SNARE motif. They however also contain a longin domain located in the N-terminal domain which is highly conserved (Filippini *et al.*, 2001). There are three longin R-SNAREs: VAMP7, Ykt6 and Sec22B. The longin

domain is a regulatory domain like the Habc domain and folds back on to the SNARE domain.

VAMP7

VAMP7 is a VAMP that is not cleaved by clostridial neurotoxins (Galli *et al.*, 1998) and is also known as the tetanus neurotoxin-insensitive VAMP (TI-VAMP). It forms complexes with other SNAREs localised at the apical plasma membrane in epithelial cells. VAMP7 co-localised with LGP120 (a lysosome marker), suggesting that it is involved in lysosome trafficking (Advani *et al.*, 1998), however a VAMP7 KO mouse model did not demonstrate impaired localisation of lysosomes, therefore other VAMPs may be able to compensate for the loss of VAMP7 (Sato *et al.*, 2011). It has also been linked to autophagic pathways as VAMP7 is involved in autophagosome-lysosome fusion (Fader *et al.*, 2009; Itakura, Kishi-Itakura and Mizushima, 2012; Guo *et al.*, 2014). VAMP7 has also been found as a mediator of secretory lysosome exocytosis (Verderio *et al.*, 2012). Neurite outgrowth requires exocytosis that appears to involve SNARE complex formation using VAMP7 (Martinez-Arca *et al.*, 2000, 2001). Neurite outgrowth is reduced in VAMP7 knockout cells (Wojnacki *et al.*, 2020). In VAMP7 knockout mice however there were no clear abnormalities observed, though axonal outgrowth was reduced (Sato *et al.*, 2011). More recently it has been described that VAMP7 may play a role in chemokine secretion in mast cells, as a knockdown of VAMP7 led to reduced secretion levels (Sakamoto *et al.*, 2024).

YKT6

Ykt6 is an unusual SNARE as it does not have a transmembrane domain and is lipid anchored to the membrane (Fukasawa *et al.*, 2004). It contains a prenylation consensus motif (CAAX box) and can exist as both an active membrane-bound form and an inactive cytosolic form (McNew *et al.*, 1997; Zhang and Hong, 2001; Fukasawa *et al.*, 2004). The biology of Ykt6 function and modification is widely debated, as it undergoes various modifications, e.g. geranylgeranylation, farnesylation, palmitoylation (Fukasawa *et al.*, 2004; Shirakawa *et al.*, 2020; Sakata *et al.*, 2021). When Ykt6 is phosphorylated at a conserved site, a conformational change occurs allowing the structure to open or close (therefore membrane-bound or cytosolic) (McGrath *et al.*, 2021).

It has been shown to be essential in yeast, where it is involved in ER-Golgi and Golgi-vacuole transport (Kweon *et al.*, 2003). In rats, Ykt6 is highly expressed in the brain, where it is concentrated in neurons, with low levels being expressed in other tissues (Hasegawa *et al.*, 2003). The depletion of Ykt6 resulted in the inhibition of autophagosome-lysosome fusion, suggesting that Ykt6 acts in this pathway (Matsui *et al.*, 2018; Takáts *et al.*, 2018). It has been proposed that the function of Ykt6 is perturbed in Parkinson's disease, as α-Synuclein has been shown to interact with Ykt6 in the cytosol, reducing the levels of membrane-bound Ykt6 that can form SNARE complexes. This results in defects in lysosomal function and protein homeostasis, causing an accumulation of proteins (Cuddy *et al.*, 2019).

Combinatorial depletion of Ykt6 and VAMP3 caused a block in secretion in Drosophila cells, leading to post-Golgi transport vesicles to accumulate (Gordon *et al.*, 2017). In addition to its involvement in ER-Golgi transport, it has also been demonstrated to be involved in exosome secretion, which is a key driver for cell-cell signalling in cancer, with increased Ykt6 expression being linked to reduced survival in non-small cell lung cancer (Ruiz-Martinez *et al.*, 2016).

Sec22B

Sec22 has three isoforms, Sec22A, B and C. Sec22B is an R-SNARE as it contains a longin domain and SNARE motif, whereas isoforms A and C are not considered SNAREs as they do not contain the SNARE motif. Sec22B is predominantly localised to the ER and Golgi where it functions in anterograde and retrograde transport, mediating fusion of COPII vesicles and Golgi membranes, COPI and ER (Sun *et al.*, 2020). It also has been shown to be involved in transport between secretory autophagosomes and the plasma membrane (Kimura *et al.*, 2017).

The R-SNAREs Ykt6 and Sec22B function in a redundant manner in Drosophila cells, as there is a notable block in secretion when both are depleted, with cargo being trapped in ER however only partial block is observed when individually depleted (Gordon *et al.*, 2017). This has also been observed in yeast where a loss of Sec22p increases levels of Ykt6p expression and Ykt6p functionally rescues the loss of Sec22p (Liu and Barlowe, 2002), and mammalian cells (Gordon *et al.*, 2017). However, in plasma cells Sec22B has a non-redundant role, as the loss of Sec22B resulted in antibody secretion deficiencies (Bonaud *et al.*, 2023).

1.2.5 R-SNAREs and intracellular trafficking

SNAREs are key drivers of membrane fusion and so play a role in the various cellular trafficking pathways in the endomembrane system (**Figure 1.5**).

Endocytosis and the endocytic recycling pathway are key intracellular processes. Endocytosis can be clathrin-dependent or clathrin-independent (Pearse, 1976; Mayor and Pagano, 2007; McMahon and Boucrot, 2011). Clathrin-mediated endocytosis involves several key steps: initiation, membrane bending, scission, and uncoating (**Figure 1.6**). The initial stage of clathrin-mediated endocytosis begins with recruitment of cargo and endocytic proteins such as AP-2 to the membrane (Godlee and Kaksonen, 2013). Actin localises to the membrane where it polymerises and aids in shaping the membrane (Merrifield *et al.*, 2002; Yang *et al.*, 2022). Myosin motor protein helps to facilitate this process (Buss *et al.*, 2001; Sun, Martin and Drubin, 2006). This polymerisation causes a pit to form in the membrane, which promotes the process of vesicle budding (Kukulski *et al.*, 2012). Clathrin forms a hexagonal/pentagonal structure around the pit, known as a clathrin-coated pit (Crowther and Pearse, 1981; G P Vigers, Crowther and Pearse, 1986). The clathrin molecules do not bind directly to the plasma membrane directly in this process but instead use adaptor proteins (e.g. AP-2 and accessory protein AP180) (G. P. Vigers, Crowther and Pearse, 1986; Morgan *et al.*, 1999). For vesicle formation to be completed, the vesicle membrane must detach from the cell membrane, a process known as vesicle scission. In clathrin-mediated endocytosis, the GTPase dynamin forms a helical structure at the top of the clathrin-coated pit, which constricts and pinches the membrane, driving vesicle scission (Robinson *et al.*, 1994; Sweitzer and Hinshaw, 1998; Stowell *et al.*, 1999). After scission of the membrane, the clathrin-coated vesicle traffics into the cytoplasm. The clathrin-coat disassembles due to the activity of HSC70 and auxilin (Barouch *et al.*, 1994; Greener *et al.*, 2000). This releases the vesicle containing its cargo allowing it to be sorted to early endosomes. After uncoating, the adaptor proteins and clathrin traffic back to the plasma membrane so they can be recycled for future endocytic events. GTPases (Rab and Arf proteins) regulate trafficking and recycling of the vesicles to their target compartments (Nielsen *et al.*, 1999; Weigert *et al.*, 2004; Kouranti *et al.*, 2006a; Navaroli *et al.*, 2012; Donaldson and and Dutta, 2016; Arrazola Sastre *et al.*, 2021). Interaction with the cytoskeleton and motor proteins allows for the vesicles to travel through the cytoplasm to the required organelle, for example Rab5

is involved in microtubule and early endosome interactions (Nielsen *et al.*, 1999). The vesicle fuses with the target membrane and the cargo is delivered, allowing the receptors to recycle back to the plasma membrane and await cargo binding.

Cargo is trafficked from the cell surface to early endosomes, then recycled back to the cell surface either via the rapid recycling route (direct to cell surface) or it is sorted to late endosomes/recycling endosomes (Grant and Donaldson, 2009). Once at the recycling endosome the cargo is returned to the cell surface. Early endosomes receive cargo from vesicles made by endocytosis. As the lumen of the early endosome is acidic, ligand release from receptors can be facilitated. If we look at a classic model of endocytic recycling, the transferrin pathway is a key pathway for iron transport in cells (**Figure 1.6**). Holo-transferrin binds to the transferrin receptor at the cell surface. It is then internalised and trafficked to endosomes. Here, the acidic lumen causes the iron to dissociate from the transferrin, resulting in apo-transferrin (Dautry-Varsat, Ciechanover and Lodish, 1983). The apo-transferrin is then recycled back to the cell surface where it can then bind iron and repeat the process (Dautry-Varsat, Ciechanover and Lodish, 1983). The fast-recycling pathway is used by proteins such as transferrin receptor (TF-R) and glycosphingolipids (Sharma *et al.*, 2003). Proteins such as RAB4 and RAB35 are often implicated in these pathways, along with R-SNAREs such as VAMP3 (van der Sluijs *et al.*, 1992; Daro *et al.*, 1996; Kouranti *et al.*, 2006b; Navaroli *et al.*, 2012). Transferrin transport also utilises the slow-recycling pathway, where transferrin and it's receptor traffic to the recycling endosome and relies on proteins such as Rab11 to transport the transferrin back to the plasma membrane (Schlierf *et al.*, 2000).

There are two pathways of secretion in cells, regulated, and constitutive secretion. Regulated secretion is typically found in specific cell types, such as endocrine and neuronal cells. It involves the transport of newly synthesised proteins (such as neurotransmitters) from the Golgi to secretory granules or vesicles in the cytoplasm, where they are stored until they are triggered for release by an external stimuli (Kelly, 1985). This causes an increase in Ca^{2+}, which results in vesicle fusion. Constitutive secretion involves the transport of proteins from the ER to the plasma membrane and is governed by the rate of protein synthesis rather than by external stimuli (Kelly, 1985). This occurs continuously and is also known as bulk flow.

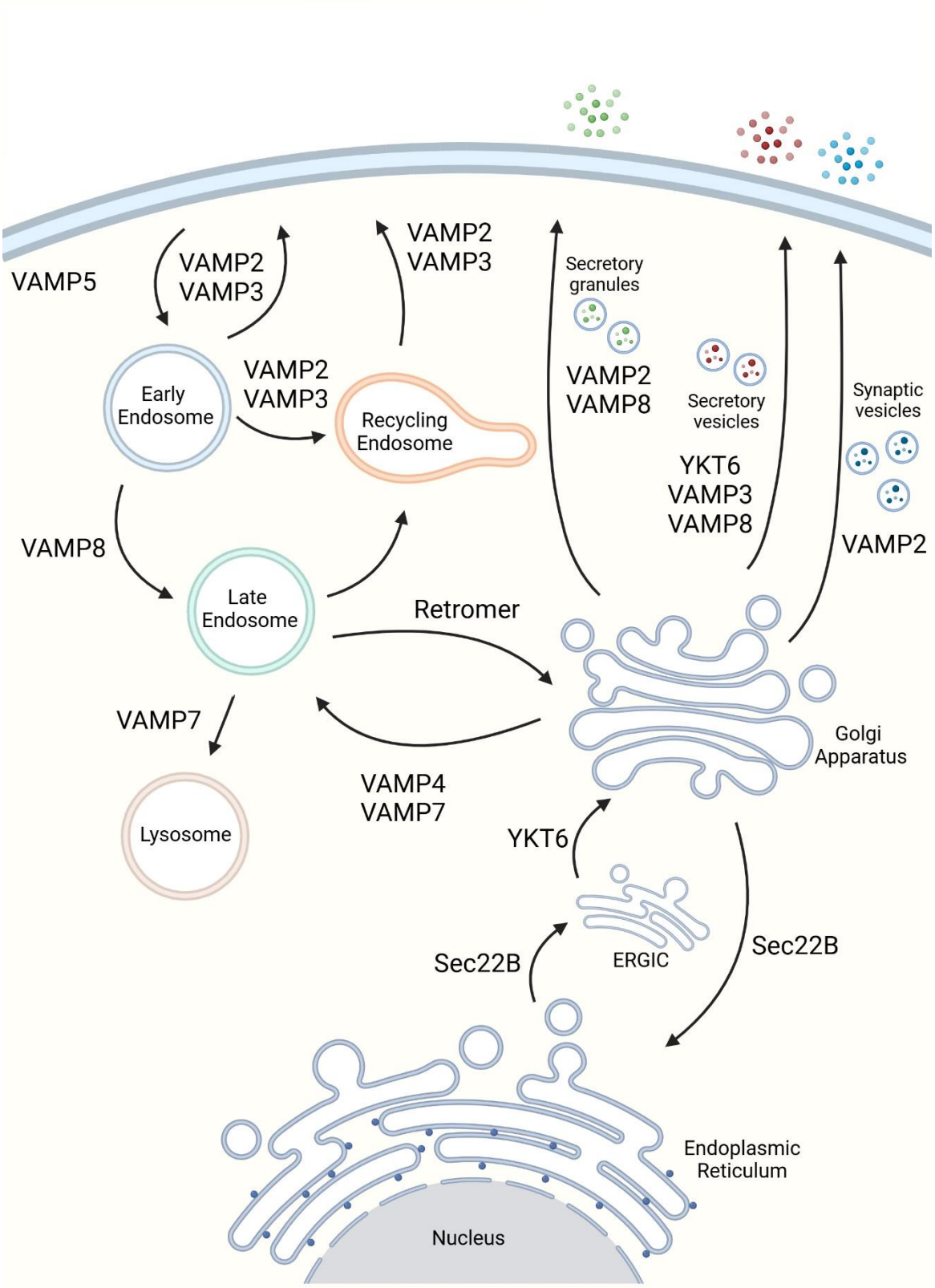

Figure 1.5. R-SNARE intracellular trafficking pathways

R-SNAREs are involved in numerous intracellular trafficking pathways as shown above. Abbreviations as follows: ERGIC - Endoplasmic-reticulum-Golgi intermediate compartment. Created with BioRender.com.

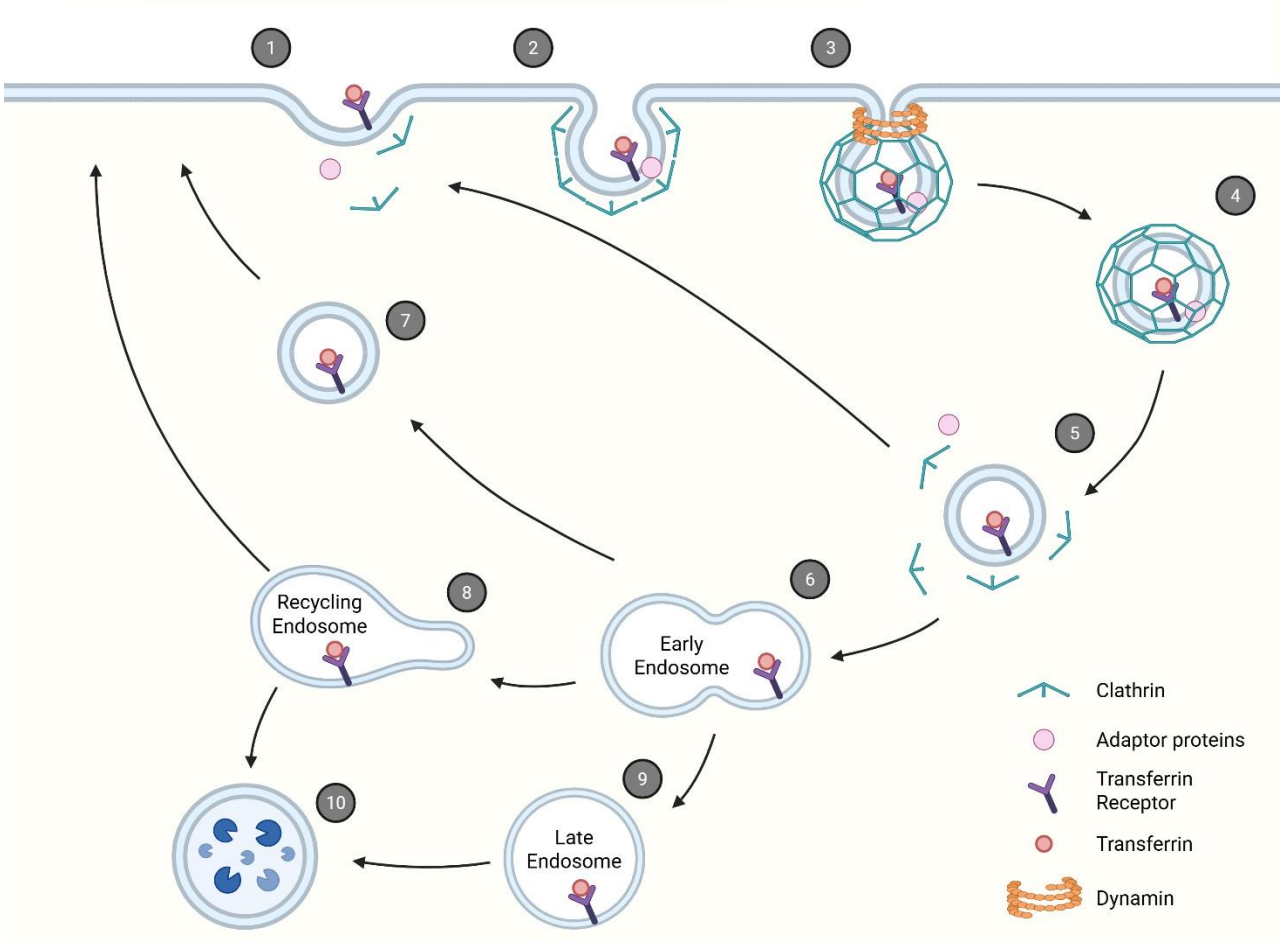

Figure 1.6. Summary of the clathrin-mediated endocytosis pathway and transferrin recycling (1) Initiation: Adaptor proteins recruited to the membrane. (2) Membrane bending and pit formation. (3) Scission: Dynamin facilitates the clathrin-coated pit detaching from the membrane. (4) Clathrin-coated vesicle formation: The vesicle is formed and released into the cytoplasm. (5) Vesicle uncoating: Clathrin and adaptor proteins detach from the vesicle and traffic back to the membrane. (6) Fusion of the vesicle with endosomes: The cargo then can recycle directly to the plasma membrane (7), be sorted to recycling endosomes for delivery to the plasma membrane (8), late endosomes (9), or lysosomal degradation (10). Created in BioRender.com.

1.2.6 Role of Q-SNAREs in membrane fusion

Q-SNAREs are also essential for membrane fusion, forming the SNARE complex along with R-SNAREs. Historically some of the best studied SNAREs are the Q-SNAREs involved in neurotransmitter release, such as SNAP-25. Synaptosomal associated protein 25 (SNAP-25) is one of the main SNARE proteins involved in

membrane fusion at the presynaptic terminal, where it is attached to the cell membrane via lipid modifications e.g. palmitoylation and contains cysteine residues in the coil region to dock it to the target membrane (Hess *et al.*, 1992; Veit, Söllner and Rothman, 1996).

In neuronal cells, SNAP-23 is able to compensate for the loss of SNAP-25 and prevent cell death, however in differentiated cells there is a notable loss of SNAP-23 expression (Rust *et al.*, 2016). SNAP-25 is expressed in neuronal and neuroendocrine cells, whereas SNAP-23 is ubiquitously expressed. There appears to be a level of genetic redundancy in SNAREs, for example SNAP-23 K/O mice are non-viable (Suh *et al.*, 2011) however, in some cells that contain both SNAP-23 and SNAP-25, such as pancreatic islet cells, SNAP-23 is redundant in the presence of SNAP-25 (Liang *et al.*, 2020).

In addition to neurotransmitter exocytosis, Q-SNAREs are also involved in endocytic and constitutive delivery of cargo to the plasma membrane. Late endosome-lysosome fusion has been shown to involve Syntaxin 7 and Syntaxin 8, where they are able to form SNARE complexes with VAMP7 and VAMP8 (Pryor *et al.*, 2004). In *Dictyostelium discoideum*, endosome-lysosome fusion in macropinocytosis requires a SNARE complex comprising Syntaxin 7, Syntaxin 8, Vti1 and VAMP7 (Bogdanovic *et al.*, 2002). Syntaxin 4 is known to be involved in insulin exocytosis (Yang, Coker, *et al.*, 2001). Syntaxin 5 forms SNARE complexes with Sec22B to facilitate ER-Golgi transport (Dascher, Matteson and Balch, 1994) and has a role in autophagy (Renna *et al.*, 2011). In constitutive secretion, Syntaxin 19 is involved in Golgi-plasma membrane trafficking/fusion and is able to form SNARE complexes with SNAP-23, SNAP-25, SNAP-29, VAMP3 and VAMP8 (Gordon *et al.*, 2010).

There appears to be a critical role of Q-SNAREs in functions outside of membrane trafficking, it has recently been shown that they are involved in cell survival and cell cycle, where SNAP-29 is involved in kinetochore formation, and plays a role in chromosomal segregation during mitosis/meiosis (Morelli *et al.*, 2016). Syntaxin 1 has been shown to be involved in glioblastoma multiforme progression, where a loss of Stx1 aids in reducing the proliferation and cell invasion of the tumour (Ulloa *et al.*, 2015).

1.2.7 SNARE mutations and disease (SNAREopathies)

A number of disease-causing mutations in SNAREs have been identified (Kovačević *et al.*, 2018; Salpietro *et al.*, 2019; Vardar *et al.*, 2020; Verhage and Sørensen, 2020). A SNAP-25 mutant was identified that impairs SNARE complex assembly, causing intellectual disability, hyperexcitability, ataxia and myasthenia in humans (Rebane *et al.*, 2018). Studies have suggested a link between mutations in the SNAP-25 gene with conditions such as ADHD, bipolar disorder, schizophrenia and epileptic encephalopathy (Young *et al.*, 1998; Barr *et al.*, 2000; Brophy *et al.*, 2002; Kustanovich *et al.*, 2003; Etain *et al.*, 2010; Klöckner *et al.*, 2021). Another example is in VAMP1 where a mutation has been shown to cause hereditary spastic ataxia in humans (Bourassa *et al.*, 2012). A VAMP2 mutation (S75P) results in a neurodevelopmental disorder, causing reduced fusion of VAMP2 vesicles and prevents Munc18 interaction (Salpietro *et al.*, 2019).

1.2.8 SNAREs in cell division

Cell survival and division relies on the successful progression of cells through the cell cycle. The cell cycle is made up of four key stages: G0/G1 (gap 1), S (synthesis), G2 (gap 2) and M (mitosis). In G1, cells increase their size, causing the expansion of the plasma membrane. In S phase, there is synthesis of DNA for the daughter cell. G2 phase involves rapid cell growth and protein synthesis. M phase is where cell division occurs. For cell division to occur, the replicated chromosomes segregate to opposite poles of the cell, prior to undergoing cytokinesis - the physical separation of the cells (Barr and Gruneberg, 2007). This segregation of chromosomes requires the assembly of kinetochores, which involves the SNARE SNAP-29 (Boucrot and Kirchhausen, 2007; Morelli *et al.*, 2016). The completion of cytokinesis relies on the abscission of the plasma membrane, a process that requires the action of SNARE proteins such as Syntaxin 2/16 and VAMP8 (Low *et al.*, 2003; Gromley *et al.*, 2005; Song *et al.*, 2009; Schiel *et al.*, 2011). SNAP-25 and VAMP2 have also been localised in the cleavage furrow during cytokinesis (Ming Li *et al.*, 2006). As well as the reformation of the plasma membrane during cell division, nuclear envelope reformation is potentially a SNARE-mediated fusion event (Jantsch-Plunger and Glotzer, 1999; Baur *et al.*, 2007).

1.2.9 Cytotoxicity of BoNTs

It is known that whilst BoNT intoxication can be lethal in whole organisms, they show limited cytotoxic action in cells. When SNAP-25 or VAMPs1-3 are cleaved by BoNTs there is no cell death, suggesting that cell viability is not reliant on synaptic vesicle fusion (Osen-Sand *et al.*, 1996). This is further supported by VAMP2 and SNAP-25 knockout mice which remain viable until birth (Schoch *et al.*, 2001; Washbourne *et al.*, 2002). There have been studies that demonstrate cytotoxicity from some BoNT serotypes, notably BoNT C and E (Osen-Sand *et al.*, 1996; Peng *et al.*, 2013). The potential for BoNTs to be used as a cancer therapy has been previously studied in BoNT/C, as intoxication resulted in cytotoxicity in neurons and neuroendocrine cells (Williamson and Neale, 1998; Peng *et al.*, 2013; Arsenault *et al.*, 2014). The overexpression of syntaxins (2/3/4) and SNAP-23 were able to rescue the cytotoxicity, possibly by acting in a compensatory manner (Peng *et al.*, 2013). This was an interesting finding as cell survival should not be affected if the BoNT solely acts by blocking neurotransmitter release as neuron development or survival is not dependent on synaptic vesicle exocytosis (Osen-Sand *et al.*, 1996). The disruption of plasma membrane recycling processes could be a possible explanation for the cytotoxicity seen in these cells (Peng *et al.*, 2013).

1.3 BoNT/X

Since the discovery of BoNT/G in 1969, there had been no new BoNT serotypes recorded, with only subtypes and mosaic toxins being identified (BoNT/FA, A1-7, CD etc). Interestingly when analysing BoNT strains, there have been cases where silent toxin genes are found in the genome of the bacteria. For example, the bacterial strain produces BoNT/A but also encodes BoNT/B gene which is not expressed (Franciosa, Ferreira and Hatheway, 1994; Barash and Arnon, 2014).

In 1996 a report of infant botulism in Japan was identified which was caused by clostridium botulinum strain 111, which expresses BoNT/B (Kakinuma *et al.*, 1996). Computational analysis of the bacterial genome from this strain by Zhang et al (2017) identified a region in the genome which shared homology with botulinum toxins suggesting this strain may encode an additional toxin. Further analysis of this sequence revealed a gene located on the chromosome which they named BoNT/X. It

was established that BoNT/X is a novel serotype as it had a low sequence similarity to other known BoNTs, no known antisera could neutralise the toxin and yet it possesses the conserved HEXXH and SXWY motifs in the protease and binding domains respectively (Zhang *et al.*, 2017). The C. botulinum strain 111 therefore appears to be a dual toxin producing strain, and it is currently assumed that the gene for BoNT/X is silent or that it is non-toxic.

1.3.1 BoNT/X substrate specificity

To identify which SNAREs BoNT/X cleaves Zhang et al (2017) produced a His6-tagged version of the LC and incubated the toxin with recombinant VAMP2. BoNT/X cleaves VAMP2 at a novel site (R66-A67), which is in the SNARE motif of the protein (Zhang *et al.*, 2017). To validate the specificity of the LC/X they used transient transfections to express HA-tagged VAMP1, VAMP3, VAMP7, VAMP8, Myc-tagged Sec22b and Ykt6. This revealed that VAMP1, VAMP3 and Ykt6 were cleaved, whilst VAMP7, VAMP8 and Sec22b were resistant to cleavage. They also discovered that GST-tagged VAMP4 and VAMP5 could be cleaved (Zhang *et al.*, 2017). The cleavage site of VAMP4, VAMP5 and Ykt6 is in the homologous location as R66-A67 in VAMP2, however the residues are different (KS in VAMP4 and Ykt6, and RS in VAMP5), with K87-S88 in VAMP4 and R40-S41 in VAMP5. The location of the cleavage site is also conserved in VAMP1 and VAMP3 (Zhang *et al.*, 2017). Kinetics studies showed that LC/X cleaves VAMP1 with ten times higher efficiency than BoNT/B and TeNT (Masuyer *et al.*, 2018).

BoNT/X is the only known BoNT that cleaves VAMP4, VAMP5 and Ykt6, which makes it a potentially powerful tool to study their roles in intracellular trafficking, but also could be utilised as a potential therapeutic. Previous work in the Peden lab (Asnawi, 2021) demonstrated that BoNT/X cleaved VAMPs1-4 and Ykt6 in vivo, causing significant perturbations in endocytic and biosynthetic trafficking pathways. Intoxication resulted in reduced surface protein levels and block of delivery of cargo to the cell surface.

At present it is not known how BoNT/X binds to neurons as the sites known to bind gangliosides and neuronal receptors in the protein are not well conserved. Potential binding targets have been assessed (GT1b, GD1a, GM1, SV2), however very weak binding to these receptors was shown, or the sites lacked conserved residues for the

binding interaction (Martínez-Carranza *et al.*, 2024). Due to the structure of BoNT/X, the binding sites of synaptotagmins 1 and 2 are not accessible, and so are also unlikely targets (Martínez-Carranza *et al.*, 2024).

Due to its broad substrate specificity, and ability to cleave SNAREs with different residues at the cleavage site, it was thought that the BoNT/X protein would likely be able to adjust to residue changes well. This could make the molecule a useful tool to engineer new variants that could perhaps cleave currently untargeted SNAREs such as VAMP7 and VAMP8 (Masuyer *et al.*, 2018). Newly engineered BoNT/X proteins were developed that selectively cleave VAMP4 or Ykt6 over the other substrates in vitro (Blum *et al.*, 2021), demonstrating the potential for new versions of the toxin to be developed in the future.

1.3.2 Therapeutic potential of BoNT/X

Previous work in the Peden lab (Asnawi, 2021) has shown that when HeLa cells were transfected with the light chain of BoNT/X, the morphology of the cells changed and showed a more rounded shape and a decreased cell size, suggesting that BoNT/X may be having a cytotoxic effect on cells. There were also fewer cells present in the BoNT/X transfected cells, which could imply that there is a reduction in cell proliferation or possible apoptosis. Current BoNT therapeutics rely on the cleavage of SNAREs involved with neurotransmitter release that then induce paralysis, however as BoNT/X cleaves SNAREs involved in other processes this molecule could be utilised therapeutically for new indications not currently treated using BoNTs.

Due to safety restrictions, a sortase-mediated ligated version of the toxin was generated using two fragments of BoNT/X that are non-toxic individually but with the addition of sortase form a full-length toxin to assess the activity of the toxin (Zhang *et al.*, 2017). This ligated BoNT/X caused flaccid paralysis *in vivo* when injected into mouse muscle, demonstrating that the toxin is functional (Zhang *et al.*, 2017). However, it was less potent and less toxic than other BoNTs, as lethal doses are typically in picogram levels, whereas the mice survived a dose of 1 µg (Zhang *et al.*, 2017). Initially there was no anti-BoNT/X antiserum, which limited native full-length toxin production due to safety concerns. However, it is now available, allowing for the native toxin to be studied (Gregg *et al.*, 2024). Studies using the native and recombinant BoNT/X protein

have confirmed that BoNT/X is less potent than other BoNTs, likely in part due to its inability to bind to cell targets (Gregg *et al.*, 2024; Martínez-Carranza *et al.*, 2024). Together, the existing data suggest that BoNT/X is not toxic to vertebrates or humans. This could be due to the inability of the toxin to enter neurons, as a chimeric toxin using the receptor binding domain of BoNT/A demonstrates toxicity (Miyashita *et al.*, 2021; Gregg *et al.*, 2024).

1.4 Summary

Studies have shown that BoNT/X acts on previously untargeted SNAREs, which could mean that it acts on different cellular pathways compared to existing known toxins. Previous work from the Peden lab (Asnawi, 2021) has shown that BoNT/X severely perturbs trafficking within the endomembrane system and blocks the delivery of proteins to the cell surface. We do not currently know if this is a result of SNARE cleavage or because the toxin is cleaving non-SNARE proteins. In addition to this, the roles of various R-SNAREs are not fully understood, and the impact of disease-causing mutations are hard to study using existing models. We can therefore use BoNT/X as a tool to study R-SNARE function.

1.5 Aims and objectives

1. Develop novel reporters for measuring BoNT/X activity.

As BoNT/X is a novel toxin, there are limited tools developed to monitor its activity, as existing assays focus on SNAP-25/VAMP2 cleavage. As novel toxins are discovered and engineered, it will be important to be able to characterise and monitor their activity. The development of simple assays to assess SNARE cleavage and function will aid those studying the biology of these toxins and provide new insight into the role of SNARE proteins in intracellular trafficking.

2. Determine if the trafficking phenotypes observed during BoNT/X intoxication are specifically due to SNARE cleavage.

We know that BoNT/X is able to cleave a broad range of R-SNAREs not previously targeted by other toxin serotypes (VAMPs1-5 and Ykt6) (Asnawi, 2021). In addition, intoxication leads to pleiotropic changes in both endocytic and biosynthetic transport. However, it is unclear whether these phenotypes are specifically caused by SNARE cleavage. By generating cleavage resistant SNAREs, we can determine if these phenotypes are specific to R-SNARE proteolysis.

3. Explore whether the BoNT/X reconstitution system can be used to model the impact of disease-causing mutations on SNARE function.

By establishing cleavage resistant SNAREs, we can investigate key residues of interest in SNAREs and assess their function. There are many disease-causing mutations, if these can be studied using cell-based systems, it could help to uncover their role in disease without reliance on animal models.

4. Investigate the mechanisms by which BoNT/X intoxication affects cell viability and cell division.

We know that R-SNAREs are required for both endocytic and secretory trafficking. However, their roles in cell homeostasis and cell survival remain to be fully elucidated. Characterising the impact of BoNT/X intoxication on these processes may shed new light into the role of R-SNAREs in these processes.

Chapter 2

2. BoNT/X a new tool for studying the function of R-SNAREs in post-Golgi trafficking and constitutive secretion

Declaration

This chapter has been submitted for examination in the format of a journal manuscript in accordance with the University of Sheffield's thesis format guidelines.

The manuscript was written by Pollyanna A Rouse and Andrew A Peden.

The following data is my own work:

Figure 1B - Western blot.

Figure 4 - All data.

Figure 5 - All data.

Figure 6 - All data.

Figure 7 - All data.

Supplemental 2B,C – Flow cytometry.

The following data is not my own work:

Figure 1A,C,D - This was conducted by Asral W. Asnawi.

Figure 2 - This was conducted by Asral W. Asnawi.

Figure 3 - This was conducted by Asral W. Asnawi.

Supplemental 1 - This was conducted by Asral W. Asnawi.

Supplemental 2A – This was conducted by Amber Robinson.

BoNT/X a new tool for studying the function of R-SNAREs in post-Golgi trafficking and constitutive secretion

Authors: Pollyanna A. Rouse*, Asral W. Asnawi*, Jesse Hay, Mark Elliott, Matthew Beard, Min Dong and Andrew A. Peden

*Contributed equally to the work.

Abstract

Botulinum neurotoxins inhibit neurotransmitter release by cleaving SNARE proteins. A novel serotype, BoNT/X was recently discovered which has a broader substrate specificity compared to BoNT/B, D, F and G. In this study we have demonstrated that the light chain of BoNT/X cleaves VAMPs 1-4, and Ykt6 in cells, and perturbs endocytic and secretory trafficking. Specifically, we have observed a significant reduction in transferrin uptake in intoxicated cells caused by the loss of the transferrin receptor from the cell surface and a dramatic block in the delivery of newly synthesised proteins to the plasma membrane. To establish if these phenotypes were due to R-SNARE proteolysis, we have generated cleavage resistant R-SNAREs and developed a simple genetic reconstitution assay to assess their function in post-Golgi trafficking. Using this approach we have identified an unexpected role for Ykt6 in transferrin receptor trafficking and uncovered roles for VAMPs 1-3 and 8 in the fusion of post-Golgi vesicles with the cell surface when the function of Ykt6 is disrupted. To further explore the utility of the genetic reconstitution assay, we have introduced a series of mutations into VAMP3 and investigated their impact on transferrin receptor trafficking. Introduction of the neurodevelopmental disease-causing proline substitution (S75P) from VAMP2 into VAMP3 abolishes VAMP3 function.

Introduction

SNARE proteins are core components of the machinery required for intracellular transport and membrane fusion (Söllner *et al.*, 1993). They have a highly conserved region termed the SNARE motif that forms complexes with other SNAREs (Jahn and Scheller, 2006). For membrane fusion to occur, SNAREs on opposing membranes must come together and zipper up to form a SNARE complex (Sutton *et al.*, 1998). SNAREs were originally classified as either vesicle associated, or target membrane associated SNAREs. However, they have been reclassified as either R or Q-SNAREs depending on the presence of a conserved arginine or glutamine in their SNARE motif (R-SNAREs are all v-SNAREs) (Kloepper, Kienle and Fasshauer, 2007). The biology of R-SNAREs have been studied extensively, and there is a good understanding of where these proteins are localised within the endomembrane system and biochemical evidence to support the pathways they act on (Jahn and Scheller, 2006). However, their disruption in cells and/or mice does not always yield the anticipated phenotypes (Bethani *et al.*, 2009; Gordon *et al.*, 2010). For example, mice lacking VAMPs 3, 4 and 7 are viable and have no gross abnormalities even though these R-SNAREs have been implicated in a range of key intracellular processes in which should be essential for viability (e.g. transferrin receptor recycling and iron uptake for VAMP3) (Yang *et al.*, 2001; Sato *et al.*, 2011; Ivanova *et al.*, 2021). One interpretation of these data is that the functions of the missing SNAREs are being replaced by the upregulation of other post-Golgi R-SNAREs. However, in most instances there seems to be little evidence to support this hypothesis (Gordon *et al.*, 2010). Thus, it is possible that alternative R-SNAREs not thought to function in post-Golgi trafficking, may be taking over their role and/or may normally act in this process. In support of this hypothesis, we have found that the Ykt6 may be playing this role. For example, we have observed that both Ykt6 and VAMP3 must be depleted to completely block delivery of biosynthetic cargo to the cell surface and that endosome-lysosome fusion can only be fully inhibited when the function of Ykt6 is disrupted in combination with VAMPs 7 and 8 (Davis *et al.*, 2021). Ykt6 is an unusual R-SNARE that does not have a proteinaceous membrane anchor like other R-SNAREs so is capable of cycling on and off membranes (McNew *et al.*, 1997; Fukasawa *et al.*, 2004). Thus, it is possible that Ykt6 is directly recruited to sites of membrane fusion without the need for intracellular trafficking.

Botulinum neurotoxins are produced by anaerobic bacteria and specifically inhibit neurotransmitter release through their cleavage of SNARE proteins. There are 7 well-characterised serotypes which have varying specificity for the SNARE molecules they cleave (BoNT/A and E target SNAP-25, BoNT/C targets syntaxin and SNAP-25, and BoNT/B, D, F and G target VAMPs1-3) (Pirazzini *et al.*, 2017). Due to their potency and specificity, they have been extensively used to dissect the role of SNAREs in regulated exocytosis (Schiavo *et al.*, 1992; Gaisano *et al.*, 1994; Steinhardt, Bi and Alderton, 1994; Regazzi *et al.*, 1995). Botulinum toxins have a highly conserved domain architecture that consists of a receptor binding domain, a translocation domain and a zinc dependent protease which cleaves SNAREs (also known as the light chain, LC). In 2017 a novel botulinum-like molecule was identified through a detailed bioinformatic analysis of published *C. botulinum* genomic sequences (Zhang *et al.*, 2017). The protein has the lowest sequence homology to any known toxin serotype and so was named BoNT/X. BoNT/X was shown to cleave a broad range of recombinant R-SNAREs (VAMPs 1-5 and Ykt6) in contrast to other R-SNARE cleaving toxins which can only cleave VAMPs 1-3 (Pirazzini *et al.*, 2017). The broader substrate specificity of BoNT/X not only allows the function of a wider range of SNAREs to be studied but also potentially increases the range of physiological processes which can be targeted by these toxins. The light chain of BoNT/X cleaves its substrates at a unique position which is found within the SNARE motif (VAMP3: R53-A54; VAMP4: K87-S88; Ykt6: K173-S174) (Zhang *et al.*, 2017). However, BoNT/X does not cleave recombinant VAMPs 7, 8 and Sec22b suggesting it has some degree of substrate specificity.

To elucidate the impact of BoNT/X intoxication on intracellular trafficking we have generated a tagged recombinant light chain and characterised its activity in cells. LC/X is capable of cleaving VAMPs 1-4 and Ykt6 in cells and leads to pleiotropic defects in both endocytic and biosynthetic transport. To determine if these phenotypes are specific to SNARE cleavage, we have developed a simple genetic reconstitution assay utilising SNAREs which are resistant to the action of the toxin. Using this approach we have observed that YKt6 appears to have an unexpected role in transferrin receptor trafficking and can rescue delivery of cargo to the plasma membrane. In addition, VAMPs 1-3 and 8 can also mediate the fusion of biosynthetic vesicles with the cell surface when Ykt6 has been lost from cells. This assay can also be used to dissect

mechanistic functions of SNAREs and disease-causing mutations, we have shown a neurodevelopmental disorder mutation in VAMP2 when introduced in VAMP3 causes loss of function. The use of this genetic reconstitution system should allow for new mechanistic insight into the role of R-SNAREs in post-Golgi trafficking and membrane fusion.

Materials

Antibodies and ligands

The following antibodies were used in this study: Rabbit anti-VAMP3, hamster anti-VAMP4, mouse anti-VAMP7, rabbit anti-VAMP8 were previously described in (Gordon *et al.*, 2010). An affinity-purified rabbit anti-Ykt6 was a gift from Dr Jesse C. Hay (University of Michigan) to A.A.P. as previously reported (Gordon *et al.*, 2010) and was raised against the peptide DGHLSRYQNPREADPMSKC. Rabbit anti-Sec22B (SySy - 186 003), Precision Protein StrepTactin-HRP conjugate (1:5000, Bio-Rad, 1610380), anti-GFP (Abclonal AE012, 1:2000), mouse anti-gamma adaptin (MAB100.3, prepared in-house), DyLight 800 Goat Anti-mouse secondary (ThermoFisher, SA5-35521, 1:5000), Anti-tubulin (Protein-tech, 66240-1-1g), Rat anti-RFP (Chromotek 5F8), mouse anti-CD71-APC (BD Biosciences, M-A712), APC anti-mouse CD63 (1:100, Biolegend, 143906), APC mouse anti-human CD8 (1:20, BD Biosciences, 555369), anti-human CD8 1:100 (Serotec, LT8 MCA1226), anti-mouse CD63 1:100 (Biolegend, NVG-2 143902), anti-HA (1:500, Biolegend, 901502), Cy™5 anti-mouse antibody (Jackson ImmunoResearch 115-175-146, 1:500). For immunofluorescence, secondary antibodies used were Donkey anti-mouse Alexa Fluor™ 647 (ThermoFisher, A-31571) and Goat anti-rat Alexa Fluor™ 594 (ThermoFisher, A-11007). Secondary HRP-conjugated antibodies for immunoblotting were HRP conjugated goat anti-mouse (1:5000, Jackson ImmunoResearch 115-035-008) and HRP conjugated goat anti-rabbit (1:5000, Jackson ImmunoResearch 111-035-144). The following ligands and markers were used: Wheat Germ Agglutinin AlexaFluor™ 647 (Invitrogen, W32466), Transferrin AlexaFluor ™ 647 and AlexaFluor™ 594 (Invitrogen T23366, T13343).

Plasmids

HA-tagged human R-SNARE and cleavage resistant versions of these constructs were synthesised by Genscript and cloned into pIRES-Neo2. The MAO tagged human R-SNAREs and cleavage resistant versions of these constructs were synthesised by Genscript and cloned into eGFP-C3 (Clontech). The light chains of BoNT/D and X (active and inactive) were synthesised by Genscript and cloned into eGPF-C3 (Clontech). mCherry and non-fluorescent versions of BoNT/X were then generated by replacing the eGFP with either mCherry, miRFP670 or a StrepII tag. For full list/details of plasmids used, see Supplemental Table 1.

Methods

Cell culture and plasmid transfections

HeLa-M and HEK-293T cells were cultured and maintained in high glucose DMEM media (Sigma) supplemented with 10% fetal bovine serum, 100 IU/mL penicillin, 100 µg/mL streptomycin and 2 mM glutamine at 37℃ in a 5% CO_2 humidified incubator. HeLa-C1 cells (Gordon *et al.*, 2010) and HA-Ykt6^{VT} stable cells were maintained with the addition of the appropriate antibiotic selection, 1 µg/mL puromycin and 1 mg/mL G418 respectively. The Cherry-VAMP stable cells were maintained with the addition of G418. Plasmids were transfected into cells using either polyethylenimine (PEI) (3 µg PEI to 1 µg plasmid DNA) or Lipofectamine 2000 (1.25:1 Lipofectamine 2000 to plasmid DNA).

Stable cell line generation

Stable cell lines expressing mCherry-VAMPs were generated by transfecting HeLa-M cells with mCherry VAMPs 3, 4, 7 and 8 and selecting the cells with G418 for 2 weeks. mCherry positive cells were autocloned using flow cytometry and screened for expression. Cells with moderate expression were selected. HA-tagged Ykt6^{VT} was synthesised by GenScript and cloned into the retroviral expression vector pLXIN (Clontech). HEK-293T cells were transfected with the pLXIN construct, puMVC (Addgene) and pCMV VSV-G (Addgene) using PEI. The cell culture media was collected 48 hours post-transfection, polybrene was added (5 µg/mL) and filtered using a 0.45 µm syringe filter (Sartorius). HeLa-M cells were infected with the retrovirus particles and centrifuged at 2000 x g for 1 hour at room temperature, prior to incubation

at 37℃. Post-transduction, cells were placed into G418 selection (Roche) and auto-cloned into a 96 well plate using a FACSMelody cell sorter (BD Biosciences). Clonal cell lines were screened for expression by staining with an anti-HA antibody.

Immunoblotting

R-SNARE cleavage blots

HeLa-M cells were transfected with either GFP, GFP-LC/X WT or GFP-LC/X inactive using Lipofectamine2000 transfection reagent. Cells were trypsinised prior to sorting for GFP-positive cells using a FACSMelody cell sorter (BD Biosciences). The sorted cells were collected, and approximately 160,000 GFP-positive cells were used per sample. Sorted cells were lysed in SDS-PAGE sample buffer (Bio-Rad) supplemented with 5% (v/v) mercaptoethanol and boiled at 95℃, prior to separation using SDS-PAGE gel electrophoresis. Proteins were then transferred overnight onto PVDF membranes using wet transfer methods. The membranes were blocked using 5% milk in 1X PBS-Tween20. The membranes were probed with antibodies against R-SNAREs and beta tubulin (loading control). The bound antibodies were detected using secondary antibodies conjugated to HRP and developed using ECL substrate. Membranes were imaged using LI-COR C-DiGit® blot scanner (LI-CORE Biosciences) and Image Studio Lite Software (LI-COR Biosciences).

VAMP-MAO blots

HEK-293T cells were transfected with various VAMP-MAO constructs with or without StrepTag-LC/X (9:1) using PEI. Cells were collected post-transfection and lysed in SDS-PAGE sample buffer (Bio-Rad). The lysates were boiled at 95℃ prior to separation by SDS-PAGE gel electrophoresis. Proteins were transferred overnight onto nitrocellulose membranes by wet transfer. The membranes were blocked using 5% milk in 1X PBS-Tween20. The membranes were probed with antibodies against GFP and gamma adaptin. Secondary antibodies conjugated to DyLight 800 were used to detect the primary antibodies. A HRP-conjugated StrepTactin (Bio-Rad) was used to detect the StrepTagged BoNT/X. StrepTactin-HRP blots were developed using ECL substrate (Bio-Rad). Membranes were imaged using LI-COR C-DiGit® blot scanner (LI-COR Biosciences) and LI-COR OdysseySA imaging system (LI-COR

Biosciences). Images were obtained using the Image Studio Lite Software (LI-COR Biosciences).

Fluorescence microscopy and image analysis

Cells were grown on glass coverslips overnight prior to transfection. Cells were fixed in 4% paraformaldehyde (PFA) 1 day post-transfection, the PFA was quenched using 0.1 M Glycine, then washed with PBS. The coverslips were mounted on microscope slides using ProLong Gold antifade mountant (Invitrogen). Images were captured using a Nikon A1 confocal microscope with a 60x Plan Apochromat oil objective lens.

VAMP-MAO microscopy

HeLa-M cells that stably express HA-Ykt6^{VT} were seeded onto glass coverslips and co-transfected with the indicated VAMP-MAO constructs and mCherry-LC/X using PEI. Cells were fixed, mounted onto glass slides using ProLong Gold antifade mountant (Invitrogen).

Immunolabeling for microscopy

PFA fixed cells were permeabilised using 0.1% saponin (Sigma S4521), 1% BSA (Fisher Scientific) solution in PBS (IF buffer), prior to incubating with the appropriate primary and secondary antibodies. Coverslips were washed with PBS and mounted onto microscope slides using ProLong Gold antifade mountant (Invitrogen).

Transferrin uptake microscopy

Cells were incubated with transferrin-Alexa Fluor™ 647 (25 µg/mL, Invitrogen) for 10 minutes at 37℃, washed with media then fixed with 4% paraformaldehyde. The coverslips were mounted as above using ProLong Gold. Images were captured using an Olympus BX61 wide-field epifluorescence microscope with a 60x UplanApo oil immersion objective lens.

CD8 and CD63 surface-labelling

HeLa-M cells expressing either CD8 or CD63 were chilled on ice and incubated with the indicated antibodies diluted in ice cold media for 30 minutes. Coverslips were washed using cold media prior to fixation with 4% PFA. Cells were quenched with 0.1

M glycine in PBS and washed with PBS. Cells were permeabilised in IF buffer, prior to incubation for 30 minutes at room temperature with the appropriate secondary antibody diluted in IF buffer. Coverslips were washed with PBS and mounted onto glass slides using ProLong Gold mountant (Invitrogen). Representative images were captured using an Olympus BX61 wide-field epifluorescence microscope. The images were analysed using ImageJ (Schindelin *et al.*, 2012), and the brightness/contrast were also adjusted.

Flow cytometry assays

Cell viability

HeLa-M cells were transfected with either GFP, GFP-LC/X active or inactive constructs. 16 hours post transfection the cells were trypsinised and stained with TO-PRO®-3 according to manufacturer's instructions. Data was acquired using a LSRII flow cytometer (BD Biosciences).

Transferrin uptake

HeLa-M cells were seeded in 12 well plates prior to transfection using PEI or Lipofectamine 2000. 16 hours post-transfection, cells were trypsinised and pelleted by centrifugation at 1500 rpm. The cells were resuspended in Transferrin Alexa Fluor™ 647 (Invitrogen) diluted in fresh media (25 µg/mL) and incubated for 10 minutes at 37℃. Cells were washed twice with fresh chilled media and resuspended in 1% PFA. Mean fluorescence intensity was measured using an LSR II cytometer (BD Biosciences) or an Attune NXT cytometer (ThermoFisher).

Cell membrane protein surface labelling

To label membrane proteins at the cell surface, cells were incubated with the appropriate antibody at 4℃ for 30 minutes prior to washing and fixation.

Secretory reporter assay

Secretory reporter cells (HeLa-C1) were transfected with mCherry-LC/X and HA-tagged R-SNAREs. Cells were incubated with 1 µM rapamycin for 120 minutes prior to trypsinisation. Cells were placed on ice in suspension to pause secretion. Mean fluorescence intensity was measured using an Attune NxT flow cytometer (Thermo Fisher Scientific). Cells expressing mCherry constructs were gated prior to quantifying

GFP fluorescence. Percentage of secreted cargo was calculated by taking a ratio between rapamycin treated and untreated samples.

Intracellular protein labelling

Transfected HeLa-M cells were trypsinised prior to fixation with 4% paraformaldehyde. The PFA was quenched using 0.1 M Glycine before the cells were permeabilised with 1X PBS containing 0.1% saponin and 1% BSA. The cells were incubated with the appropriate antibody diluted in the permeabilisation buffer for 45 minutes. For non-conjugated primary antibodies, cells were washed with the permeabilisation buffer prior to incubation with the appropriate secondary antibody for 45 minutes. Cells were resuspended in 1% PFA. Mean fluorescence intensity of the cells was measured by flow cytometry.

Statistics and analysis

GraphPad Prism version 9 for Windows (GraphPad Software, Boston, MA, USA) was used for plotting all graphical data included in figures and the associated statistical analysis (Meiringer *et al.*, 2008). FlowJo™ v10.8 Software (BD Life Sciences) was used to display flow cytometry data and calculate the mean and geometric mean fluorescence intensity.

Results

The recombinant LC of BoNT/X is active and cleaves VAMPs 3, 4 and Ykt6

It has previously been reported that the light chain of BoNT/X can cleave recombinant VAMPs 1-5; Ykt6, and endogenous VAMPs 2 and 4 in vivo (Zhang *et al.*, 2017). Thus, it could potentially be a novel tool for investigating that function of R-SNAREs in intracellular transport. To investigate the activity and specificity of the toxin in vivo we synthesised a GFP-tagged version of the light chain (residues 1-439aa), which was tagged with eGFP. As a control, an inactive form of the LC/X was also made by mutating Arg360 and Tyr363 (R360A/Y363F) (Zhang *et al.*, 2017). HeLa-M cells stably expressing mCherry-tagged R-SNAREs (VAMP3, VAMP4, VAMP7, VAMP8) were transiently transfected with the indicated light chain constructs and microscopy performed (**Figure 1A**, **Supplemental Figure 1**). In the cells transfected with the active BoNT/X construct, the signal for VAMP3 and VAMP4 were reduced and became

predominantly cytoplasmic, whereas the levels and/or localisation of VAMP7 and VAMP8 were not affected. As expected, an inactive version of the BoNT/X LC has no impact on the levels of VAMP3 or its localisation. To determine whether BoNT/X can cleave endogenous R-SNAREs cells were transfected with the indicated constructs, enriched using cell sorting and analysed by immunoblotting against a panel of well characterised R-SNARE antibodies (**Figure 1B**). As expected, the levels of VAMP3 and VAMP4 were greatly reduced in the cells expressing the active construct. In addition, a lower molecular weight band for Ykt6 was observed, suggesting that the protein had been proteolytically cleaved. No loss of signal was observed for VAMP7, VAMP8 or Sec22B, indicating that they are not cleaved by the LC/X and the specificity of the toxin had not been altered by the tag. It is likely that HeLa-M cells also express VAMP2 (Kubo *et al.*, 2015) which is cleaved by the light chain of BoNT/X. However, due to technical difficulties we are unable to detect this R-SNARE by immunoblotting.
In performing these experiments, it was noticed that there were fewer cells in samples transfected with the active light chain. To directly quantify this, the cell number and cell viability was measured using an automatic cell counter and flow cytometry (**Figure 1C and D**). In samples transfected with BoNT/X there was no significant drop in cell viability after 16 hours. However, there was a significant decrease in cell number suggesting that there may be a reduction in cell proliferation in intoxicated cells.

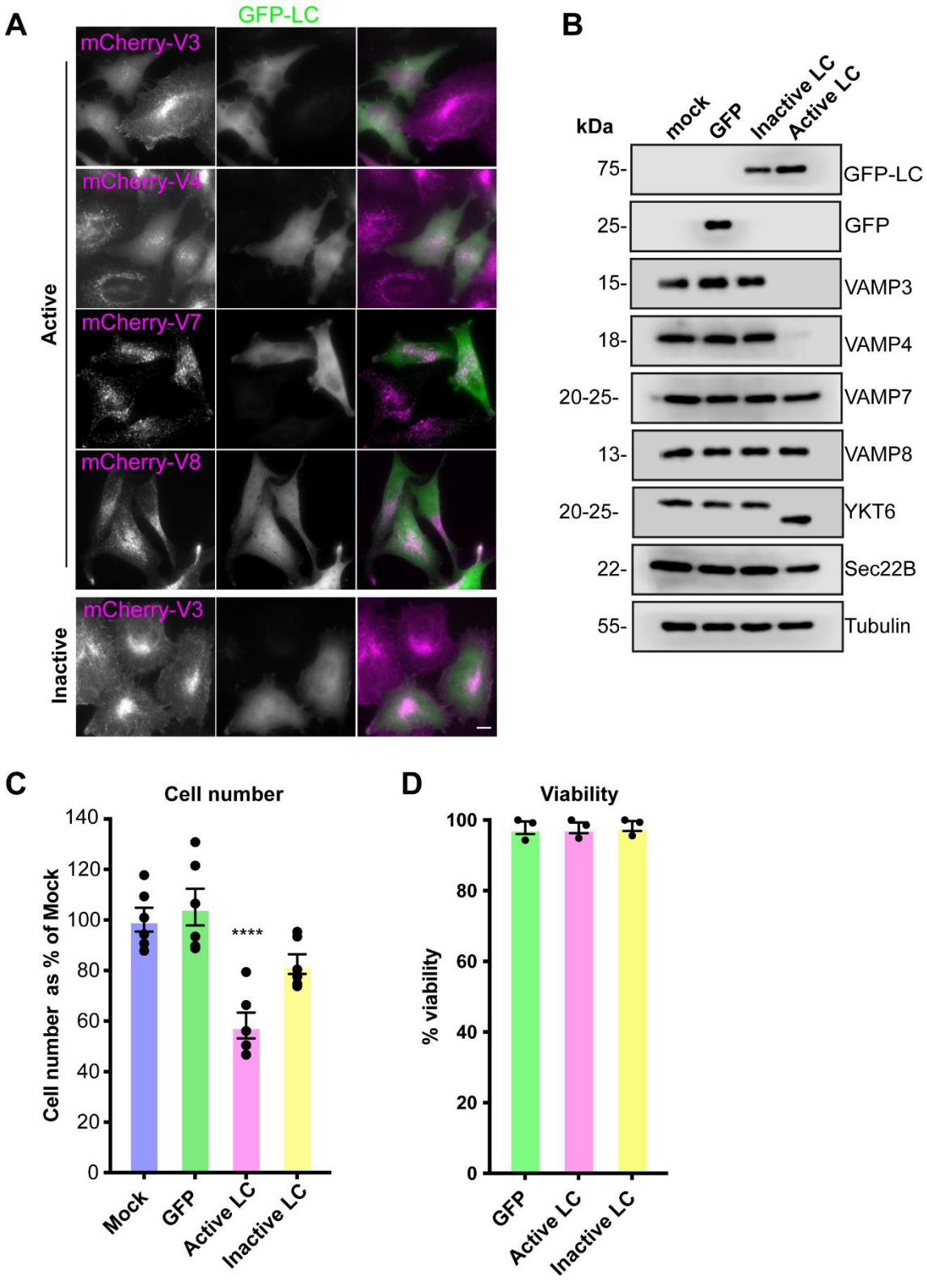

Figure 1. The recombinant LC of BoNT/X is active and specifically cleaves VAMPs 3, 4 and Ykt6

(**A**) HeLa-M cells expressing mCherry-tagged VAMPs were grown on coverslips and transiently transfected with either active or inactive light chain of BoNT/X tagged with

GFP. Cells were fixed and representative images captured. Scale bar = 10 µm. (**B**) HeLa-M cells were transiently transfected with either GFP, GFP-LC/X active or inactive constructs. GFP-positive cells were sorted using flow cytometry, lysed in SDS-PAGE sample buffer and transferred to PVDF membranes. Blots were probed with antibodies against GFP, VAMP3, VAMP4, VAMP7, VAMP8, Ykt6 and Sec22B. Tubulin was used as a loading control. (**C, D**) HeLa-M cells were transfected with either GFP, GFP-LC/X active or inactive or constructs, the cell number and cell viability measured 16 hours post-transfection. An automatic cell counter was used for cell number estimation (n=5). One-way ANOVA with Dunnett's multiple comparison was performed for analysis, **** $P<0.0001$. To assess cell viability, cells were stained with TO-PRO®-3 prior to acquisition by flow cytometry (n=3). Error bars show SEM.

Expression of the BoNT/X light chain perturbs the trafficking of the TF-R

The immunoblotting data suggests that BoNT/X can cleave a broad number of R-SNAREs in HeLa-M cells (VAMPs (2) 3, 4 and Ykt6) so it is likely that there will be significant alterations in intracellular trafficking. To investigate this, cells were transfected with the light chain of BoNT/X and the uptake of fluorescent transferrin assessed using immunofluorescence microscopy and flow cytometry (**Figure 2A and B**). In intoxicated cells, almost no detectable transferrin uptake was observed. To check that this phenotype was specific to BoNT/X and its broader substrate specificity we transfected cells with BoNT/D light chain constructs which were GFP tagged. BoNT/D only cleaves VAMPs 2 and 3 (Yamasaki *et al.*, 1994 and **Supplemental 1**). In BoNT/D intoxicated cells no significant alteration in transferrin uptake was observed (**Figure 2C**) suggesting that it is likely to be the additional loss of VAMP4 and/or Ykt6 which is causing this phenotype.

To determine if this reduction of transferrin uptake is due to a loss of the transferrin receptor (TF-R) from the cell surface, its localisation and levels were determined using fluorescence microscopy and flow cytometry (**Figure 2D-G**). In control cells the receptor is present in a perinuclear pool and punctate structures dispersed throughout the cytoplasm, most likely early and recycling endosomes (van der Sluijs *et al.*, 1992; Ullrich *et al.*, 1996). However, in intoxicated cells there was a dramatic reduction in signal accompanied with a clear alteration in its localisation (**Figure 2D**). In support of this observation the levels of the receptor were also dramatically reduced at the cell

surface (**Figure 2E**) suggesting a possible block in the delivery and/or recycling of the receptor with the cell surface. As expected, BoNT/D intoxication did not alter the surface levels of the TF-R (**Figure 2F**) indicating that the observed phenotypes are BoNT/X specific. To further explore the impact of BoNT/X on TF-R trafficking, the total levels of the receptor were also measured using flow cytometry (**Figure 2G**). In the intoxicated cells there was a significant reduction in the receptor levels, possibly indicating a misrouting of the receptor to lysosomes.

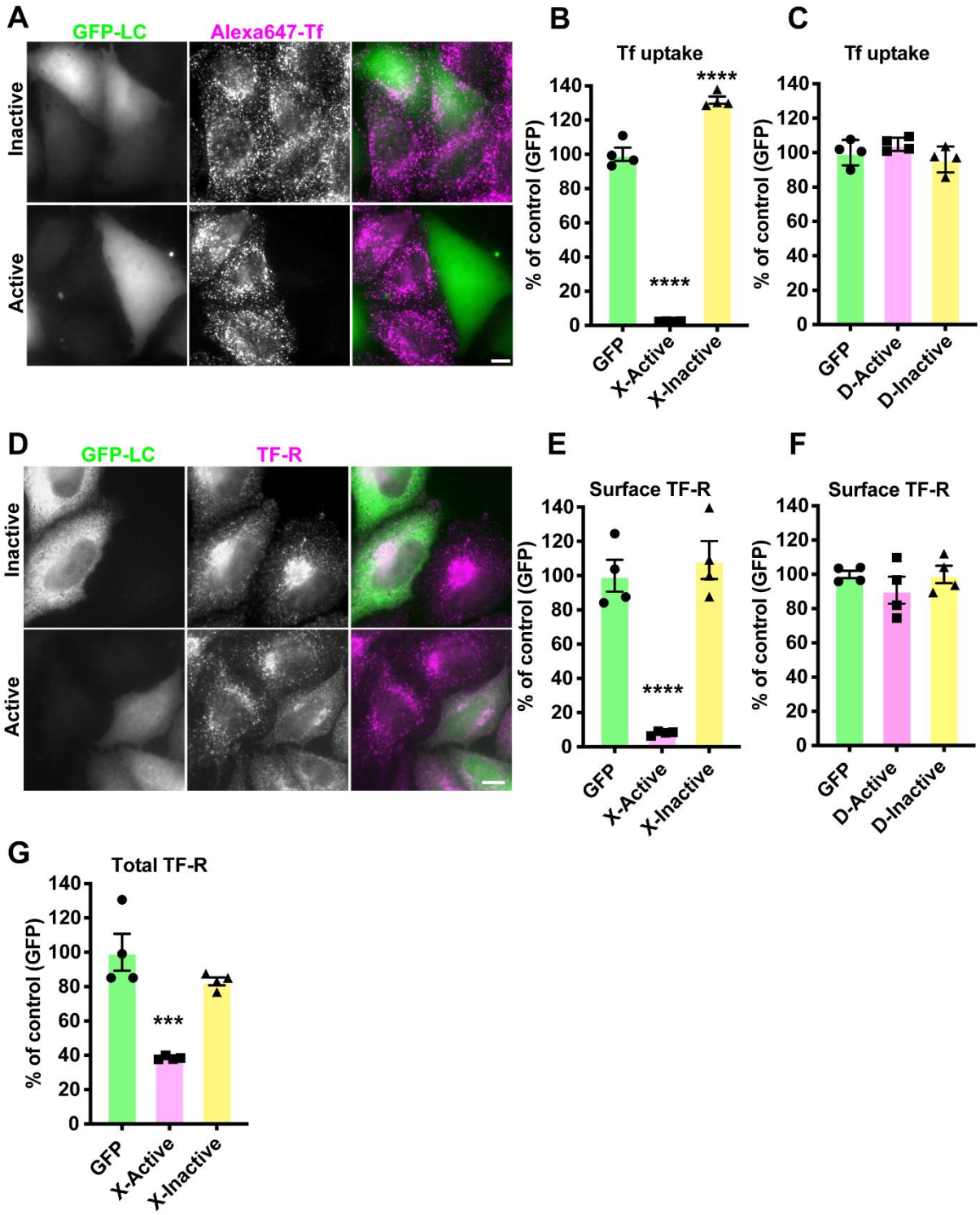

Figure 2. The LC of BoNT/X is a potent inhibitor of Transferrin receptor trafficking

(**A**) To determine the effect of BoNT/X on receptor-mediated endocytic trafficking, HeLa-M cells were grown on glass coverslips and transiently transfected with either active or inactive BoNT/X constructs tagged with GFP. The cells were then incubated with Transferrin Alexa Fluor™ 647 for 10 minutes at 37℃. The cells were fixed using

4% PFA and representative images captured. Scale bar = 10 µm. (**B**) To quantify the amount of transferrin taken up by the transfected cells, the experiments were repeated in suspension and the mean fluorescent intensity of the cells measured using flow cytometry (n=4). The amount of transferrin internalised by the cells was normalised to the GFP control. Error bars represent SEM. One-way ANOVA with Dunnett's multiple comparison was performed for analysis, **** P<0.0001. (**C**) To determine if this phenotype was specific to BoNT/X intoxication, HeLa-M cells were transfected with either the active or inactive GFP tagged light chain of BoNT/D and the transferrin uptake assay repeated as above. The amount of transferrin internalised by the cells was normalised to the GFP control. Error bars represent SEM. (**D**) To determine if BoNT/X intoxication impacts the localisation of the transferrin receptor (TF-R) HeLa-M cells were transfected with either active or inactive BoNT/X constructs tagged with GFP. Cells were fixed with 4% PFA and permeablised with IF buffer, prior to staining with anti-CD71 antibody for 30 minutes at 4℃. Cells were then washed with PBS and representative images captured. Scale bar = 10 µm. (**E**) To measure the levels of TF-R on the cell surface, HeLa-M cells were transfected with either the active or inactive versions of BoNT/X LC. Cells were harvested and stained with the anti-TF-R (CD71) antibody at 4℃. Cells were then fixed, and the mean fluorescent intensity of the cells were measured by flow cytometry (n=4). Error bars represent SEM. One-way ANOVA with Dunnett's multiple comparison was performed for analysis, **** P<0.0001. (**F**) As a control, surface levels of transferrin receptor were measured with HeLa-M cells transfected with active or inactive BoNT/D constructs by flow cytometry (n=4). Error bars represent SEM. (**G**) To measure the total TF-R levels, cells were transfected with active and inactive BoNT/X LC, fixed and permeabilised prior to staining with anti-CD71. Mean fluorescent intensity of the cells were measured by flow cytometry (n=4). One-way ANOVA with Dunnett's multiple comparison was performed for analysis, *** P= 0.0001. Error bars show SEM.

BoNT/X intoxication blocks the delivery of newly synthesised membrane proteins to the cell surface

To determine if the trafficking of newly synthesised membrane proteins to the cell surface was perturbed in BoNT/X intoxicated cells, the localisation of transiently transfected GFP tagged CD8 and GFPSpark CD63 was assessed by microscopy and flow cytometry (**Figure 3**). CD8 is a transmembrane glycoprotein that localises to the

surface of T cells and is not expressed in HeLa-M cells. CD63 is an endosomal/lysosomal protein that actively traffics to the cell surface so can also be used to measure biosynthetic transport. To be able to specifically detect transfected CD63, murine CD63 and a species specific antibody was used. As both reporter constructs were GFP tagged, a non-fluorescent version of the BoNT/X LC was used. In cells transfected with the inactive toxin, there was strong plasma membrane staining for both CD8 and CD63 suggesting that the reporter constructs were efficiently delivered to the cell surface. However, in the intoxicated cells, the surface staining was dramatically reduced and strong intracellular labelling reminiscent of the ER and Golgi was observed suggesting that the constructs were becoming trapped in the early biosynthetic pathway. To quantitatively measure the levels of CD8 and CD63 at the cell surface, the experiments were repeated, and flow cytometry performed. As expected, the levels of CD8 and CD63 were significantly reduced in the intoxicated cells compared to that of the inactive control. To determine if the delivery of soluble biosynthetic cargo to the plasma membrane was also perturbed in the BoNT/X intoxicated cells the experiments were repeated using reporter assay previously developed by our group (Gordon *et al.*, 2010) (**Figure 3E**). In this assay, the secretion of GFP is regulated by the addition Rapamycin or AP21998 which controls the oligomerisation state of the reporter molecule (Gordon *et al.*, 2021). In intoxicated cells, we observed that there was almost no secretion of the reporter construct as measured by flow cytometry suggesting that BoNT/X intoxication blocks the transport of soluble cargo to the cell surface.

As we observed a significant reduction in the cell surface levels of the TF-R, CD8, CD63 and a block in the delivery of soluble cargo to the cell surface we wondered whether BoNT/X intoxication could be having a more global impact on the levels of cell surface receptors. To test this hypothesis, we measured the amount of wheat germ agglutinin (WGA) binding to the cell surface of transfected cells. WGA is a lectin that binds glycosylated proteins so should provide an estimate of the cell surface levels of any glycosylated protein (**Figure 3F**). WGA binding was reduced by approximately 50% in BoNT/X intoxicated cells compared to either GFP or the inactive control. These results suggest that there is a global change in the levels of glycosylated proteins at the cell surface in intoxicated cells.

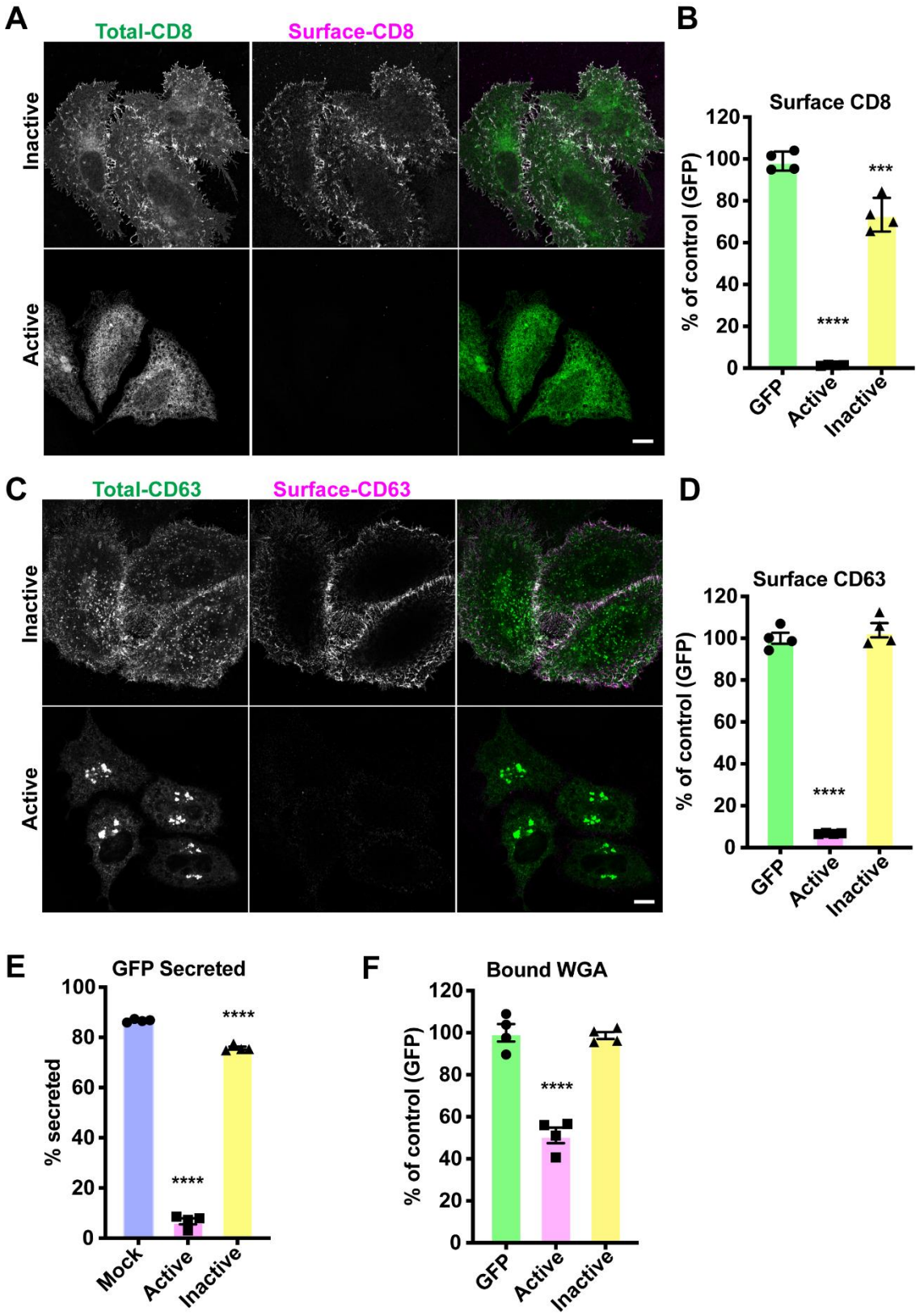

Figure 3. The LC of BoNT/X blocks the transport of a wide range of proteins to the cell surface

(**A**) To determine if BoNT/X blocks the delivery of CD8 to the cell surface, HeLa-M cells were grown on coverslips and co-transfected with active or inactive BoNT/X and

eGFP-CD8α. To detect surface expression of CD8 the cells were labelled with the anti-CD8 antibody at 4℃ prior to fixation. Scale bar = 10 μm. (**B**) The surface levels of CD8 were also measured by flow cytometry by collecting the cells in suspension prior to staining with anti-CD8-APC. Mean fluorescence intensity was calculated and normalised to the GFP control. Error bars represent the SEM. One-way ANOVA with Dunnett's multiple comparison was performed for analysis, *** P=0.0002, **** P<0.0001. (**C**) To determine if BoNT/X blocks the delivery of CD63 to the cell surface, HeLa-M cells were grown on coverslips and co-transfected with the active or inactive BoNT/X and murine CD63-GFP. To detect surface expression of CD63 the cells were labelled with a mouse-specific anti-CD63 antibody at 4℃ prior to fixation. Scale bar = 10 μm. (**D**) Surface levels of CD63 were measured by flow cytometry by collecting the cells in suspension prior to staining with anti-CD63-APC. Mean fluorescence intensity was calculated and normalised to the GFP control. Error bars represent the SEM. One-way ANOVA with Dunnett's multiple comparison was performed for analysis, **** P<0.0001. (**E**) To determine the effects of LC/X intoxication on secretion, secretory reporter cells were transfected with mCherry-tagged active and inactive BoNT/X LC. Post-transfection, the cells were trypsinised and treated with 1 μM Rapamycin for 120 minutes at 37℃. Mean fluorescence intensity was determined by flow cytometry. Error bars represent the SEM. One-way ANOVA with Dunnett's multiple comparison was performed for analysis, **** P<0.0001. (**F**) To measure WGA binding at the cell surface, BoNT/X LC transfected cells were incubated with WGA at 4℃ prior to being washed and fixed. Mean fluorescence intensity was measured by flow cytometry (n=4). One-way ANOVA with Dunnett's multiple comparison was performed for analysis, **** P<0.0001.

Development of BoNT/X resistant R-SNAREs

It has previously shown that SNAREs can be made resistant to the action of botulinum and tetanus toxins by altering residues at their cleavage sites (Pellizzari *et al.*, 1996; Regazzi *et al.*, 1996; Peng *et al.*, 2013). Thus, to determine if the phenotypes caused by BoNT/X intoxication are caused by the cleavage of R-SNAREs and to develop new tools for studying SNARE function we have developed cleavage resistant R-SNAREs. BoNT/X cleaves its target R-SNAREs at a novel site compared to other BoNTs; VAMPs 4, 5 and Ykt6 are cleaved between highly conserved lysine and serine (KS)

residues and VAMPs 1-3 are cleaved between arginine and alanine (RA) (**Figure 4A**). In the first instance we swapped the cleavage site residues to lysine and threonine (KT) as they are found in VAMP8 which is not cleaved by the toxin. Unfortunately, this substitution was not resistant to cleavage (**Supplemental Figure 2**). We also tested a series of additional mutations with limited success (QA, AA, HA). We then tried substituting the residues to VW, a change which protects VAMP2 against the action of tetanus toxin (Regazzi *et al.*, 1996; Randhawa *et al.*, 2000). This change partially protected VAMP3 from BoNT/X cleavage (**Supplemental Figure 2A**). Finally, we substituted the residues to valine and threonine (VT) which gave VAMP3 protection against BoNT/X (**Supplemental Figure 2A**).

To confirm these preliminary observations, we developed a simple microscopy-based assay for measuring SNARE cleavage. In this assay GFP tagged R-SNAREs are anchored to the surface of mitochondria using the targeting domain of a monoamine oxidase (MAO) and in the presence of the toxin the GFP is cleaved from the reporter molecule and becomes cytoplasmic (**Figure 4A**). The mitochondrially anchored VAMP3, VAMP4 and Ykt6 are efficiently cleaved when incubated with LC/X, resulting in a cytoplasmic GFP signal (**Figure 4B**). The VT mutation in VAMP3 and Ykt6 appears to offer good levels of protection against this cleavage and remain localised to mitochondria. To support these observations the experiments were repeated by immunoblotting (**Figure 4C**). Interestingly, VAMP4^{VT}only has partial resistance to the action of BoNT/X. In cells expressing high levels of the toxin, GFP becomes cytosolic and there is an appearance of a faint lower molecular weight band in the GFP immunoblot suggesting the construct is becoming cleaved.

BoNT/X resistant R-SNAREs are capable of rescuing BoNT/X intoxication

To determine if VT versions of the SNAREs were functional and can rescue BoNT/X intoxication we co-transfected HA-tagged VAMP3^{VT}, VAMP4^{VT} and Ykt6^{VT} with BoNT/X LC and measured transferrin uptake (**Figure 4D**). Cells overexpressing VAMP3^{VT} were able to partially rescue transferrin uptake and Ykt6^{VT} rescued this phenotype to levels comparable to the mock transfected cells. However, VAMP4^{VT} failed to restore transferrin uptake. In parallel, we also tested VAMP3^{KT} and Ykt6^{VW}. Neither construct was able to rescue transferrin uptake suggesting that the constructs are either still cleaved by the toxin and/or are non-functional (**Supplemental Figure**

2B and C). We also determined whether the VT SNAREs could also rescue the surface and total levels of the TF-R (**Figure 4E and F**). Ykt6^{VT} effectively rescued the surface levels of the receptor but only partially rescued its total levels suggesting that the trafficking of the receptor had not been fully rescued by expression of the individual SNAREs.

Based on these results, we wondered whether we would be able to use this approach to investigate the function of other R-SNAREs. In particular, it is still not fully understood which R-SNAREs act in the delivery of material to the cell surface (Antonin *et al.*, 2000; Miller *et al.*, 2011; Kubo *et al.*, 2015). Work from other labs have implicated VAMPs 2, 3, 7 and 8 as potentially having a role in this process. However, the loss of these SNAREs either through genetic disruption or RNAi based approaches does not dramatically impact this process. Thus, we generated a library of HA tagged R-SNAREs (VAMPs 1-5, 7, 8, Sec22B and Ykt6) resistant to BoNT/X. These SNAREs were then co-transfected into HeLa-M cells with LC/X and the amount of transferrin taken up by the cells measured. As expected, expression of VAMP3^{VT} and Ykt6^{VT} significantly enhanced transferrin uptake in the intoxicated cells. In addition, VAMP2^{VT} and VAMP8 also were able to partially rescue this process. In support of these findings, we also observed that these SNAREs significantly increased the cell surface levels of the TF-R (**Figure 5E**). To confirm that all the R-SNARE constructs were being expressed in the intoxicated cells we performed intracellular HA staining (**Supplemental 3A**). All of the constructs were co-expressed with the GFX-LC/X (**Supplemental Figure 3B**). However, the levels of HA-Sec22B and HA-VAMP7 were relatively low compared to the other SNAREs. To extend these observations, we looked at the surface levels of CD8, CD63 and the total levels of surface proteins using WGA (**Figure 5C, D and E**). The VT versions of VAMPs 2, 3, 8 and Ykt6 all significantly increased the amount of WGA binding to the intoxicated cells. Similar results were also observed for CD8 and CD63, except VAMP1^{VT} was also able to increase the amount of these proteins at the cell surface.

To gain a more mechanistic understanding of the role of Ykt6 in this process, we also investigated a truncated version of Ykt6 lacking its C-terminal lipid modifications (Ykt6^{VTD}) (Fukasawa *et al.*, 2004). The truncated version of Ykt6 was unable to rescue BoNT/X intoxication suggesting that the protein must be bound to membranes to function correctly. As an additional control, we also investigated the impact of co-

expressing the non-cleavage resistant version of Ykt6. Surprisingly, this construct was able to partially rescue the surface levels of CD8 and CD63 suggesting that some of the protein may remain uncleaved if it is expressed at high enough levels.

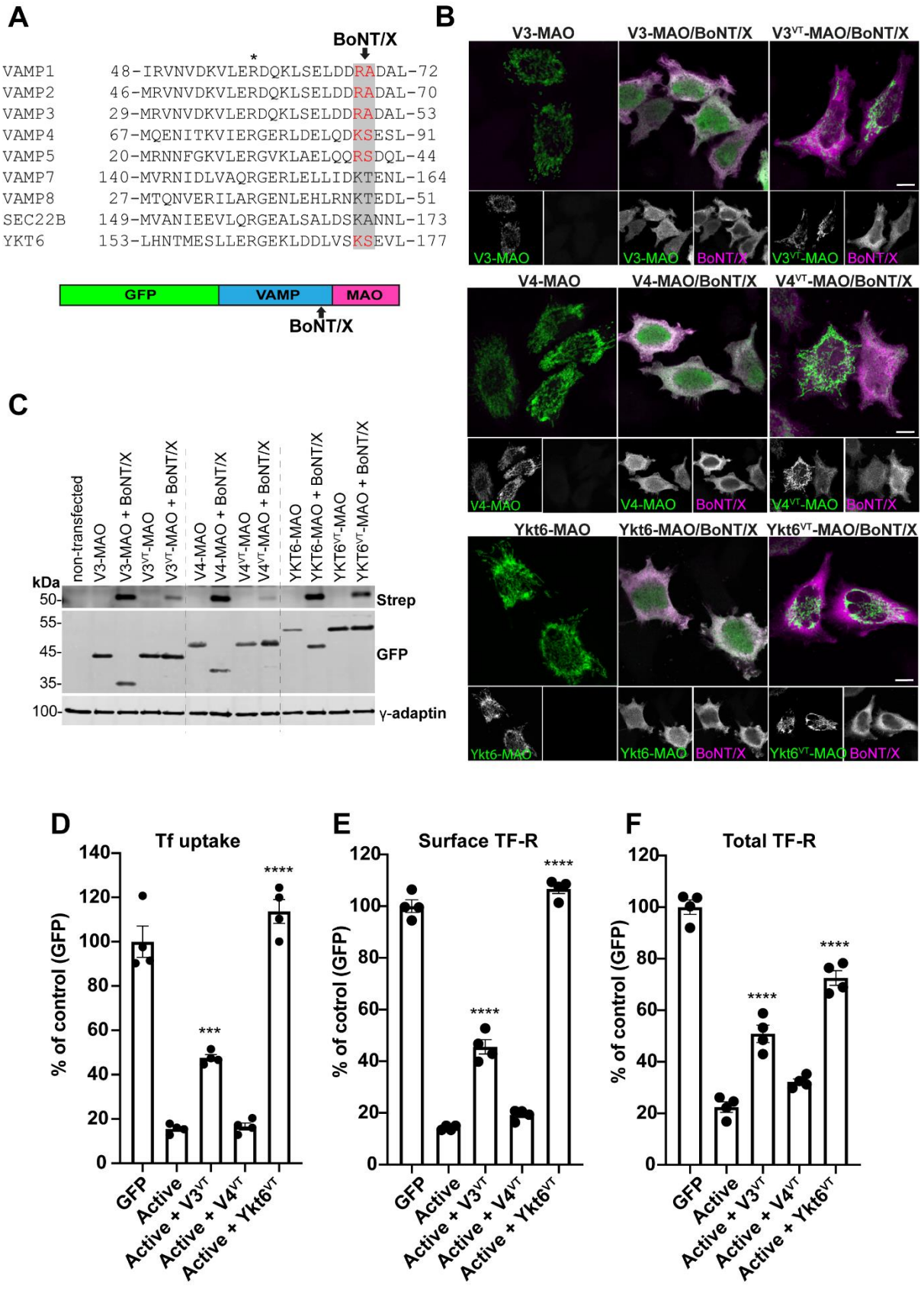

Figure 4. R-SNAREs can be engineered to have resistance to BoNT/X

(**A**) Sequence alignment of human R-SNAREs showing the BoNT/X cleavage site in red (* shows position of conserved arginine (R) in the middle of the SNARE domain).

A schematic of the VAMP-MAO reporter constructs used to measure SNARE cleavage. When the reporter construct is cleaved by BoNT/X, GFP is released into the cytoplasm. (**B**) To determine if the VT substitutions provide protection against the action of BoNT/X the indicated VT constructs were co-transfected into HeLa-M cells with mCherry-LC/X. The next day the cells were fixed using 4% PFA and representative images acquired using a confocal microscope. To make the imaging easier to perform HeLa-M cells stably expressing HA-Ykt6^{VT} were used. (**C**) HEK-293T cells were transfected with indicated VAMP-MAO constructs with and without StrepTag-LC/X. The next day, cell extracts were prepared from the cells and immunoblotting performed. Membranes were probed for GFP and StrepTactin. Gamma adaptin was used as a loading control. (**D**) To establish if cleavage-resistant R-SNAREs or overexpression could rescue the phenotype resulting from LC/X intoxication, HeLa-M cells were co-transfected with GFP-BoNT/X LC and HA-VAMP3^{VT}, VAMP4^{VT} or Ykt6^{VT}. Cells were collected and incubated with transferrin-Alexa™ 647 at 37℃ for 10 minutes prior to washing and fixation. The mean fluorescent intensity of the cells was measured by flow cytometry (n=4). The amount of transferrin internalised by the cells was normalised to the GFP control. One-way ANOVA with Dunnett's multiple comparison was performed for analysis, compared to the Active LC/X, *** P=0.0002, **** P<0.0001. Error bars represent the SEM. (**E**) The cell surface levels of transferrin receptor (TF-R) were measured on the transfected cells by incubating the cells with anti-TF-R APC at 4℃ for 30 minutes. The cells were washed, fixed using 4% PFA and the mean fluorescence intensity measured by flow cytometry (n=4). One-way ANOVA with Dunnett's multiple comparison was performed for analysis, compared to the Active LC/X, **** P<0.0001. Error bars represent the SEM. (**F**) The total TF-R levels were measured on the transfected cells by fixing the cells with 4% PFA, permeabilising them using 0.1% saponin and incubating them with an anti-TF-R APC labelled antibody for 30 minutes. The cells were washed several times, and the mean fluorescent intensity was measured by flow cytometry (n=4). One-way ANOVA with Dunnett's multiple comparison was performed for analysis, compared to the Active LC/X, **** P<0.0001. Error bars represent the SEM.

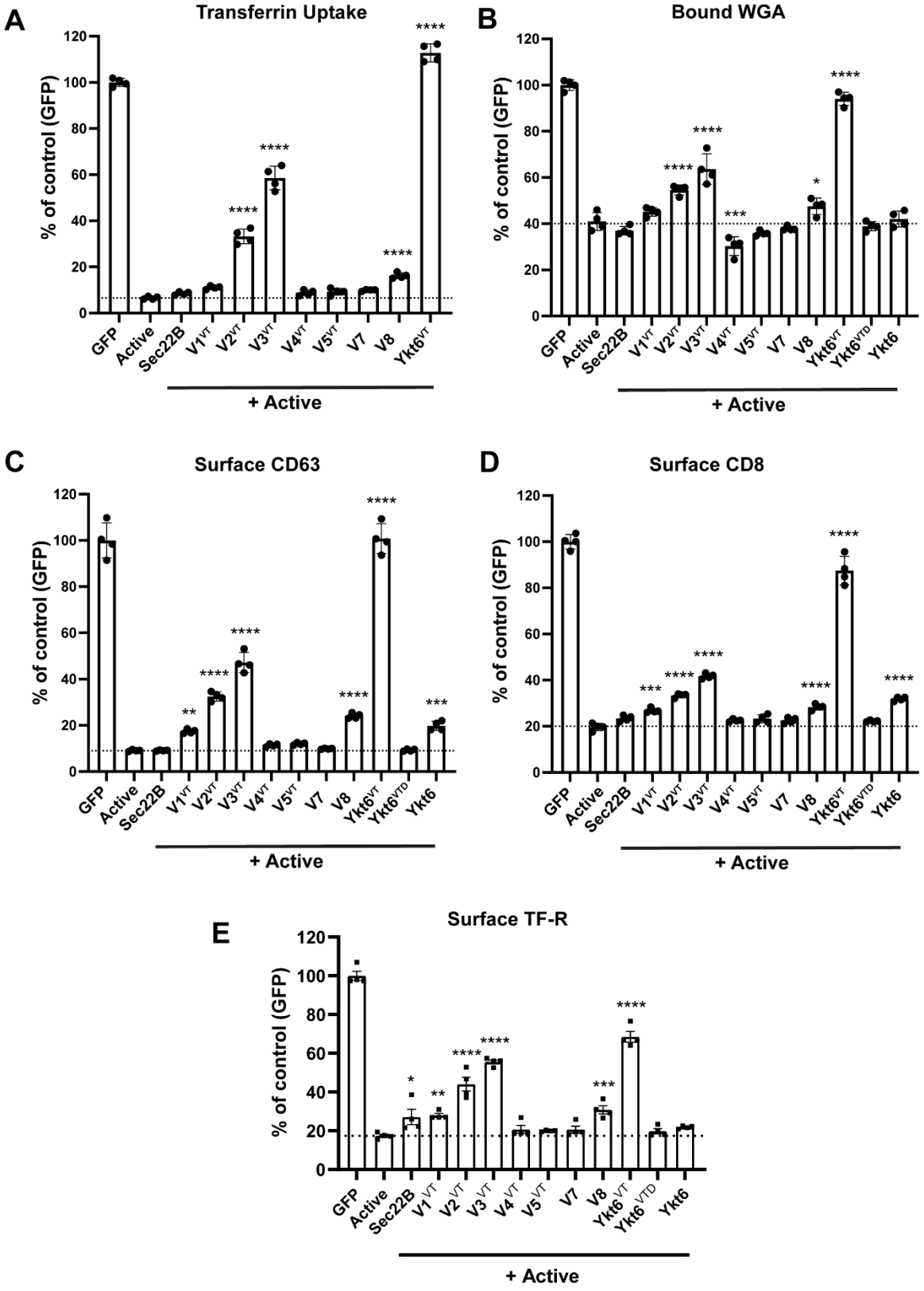

Figure 5. VAMPs 2, 3, 8 and Ykt6 are able to rescue the delivery of cargo to the cell surface in BoNT/X intoxicated cells

To establish if other R-SNAREs could rescue the phenotype resulting from LC/X intoxication, HeLa-M cells were co-transfected with GFP-BoNT/X LC and a panel of

HA-tagged R-SNAREs. (**A**) Cells were collected and incubated with transferrin-Alexa™ 647 at 37℃ for 10 minutes prior to washing and fixation. The mean fluorescence intensity was measured by flow cytometry (n=4). The amount of transferrin internalised by the cells was normalised to the GFP control. One-way ANOVA with Dunnett's multiple comparison was performed for analysis, compared to the Active LC/X, **** P<0.0001. Error bars represent the SEM. (**B**) Cells were incubated with WGA-Alexa Fluor™ 647 (Invitrogen) for 15 minutes, prior to washing with cold media. Cells were fixed and the mean fluorescence intensity measured by flow cytometry (n=4). One-way ANOVA with Dunnett's multiple comparison was performed for analysis, compared to the Active LC/X, * P=0.0490, *** P=0.0003, **** P<0.0001. Error bars represent the SEM. (**C, D**) To determine if surface levels of CD8 and CD63 could be rescued by cleavage resistant SNAREs, HeLa-M cells were transiently transfected with non-fluorescent LC/X, CD8-GFP or CD63-GFP, and the panel of HA-tagged R-SNARE constructs. The surface levels of CD8 or CD63 were measured by incubating the cells with either anti- CD8 or CD63 antibodies labelled with APC for 30 minutes at 4℃. Cells were washed, fixed and the mean fluorescence intensity measured by flow cytometry (n=4). Error bars represent the SEM. One-way ANOVA with Dunnett's multiple comparison was performed for analysis, compared to the Active LC/X, CD8: *** P=0.0005, **** P<0.0001, CD63: ** P=0.0060, *** P=0.0003, **** P<0.0001. (**E**) The cell surface levels of transferrin receptor (TF-R) were measured by incubating the transfected cells with anti-TF-R APC at 4℃ for 30 minutes. The cells were washed, fixed using 4% PFA and the mean fluorescence intensity measured by flow cytometry. Error bars represent the SEM. Adjusted P values calculated using one-way ANOVA with Dunnett's multiple comparisons test, compared to the Active LC/X, * P=0.0211, ** P=0.0099, *** P=0.0006, **** P=<0.0001.

The secretion of soluble cargo can be partially rescued by BoNT/X resistant Ykt6

We have previously shown that BoNT/X intoxication blocks the secretion of soluble cargo using a GFP reporter assay (**Figure 3E**). To determine if this phenotype can be rescued by the overexpression of cleavage resistant SNAREs we co-transfected the secretory model cell line with the indicated R-SNAREs and mCherry BoNT/X LC (**Figure 6A and B**). Expression of cleavage resistant Ykt6 significantly increases secretion of the GFP reporter in the intoxicated cells. However, we observed no

improvement in secretion with the co-expression of VAMP2^{VT} and/or VAMP3^{VT}. At present it is unclear if this lack of rescue is due to a simple technical problem or represents a physiologically important observation.

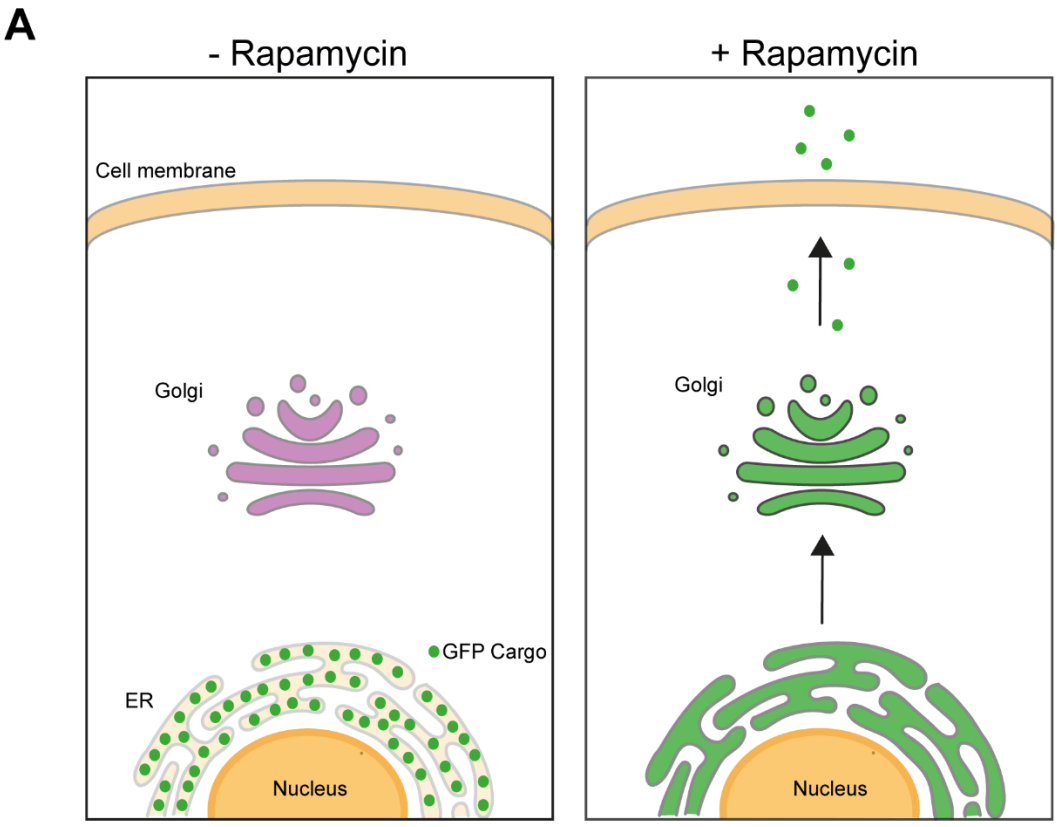

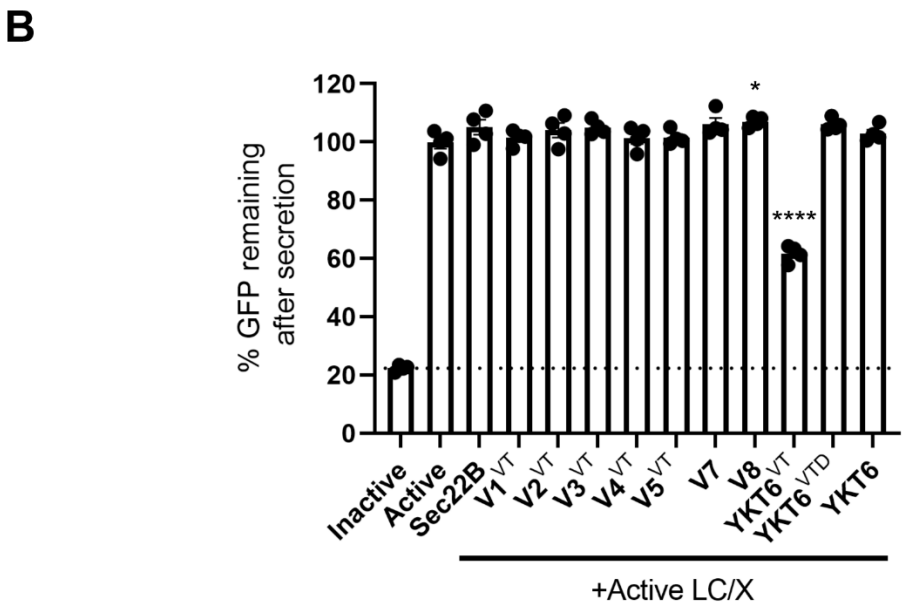

Figure 6. The secretion of soluble cargo in BoNT/X intoxicated cells can partially be rescued by overexpression of cleavage resistant Ykt6

(**A**) Schematic demonstrating the GPF secretory reporter assay. (**B**) HeLa-C1 cells stably expressing the GFP reporter were transfected with mCherry-LC/X and HA-tagged R-SNAREs. Cells were incubated for 120 mins with 1 µM rapamycin prior to trypsinisation. Cells were collected in suspension. Mean fluorescence intensity was measured by flow cytometry. Error bars represent the SEM. Adjusted P values calculated using one-way ANOVA with Dunnett's multiple comparisons test, compared to the Active LC/X, * P=0.0370, **** P=<0.0001.

BoNT/X can be used to the dissect the role of specific residues in R-SNARE function

The genetic reconstitution assay we have developed can not only be used to study the role of different R-SNAREs in intracellular trafficking but can also potentially be used to: 1) investigate the function of key residues in SNARE biology and 2) elucidate the impact of disease-causing mutations on SNARE function. We demonstrated the utility of this assay by showing that a truncated form of Ykt6 ($Ykt6^{VTD}$) which is not able to associate with membranes is unable to rescue BoNT/X associated phenotypes (**Figure 5**). To further explore the use of this assay we have also introduced a panel of mutations into cleavage resistant VAMP3 and assessed their ability to rescue transferrin uptake (**Figure 7**). It has previously shown that VAMPs 1-3 are endocytosed from the cell surface through an interaction with endocytic accessory protein PI-CALM (Harel *et al.*, 2008; Miller *et al.*, 2011) and that mutations in the N-terminal portion of the coiled-coil domain abolish this interaction (V30A/M33A). However, we were not able to assay the importance of this interaction because at the time there were no simple assays to measure VAMP3 function. Thus, we introduced the V30A/M33A mutation into HA-$VAMP3^{VT}$ and assessed the ability to rescue transferrin uptake. In parallel to these studies, we also explored the impact of altering the ionic layer of VAMP3 to a glutamine (R39Q) (Katz and Brennwald, 2000; Graham *et al.*, 2001; Scales, Yoo and Scheller, 2001), mutating the di-tryptophan motif (W71A/W72A) which is next to the transmembrane domain (Sutton *et al.*, 1998; Kweon, Kim and Shin, 2003; Borisovska *et al.*, 2012; Fang, Zhao and Lindau, 2013), and placing the HA-tag at the C-terminus of VAMP3 (Gordon *et al.*, 2009; Miller *et al.*, 2011). To confirm that the constructs were expressed we used both fluorescence

microscopy and intracellular flow cytometry (**Figure 7A and B**). The V30A/M33A, R39Q and W71A/W72A mutants partially restore transferrin uptake suggesting that these mutations have not fully disrupted the function of VAMP3. However, when VAMP3 was tagged at the C-terminus it failed to rescue transferrin uptake indicating that the tag is most likely blocking the ability of VAMP3 to drive membrane fusion. As a final experiment we assessed whether this approach could be used to model the impact of a mutation which causes a neurodevelopmental disorder (Salpietro *et al.*, 2019). It has previously been shown that the S75P substitution in VAMP2 perturbs the function of the SNARE. However, it is unclear whether the mutation causes a loss of function and/or is acting in a dominant negative fashion. VAMPs 2 and 3 share high degrees of homology and the majority of residues in the SNARE domain are 100% conserved. Thus, we introduced the equivalent StoP substitution in VAMP3 (S58P) and measured transferrin uptake. Surprisingly, this mutant abolished the ability of VAMP3 to rescue transferrin uptake suggesting that at least in this context the mutation abolishes the function of VAMP3.

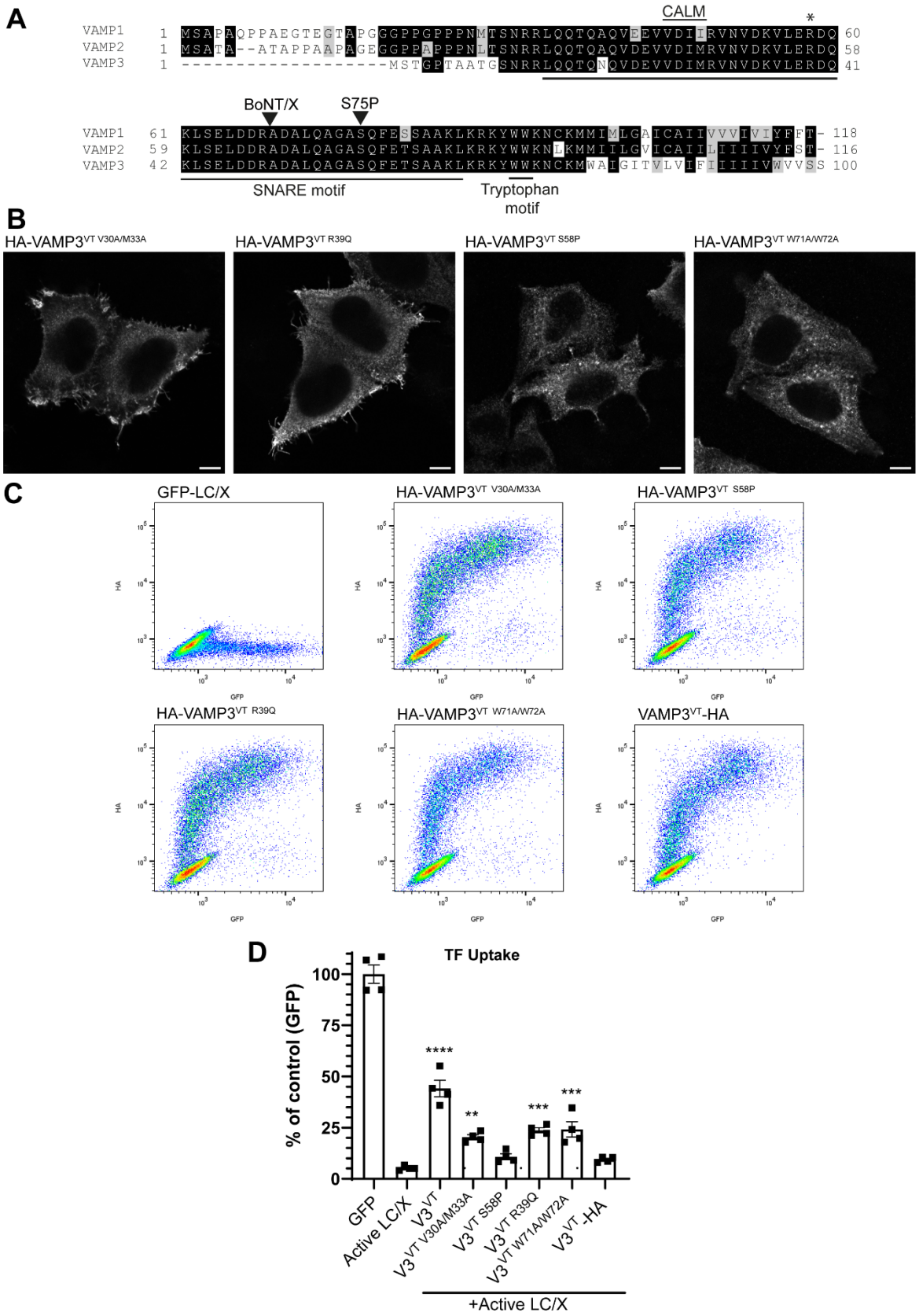

Figure 7. Functional mutations in R-SNAREs can be explored using BoNT/X

(**A**) Sequence alignment of VAMPs 1-3. The position of the mutations introduced into VAMP3 are indicated (* shows position of conserved arginine residue (R)). (**B**) HeLa-

M cells were transfected with mutated HA-VAMP3^{VT} constructs, fixed with PFA and permeabilised prior to staining with anti-HA antibody. Images captured using a Nikon A1 confocal microscope. Scale bar = 10 µm. (**C**) To determine if the HA-VAMP3^{VT} mutants and LC/X were co-expressed in cells, HeLa-M cells were co-transfected with GFP-LC/X (0.1 µg), HA-VAMP (0.5 µg) and GFP (0.4 µg, carrier to boost transfection efficiency). Cells were collected in suspension and fixed. After fixation, the cells were permeabilised, then stained with an anti-HA mouse antibody, followed by an anti-mouse Cy5 secondary. Cells were placed in 1% PFA, and fluorescence measured by flow cytometry. (**D**) To assess the effects of functional mutations in VAMP3, the transferrin uptake assay was used. Cells were collected and incubated with transferrin-Alexa Fluor™ 594 at 37℃ for 10 minutes prior to washing and fixation. Mean fluorescence intensity was measured by flow cytometry (n=4). The amount of transferrin internalised by the cells was normalised to the GFP control. Error bars represent the SEM. One-way ANOVA with Dunnett's multiple comparison was performed for analysis, compared to the Active LC/X ** P=0.0030, *** P=0.0003, **** P=<0.0001.

Discussion

In this study we aimed to understand the impact of BoNT/X intoxication on intracellular trafficking and establish if the toxin can be used as a new tool to dissect R-SNARE function. We have shown that the recombinant light chain of BoNT/X is active in cells and cleaves VAMPs 1-3 as well as the non-canonical R-SNAREs VAMP4 and Ykt6. We have demonstrated that trafficking in the endomembrane system is significantly perturbed in intoxicated cells and co-expression of cleavage resistant R-SNAREs such as VAMP3 and Ykt6 can rescue these phenotypes. The development of this simple genetic reconstitution assay has allowed the role of post-Golgi R-SNAREs in trafficking to the cell surface to be assessed in a way which has not been feasible up until now.

Does Ykt6 normally function in TF-R trafficking?

One of the most striking observations from this study is that Ykt6 is able to restore TF-R trafficking in intoxicated cells suggesting that it can mediate the fusion of TF-R containing vesicles with the plasma membrane. Based on the known literature, Ykt6 would not be expected to have this role (Galli *et al.*, 1994; Kweon *et al.*, 2003; Takáts

et al., 2018). However, Ykt6 is a promiscuous SNARE that acts several pathways including in ER-Golgi trafficking and autophagosome/lysosome fusion (McNew *et al.*, 1997; Xu *et al.*, 2002; Hasegawa *et al.*, 2003; Takáts *et al.*, 2018). In addition, Ykt6 has been implicated in the fusion of biosynthetic cargo with the cell surface (Gordon *et al.*, 2017; Watanabe *et al.*, 2024). Thus, it is feasible that Ykt6 acts in the fusion of TF-R containing vesicles with the cell surface. It has previously shown that VAMPs 2 and 3 are present on TF-R containing vesicles (Kubo *et al.*, 2015). However, their disruption does not lead to dramatic alterations in the surface levels of the TF-R. In addition, we also failed to detect any gross change in either the trafficking or cell surface levels of the TF-R in cells depleted of VAMPs 2 and 3 using BoNT/D (**Figure 2F**). Based on these observations it would seem likely that Ykt6 plays a role in TF-R trafficking. At present, we cannot rule out the possibility that Ykt6 only acts on this pathway when the function of VAMPs 2 and 3 have been disrupted. Ykt6 is a peculiar SNARE as it has the ability to cycle on and off membranes (Fukasawa *et al.*, 2004; Meiringer *et al.*, 2008) thus it is possible that Ykt6 could be recruited to transport vesicles which are lacking R-SNAREs. However, it is unclear how the cell would sense these changes and regulate this process. In the future it will be important to determine how intoxication impacts the formation of SNARE complexes at the plasma membrane. One would predict that if Ykt6 normally acts at this step the levels of Ykt6 containing SNARE complexes would not change after intoxication.

Several R-SNAREs can mediate the fusion of biosynthetic vesicles with the cell surface

The human genome encodes 7 post-Golgi R-SNAREs with many of them being implicated in mediating the fusion of biosynthetic transport vesicles with the cell surface (Galli *et al.*, 1994; Wong *et al.*, 1998; Steegmaier *et al.*, 1999; Schoch *et al.*, 2001; Gordon *et al.*, 2017). Interestingly, we only observed significant rescue with VAMPs 1-3 and 8 in the assays performed. At present it is unclear why VAMP3 is the most effective ‘brevin’ type R-SNARE in this process. It is possible that VAMP3 is the one which is most efficiently packaged into transport vesicles exiting the TGN and/or has the optimal affinity for the Q-SNAREs expressed in these cells. In agreement with this hypothesis, there is a significant pool of endogenous and tagged VAMP3 at the TGN (data not shown) suggesting that it is well placed to act in this pathway. Our

functional data suggests that VAMPs 1-3, and 8 can drive the fusion of biosynthetic vesicles with the plasma membrane. However, their role in this process is only uncovered when the function of Ykt6 is disrupted. Why is this the case? As previously discussed, it is possible that Ykt6 is taking over this process in cells where the function of these SNAREs has been disrupted. However, it is also feasible that there are multiple redundant routes to the cell surface from the TGN that are defined by these SNAREs and that their role only becomes apparent when several of these pathways are disrupted.

Can the genetic reconstitution assay be used to study functional and disease-causing mutations in R-SNAREs?

The genetic reconstitution assay provides a novel platform to assess the function of individual SNAREs in intracellular trafficking. In addition, the assay can be used to perform detailed mechanistic studies where key residues are changed within the SNAREs. For example, we have investigated the role of lipidation in regulating Ykt6 function by deleting its C-terminal cysteine containing motif and shown that the protein must be membrane anchored to function. To investigate how R-SNARE endocytic recycling impacts SNARE function we introduced mutations in VAMP3 which abolishes its interaction with clathrin adaptor protein, clathrin assembly lymphoid myeloid leukaemia (CALM) (Miller *et al.*, 2011). This mutation blocks the ability of VAMP3 to be recycled after fusion with the cell surface. Surprisingly, the mutant form of VAMP3 was able to partially rescue transferrin uptake. In the reconstitution assay the R-SNAREs are over expressed using a CMV promoter so it is possible that the biosynthetic delivery of VAMP3 to the cell surface is able to compensate for any defect in endocytic recycling. Thus, in the future it may be of interest to repeat these experiments using stable cell lines which express the mutant constructs at levels closer to that of the endogenous SNAREs (Gordon *et al.*, 2009). It has previously been shown that substitution of a serine for a proline residue (S75P) in the SNARE domain of VAMP2 causes a serious neurodevelopmental disorder (Salpietro *et al.*, 2019). It is thought that this mutation prevents Munc18 from activating SNARE complex assembly and membrane fusion. When a comparable mutation is introduced into VAMP3 the protein is unable to rescue transferrin uptake, suggesting that protein no longer functions. It has previously been shown that the conserved Q and R residues at the

zero layer position in the SNARE complex are important for SNARE function (Katz and Brennwald, 2000; Scales, Yoo and Scheller, 2001). Surprisingly, we observed that the VAMP3 (R39Q) mutant was still able to partially rescue transferrin uptake. Similar results have been observed by others and the RtoQ mutant of Ykt6 is able to rescue autophagy (Takáts *et al.*, 2018). VAMP2 has a pair of tryptophan residues (W89/W90) that are thought to play a role in fusion by inserting their hydrophobic side chains into the membrane. When these residues are mutated, it was previously observed that there was a ~50% decrease in activity compared to the wild type VAMP2 (Borisovska *et al.*, 2012; Fang, Zhao and Lindau, 2013). Our data suggests that these residues are also important in VAMP3 function, as we observed a significant reduction in function compared with wild type VAMP3^{VT}.

VAMP4^{VT} is only partially resistant to cleavage by LC/X

The VT substitution in VAMP4 did not fully protect the protein from the action of LC/X especially when the light chat was expressed at high levels. Thus, the functional studies looking at the role of VAMP4 in post-Golgi trafficking need to be considered with caution. At present it is unclear why this is the case as the VT substitution protects other R-SNAREs. Conducting mass spectrometry-based analysis to identify the cleavage products would provide insight into the possibility of an alternative cleavage site. It could also be interesting to model the protein residues as there could be a structural/conformational change induced in VAMP4 that facilitates proteolysis by LC/X.

In conclusion, we have demonstrated that the light chain of BoNT/X is able to cleave VAMPs 1-3 and non-canonical R-SNAREs in vivo, and this results in notable defects in intracellular trafficking. By mutating R-SNAREs targeted by BoNT/X to resist cleavage we have established that the phenotypes caused by intoxication are specific to SNARE proteolysis. We have developed a simple and robust genetic constitution assay to explore the role of R-SNAREs in post-Golgi trafficking. We have uncovered an unexpected role for Ykt6 in transferrin receptor trafficking and identified key residues in VAMP3 that are important for its function. BoNT/X is an exciting novel tool for studying the function of R-SNAREs in post-Golgi trafficking.

Supplementals

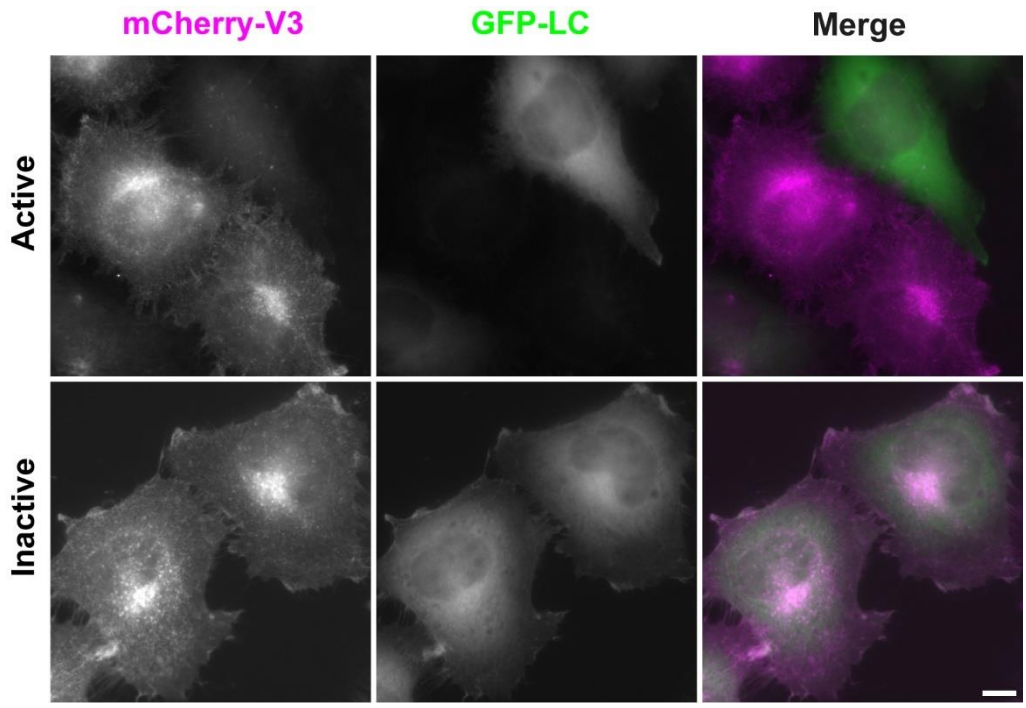

Supplemental Figure 1. BoNT/D cleaves VAMP3 in vivo

A GFP-tagged active BoNT/D light chain (residues 1-430aa) was synthesised, and an inactive version was also generated (Y168D/L200D) (Guo and Chen, 2013). HeLa-M cells expressing mCherry-tagged VAMPs were grown on coverslips and transiently transfected with either active or inactive light chain of BoNT/D tagged with GFP. Cells were fixed and representative images captured. Scale bar = 10 µm.

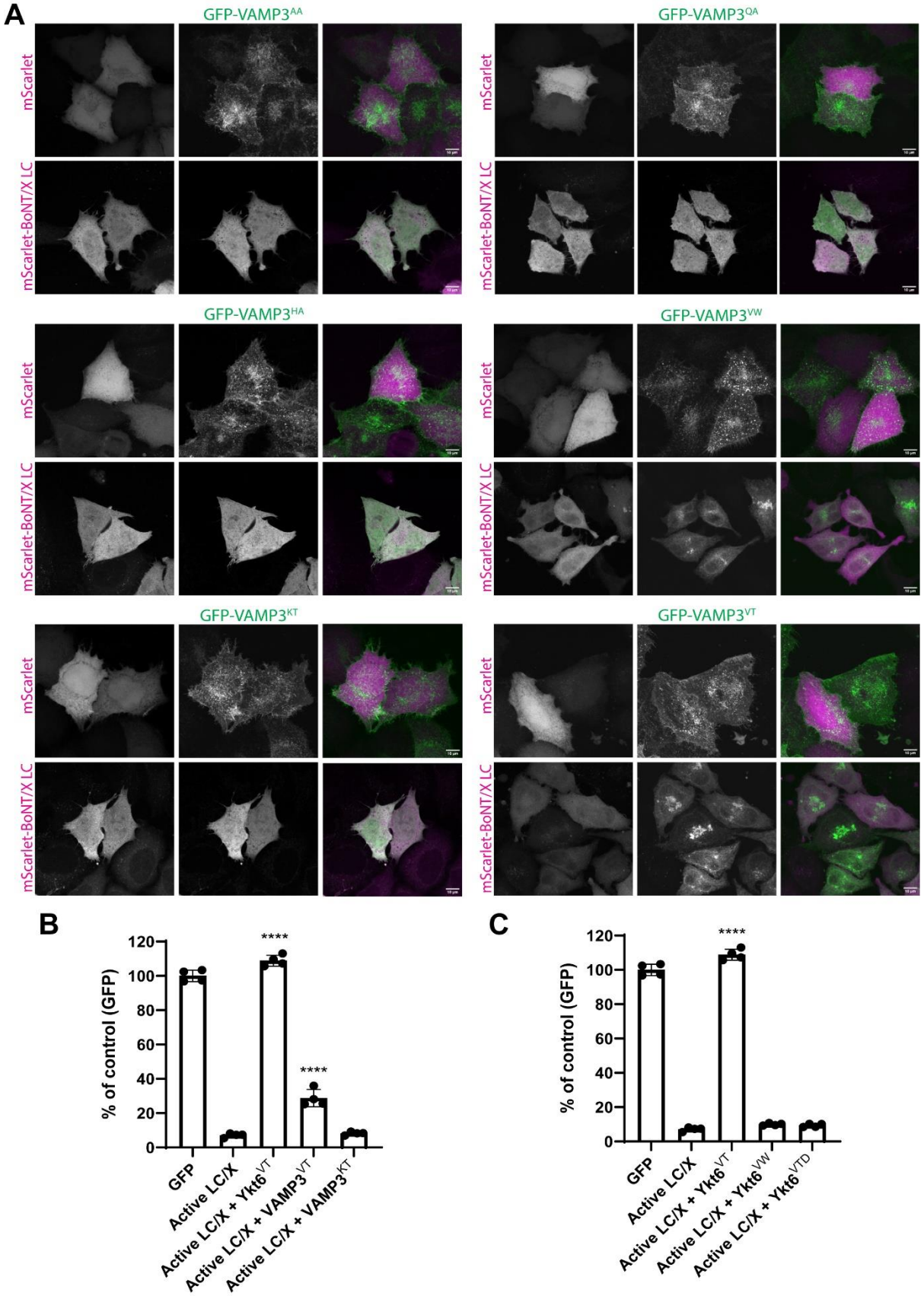
A
GFP-VAMP3AA
GFP-VAMP3QA
GFP-VAMP3HA
GFP-VAMP3VW
GFP-VAMP3KT
GFP-VAMP3VT
mScarlet
mScarlet-BoNT/X LC
B
% of control (GFP)
120
100
80
60
40
20
0
****
****
GFP
Active LC/X
Active LC/X + Ykt6VT
Active LC/X + VAMP3VT
Active LC/X + VAMP3KT
C
% of control (GFP)
120
100
80
60
40
20
0
****
GFP
Active LC/X
Active LC/X + Ykt6VT
Active LC/X + Ykt6VW
Active LC/X + Ykt6VTD

Supplemental Figure 2. Testing mutations in R-SNAREs to protect against BoNT/X LC

(**A**) Immunofluorescence of VAMP3 mutants. HeLa-M cells were co-transfected with the indicated GFP-tagged VAMP3 mutants and either mScarlet or mScarlet-BoNT/X LC. Cells were fixed with PFA and representative images captured. Scale bar = 10 µm. (**B,C**) To establish if the mutations could rescue the phenotype resulting from LC/X intoxication, HeLa-M cells were co-transfected with GFP-BoNT/X LC and HA-VAMP3^{KT}, HA-VAMP3^{VT}, myc-Ykt6^{VW}, HA-Ykt6^{VT}, HA-Ykt6^{VTD}. Cells were collected and incubated with transferrin-Alexa™ 647 at 37 ℃ for 10 minutes prior to washing and fixation. The mean fluorescent intensity of the cells was measured by flow cytometry (n=4). The amount of transferrin internalised by the cells was normalised to the GFP control. Adjusted P values calculated using one-way ANOVA with Dunnett's multiple comparisons test, compared to the Active LC/X. **** P=<0.0001.

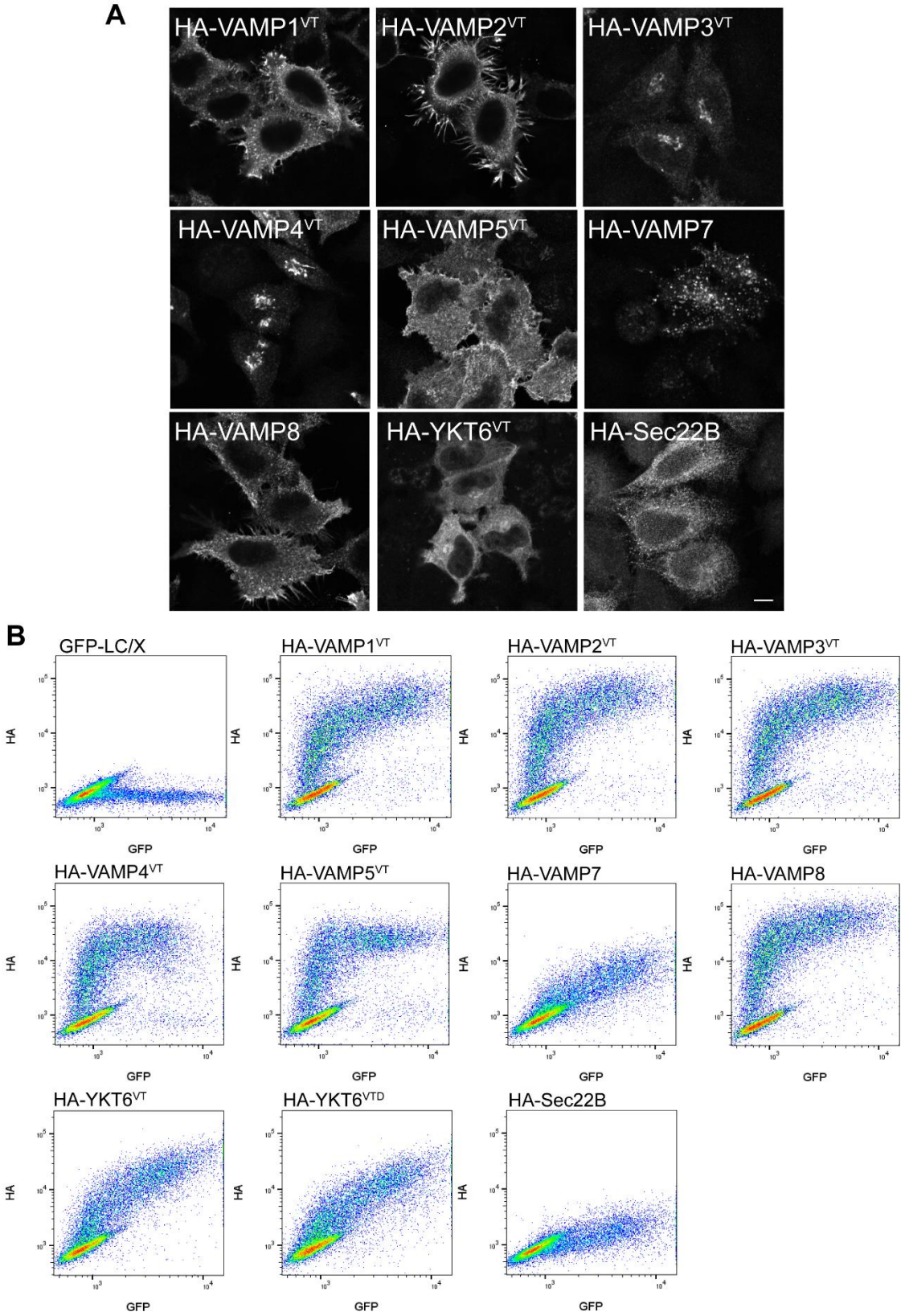

Supplemental Figure 3. HA-tagged R-SNARE expression

(**A**) Steady state immunofluorescence of resistant HA-tagged R-SNAREs. HeLa-M cells were transfected with the VT mutant HA-tagged R-SNAREs. Cells were fixed with

PFA and permeabilised with IF buffer prior to staining with anti-HA antibody and representative images captured. Scale bar = 10 µm. (**B**) HA-tagged R-SNAREs transiently co-expressed with GFP-LC/X. To determine if HA-tagged R-SNARE and LC/X were co-expressed in cells, HeLa-M cells were co-transfected with GFP-LC/X (0.1 µg), HA-tagged R-SNARE (0.5 µg) and GFP (0.4 µg, carrier to boost transfection efficiency). Cells were collected in suspension and fixed. After fixation, the cells were permeabilised, then stained with an anti-HA mouse antibody, followed by anti-mouse Cy™5 secondary. Cells were placed in 1% PFA and acquired by flow cytometry.

Supplemental Table 1. Plasmid constructs and mutations

Construct	Vector	Notes
GFP-BoNT/X LC active	pEGFP-C3 (Clontech/Takara)	The light chain of BoNT/X (1-439aa) was codon optimised, synthesised and cloned into the vector using XhoI and EcoRI.
GFP-BoNT/X LC inactive	pEGFP-C3 (Clontech/Takara)	The inactive version of the light chain (R360A/Y363F) was generated using site directed mutagenesis.
mCherry-BoNT/X LC active	pEGFP-C3 (Clontech/Takara)	The construct was made by swapping eGFP with mCherry (NheI/BsrG1).
mCherry-BoNT/X LC inactive	pEGFP-C3 (Clontech/Takara)	The construct was made by swapping eGFP with mCherry (NheI/BsrGI).
StrepII tag-BoNT/X LC active	pEGFP-C3 (Clontech/Takara)	The construct was made by swapping eGFP with StrepII tag (AgeI/XhoI).
StrepII tag-BoNT/X LC inactive	pEGFP-C3 (Clontech/Takara)	The construct was made by swapping eGFP with StrepII tag (AgeI/XhoI).
miRFP670-BoNT/X LC active	pEGFP-C3 (Clontech/Takara)	The construct was made by swapping eGFP with miRFP670 (AgeI/XhoI). For unknown reasons the fusion protein was not fluorescent, so it was used as a dark version of BoNT/X LC.
miRFP670-BoNT/X LC inactive	pEGFP-C3 (Clontech/Takara)	The construct was made by swapping eGFP with miRFP670 (AgeI/XhoI). For unknown reasons the fusion protein was not fluorescent, so it was used as a dark version of BoNT/X LC.
mScarlet-BoNT/X LC active	pEGFP-C3 (Clontech/Takara)	The construct was made by swapping eGFP with mScarlet (AgeI/XhoI).
mScarlet	pScarlet-N1	The construct was obtained from Addgene (Plasmid #128060).
GFP-BoNT/D LC active	pEGFP-C3 (Clontech/Takara)	The light chain of BoNT/D (1-430aa) was codon optimised, synthesised and cloned into the vector using XhoI and EcoRI.

GFP-BoNT/D LC inactive	pEGFP-C3 (Clontech/Takara)	The inactive version of the light chain (Y168D/L200D) was generated using site directed mutagenesis.
HA-VAMP1 (VT mutant)	pIRES-Neo2 (Clontech/Takara)	Human VAMP1 (Refseq NM_014231.5) was synthesised with an N-terminal HA tag, R68V/A69/T substitutions and cloned into the expression plasmid using EcoRI and NotI.
HA-VAMP2 (VT mutant)	pIRES-Neo2 (Clontech/Takara)	Human VAMP2 (Refseq NM_014232.3) was synthesised with an N-terminal HA tag, R66V/A67T substitutions and cloned into the expression plasmid using EcoRI and NotI.
HA-VAMP3 (VT mutant)	pIRES-Neo2 (Clontech/Takara)	Human VAMP3 (Refseq NM_004781.4) was synthesised with an N-terminal HA tag, R49V/A50T substitutions and cloned into the expression plasmid using EcoRI and NotI.
HA-VAMP3 (VT mutant) CALM	pIRES-Neo2 (Clontech/Takara)	HA-VAMP3 (VT mutant) as synthesised above with an additional V30A/M33A substitution.
HA-VAMP3 (VT mutant) S to P	pIRES-Neo2 (Clontech/Takara)	HA-VAMP3 (VT mutant) as synthesised above with an additional S58P substitution.
HA-VAMP3 (VT mutant) R to Q	pIRES-Neo2 (Clontech/Takara)	HA-VAMP3 (VT mutant) as synthesised above with an additional R39Q substitution.
HA-VAMP3 (VT mutant) WW to AA	pIRES-Neo2 (Clontech/Takara)	HA-VAMP3 (VT mutant) as synthesised above with an additional W71A/W72A substitution.
VAMP3-HA (VT mutant)	pIRES-Neo2 (Clontech/Takara)	Human VAMP3 (Refseq NM_004781.4) was synthesised with a C-terminal HA tag, R49V/A50T substitutions and cloned into the expression plasmid using EcoRI and NotI.
HA-VAMP4 (VT mutant)	pIRES-Neo2 (Clontech/Takara)	Human VAMP4 (Refseq NM_003762.5) was synthesised with an N-terminal HA tag, K87V/S88T substitutions and cloned into the expression plasmid using EcoRI and NotI.
HA-VAMP5 (VT mutant)	pIRES-Neo2 (Clontech/Takara)	Human VAMP5 (Refseq NM_006634.3) was synthesised with an N-terminal HA tag, R40V/S41T substitutions and cloned into the expression plasmid using EcoRI and NotI.
HA-VAMP7	pIRES-Neo2 (Clontech/Takara)	Human VAMP7 (Refseq NM_005638.6) was synthesised with an N-terminal HA tag and cloned into the expression plasmid using EcoRI and NotI.

HA-VAMP8	pIRES-Neo2 (Clontech/Takara)	Human VAMP8 (Refseq NM_003761.5) was synthesised with an N-terminal HA tag and cloned into the expression plasmid using EcoRI and NotI.
HA-Ykt6	pIRES-Neo2 (Clontech/Takara)	Human Ykt6 (Refseq NM_006555.4, 1-198aa) was synthesised with an N-terminal HA tag and cloned into the expression plasmid using NheI and NotI.
HA-Ykt6 (VT mutant)	pIRES-Neo2 (Clontech/Takara)	Human Ykt6 (Refseq NM_006555.4, 1-198aa) was synthesised with an N-terminal HA tag, K173V/S174T substitutions and cloned into the expression plasmid using NheI and NotI.
HA-Ykt6 (VT mutant)	pLXIN-Mod (Clontech/Takara)	HA-Ykt6 (VT mutant) was cloned using XhoI/NotI.
HA-Ykt6 (VT and truncation mutant)	pIRES-Neo2 (Clontech/Takara)	Human Ykt6 (1-193aa, Refseq NM_006555.4) was synthesised with an N-terminal HA tag, K173V/S174T substitutions and cloned into the expression plasmid using NheI and NotI.
HA-Sec22B	pIRES-Neo2 (Clontech/Takara)	Human Sec22B (Refseq NM_004892.6) was synthesised with an N-terminal HA tag and cloned into the expression plasmid using EcoRI and NotI.
GFP-VAMP3-HA-MAO	pEGFP-C3 (Clontech/Takara)	Human VAMP3 (Refseq NM_004781.4) (1-77aa) was synthesised with a C-terminal HA tag and MAO targeting sequence (Refseq NM_001270458.2; isoform 1, 481-527aa) and cloned into the expression plasmid using XhoI and EcoRI.
GFP-VAMP3-HA-MAO (VT mutant)	pEGFP-C3 (Clontech/Takara)	Human VAMP3 (Refseq NM_004781.4) (1-77aa) was synthesised with a C-terminal HA tag, R49V/A50T substitutions, MAO targeting sequence (Refseq NM_001270458.2; isoform 1, 481-527aa) and cloned into the expression plasmid using XhoI and EcoRI.
GFP-VAMP4-HA-MAO	pEGFP-C3 (Clontech/Takara)	Human VAMP4 (Refseq NM_003762.5, 1-117aa) was synthesised with a C-terminal HA tag, MAO targeting sequence (Refseq NM_001270458.2; isoform 1, 481-527aa) and cloned into the expression plasmid using XhoI and EcoRI.

GFP-VAMP4-HA-MAO (VT mutant)	pEGFP-C3 (Clontech/Takara)	Human VAMP4 (Refseq NM_003762.5, 1-117aa) was synthesised with a C-terminal HA tag, K87V/S88T substitutions, MAO targeting sequence (Refseq NM_001270458.2; isoform 1, 481-527aa) and cloned into the expression plasmid using XhoI and EcoRI.
GFP-Ykt6-HA-MAO	pEGFP-C3 (Clontech/Takara)	Human Ykt6 (Refseq NM_006555.4, 1-193aa) was synthesised with a C-terminal HA tag, MAO targeting sequence (Refseq NM_001270458.2; isoform 1, 481-527aa) and cloned into the expression plasmid using XhoI and HindIII.
GFP-Ykt6-HA-MAO (VT mutant)	pEGFP-C3 (Clontech/Takara)	Human Ykt6 (Refseq NM_006555.4, 1-193aa) was synthesised with a C-terminal HA tag, K173V/S174T substitutions, MAO targeting sequence (Refseq NM_001270458.2; isoform 1, 481-527aa) and cloned into the expression plasmid using XhoI and HindIII.
mCherry-VAMP3	pmCherry-C1 (Clontech/Takara)	Rat VAMP3 (Refseq NM_057097.2) was cloned into the expression plasmid using XhoI/BamHI. Gift from Ben Nichols lab.
mCherry-VAMP4	pmCherry-C1 (Clontech/Takara)	Rat VAMP4 (Refseq NM_001108856.2) was cloned into the expression plasmid using XhoI/BamHI. Gift from Ben Nichols lab.
mCherry-VAMP7	pmCherry-C1 (Clontech/Takara)	Human VAMP7 (Refseq NM_005638.6) was cloned into the expression plasmid using HindIII/BamHI. Gift from Ben Nichols lab.
mCherry-VAMP8	pmCherry-C1 (Clontech/Takara)	Rat VAMP8 (Refseq NM_031827.2) was cloned into the expression plasmid using XhoI/BamHI. Gift from Ben Nichols lab.
GFP-VAMP3 (AA mutant)	pEGFP-C3 (Clontech/Takara)	Human VAMP3 (Refseq NM_004781.4) was synthesised with an N-terminal HA tag, R49A substitution and cloned into the expression plasmid using XhoI and EcoRI.
GFP-VAMP3 (QA mutant)	pEGFP-C3 (Clontech/Takara)	Human VAMP3 (Refseq NM_004781.4) was synthesised with an N-terminal HA tag, R49Q substitution and cloned into the expression plasmid using XhoI and EcoRI.

GFP-VAMP3 (HA mutant)	pEGFP-C3 (Clontech/Takara)	Human VAMP3 (Refseq NM_004781.4) was synthesised with an N-terminal HA tag, R49H substitution and cloned into the expression plasmid using XhoI and EcoRI.
GFP-VAMP3 (VW mutant)	pEGFP-C3 (Clontech/Takara)	Human VAMP3 (Refseq NM_004781.4) was synthesised with an N-terminal HA tag, R49V/A50W substitutions and cloned into the expression plasmid using XhoI and EcoRI.
GFP-VAMP3 (KT mutant)	pEGFP-C3 (Clontech/Takara)	Human VAMP3 (Refseq NM_004781.4) was synthesised with an N-terminal HA tag, R49K/A50T substitutions and cloned into the expression plasmid using XhoI and EcoRI.
GFP-VAMP3 (VT mutant)	pEGFP-C3 (Clontech/Takara)	Human VAMP3 (Refseq NM_004781.4) was synthesised with an N-terminal HA tag, R49V/A50T substitutions and cloned into the expression plasmid using XhoI and EcoRI.
HA-VAMP3 (KT mutant)	pIRES-Neo2 (Clontech/Takara)	Human VAMP3 (Refseq NM_004781.4) was synthesised with an N-terminal HA tag, R49K/A50T substitutions and cloned into the expression plasmid using EcoRI and NotI.
Myc-Ykt6 (VW mutant)	pCMV-Myc	myc-Ykt6 (Rat, NM_031692.3) was a gift from Prof Jesse Hay (Hasegawa *et al.*, 2004) and site directed mutagenesis was performed to introduce the changes (K173V/S174W).
CD8a-eGFP	pEGFP-N1	Human CD8 expression plasmid from Addgene (86051).
CD63-GFPSpark	pCMV3-GFPSpark	Mouse CD63 (Refseq NM_001042580.2) purchased from Sino Biological (MG50557-ACG).

References

Antonin, W. *et al.* (2000) 'The R-SNARE Endobrevin/VAMP-8 Mediates Homotypic Fusion of Early Endosomes and Late Endosomes', *Molecular Biology of the Cell*, 11(10), pp. 3289–3298.

Bethani, I. *et al.* (2009) 'Endosomal Fusion upon SNARE Knockdown is Maintained by Residual SNARE Activity and Enhanced Docking', *Traffic*, 10(10), pp. 1543–1559. Available at: https://doi.org/10.1111/j.1600-0854.2009.00959.x.

Borisovska, M. *et al.* (2012) 'Membrane-Proximal Tryptophans of Synaptobrevin II Stabilize Priming of Secretory Vesicles', *The Journal of Neuroscience*, 32(45), pp. 15983–15997. Available at: https://doi.org/10.1523/JNEUROSCI.6282-11.2012.

Davis, L.J. *et al.* (2021) 'Organelle tethering, pore formation and SNARE compensation in the late endocytic pathway', *Journal of Cell Science*, 134(10), p. jcs255463. Available at: https://doi.org/10.1242/jcs.255463.

Fang, Q., Zhao, Y. and Lindau, M. (2013) 'Juxtamembrane tryptophans of synaptobrevin 2 control the process of membrane fusion', *FEBS Letters*, 587(1), pp. 67–72. Available at: https://doi.org/10.1016/j.febslet.2012.11.002.

Fukasawa, M. *et al.* (2004) 'Localization and activity of the SNARE Ykt6 determined by its regulatory domain and palmitoylation', *Proceedings of the National Academy of Sciences*, 101(14), pp. 4815–4820. Available at: https://doi.org/10.1073/pnas.0401183101.

Gaisano, H.Y. *et al.* (1994) 'Tetanus toxin light chain cleaves a vesicle-associated membrane protein (VAMP) isoform 2 in rat pancreatic zymogen granules and inhibits enzyme secretion.', *Journal of Biological Chemistry*, 269(25), pp. 17062–17066. Available at: https://doi.org/10.1016/S0021-9258(17)32520-6.

Galli, T. *et al.* (1994) 'Tetanus toxin-mediated cleavage of cellubrevin impairs exocytosis of transferrin receptor-containing vesicles in CHO cells.', *Journal of Cell Biology*, 125(5), pp. 1015–1024. Available at: https://doi.org/10.1083/jcb.125.5.1015.

Gordon, D.E. *et al.* (2009) 'Coiled-coil interactions are required for post-Golgi R-SNARE trafficking', *EMBO reports*, 10(8), pp. 851–856. Available at: https://doi.org/10.1038/embor.2009.96.

Gordon, D.E. *et al.* (2010) 'A targeted siRNA screen to identify SNAREs required for constitutive secretion in mammalian cells', *Traffic (Copenhagen, Denmark)*, 11(9), pp. 1191–1204. Available at: https://doi.org/10.1111/j.1600-0854.2010.01087.x.

Gordon, D.E. *et al.* (2017) 'VAMP3/Syb and YKT6 are required for the fusion of constitutive secretory carriers with the plasma membrane', *PLOS Genetics*, 13(4), p. e1006698. Available at: https://doi.org/10.1371/journal.pgen.1006698.

Gordon, D.E. *et al.* (2021) 'Quantitative Flow Cytometry-Based Assays for Measuring Constitutive Secretion', *Methods in Molecular Biology (Clifton, N.J.)*, 2233, pp. 115–129. Available at: https://doi.org/10.1007/978-1-0716-1044-2_8.

Graham, M.E. *et al.* (2001) 'SNAP-25 with mutations in the zero layer supports normal membrane fusion kinetics', *Journal of Cell Science*, 114(24), pp. 4397–4405. Available at: https://doi.org/10.1242/jcs.114.24.4397.

Guo, J. and Chen, S. (2013) 'Unique Substrate Recognition Mechanism of the Botulinum Neurotoxin D Light Chain', *The Journal of Biological Chemistry*, 288(39), pp. 27881–27887. Available at: https://doi.org/10.1074/jbc.M113.491134.

Harel, A. *et al.* (2008) 'Evidence for CALM in Directing VAMP2 Trafficking', *Traffic*, 9(3), pp. 417–429. Available at: https://doi.org/10.1111/j.1600-0854.2007.00694.x.

Hasegawa, H. *et al.* (2003) 'Mammalian Ykt6 Is a Neuronal SNARE Targeted to a Specialized Compartment by its Profilin-like Amino Terminal Domain', *Molecular Biology of the Cell*, 14(2), pp. 698–720. Available at: https://doi.org/10.1091/mbc.E02-09-0556.

Hasegawa, H. *et al.* (2004) 'Intramolecular protein-protein and protein-lipid interactions control the conformation and subcellular targeting of neuronal Ykt6', *Journal of Cell Science*, 117(19), pp. 4495–4508. Available at: https://doi.org/10.1242/jcs.01314.

Ivanova, D. *et al.* (2021) 'Control of synaptic vesicle release probability via VAMP4 targeting to endolysosomes', *Science Advances*, 7(18), p. eabf3873. Available at: https://doi.org/10.1126/sciadv.abf3873.

Jahn, R. and Scheller, R.H. (2006) 'SNAREs — engines for membrane fusion', *Nature Reviews Molecular Cell Biology*, 7(9), pp. 631–643. Available at: https://doi.org/10.1038/nrm2002.

Katz, L. and Brennwald, P. (2000) 'Testing the 3Q:1R "Rule": Mutational Analysis of the Ionic "Zero" Layer in the Yeast Exocytic SNARE Complex Reveals No Requirement for Arginine', *Molecular Biology of the Cell*, 11(11), pp. 3849–3858.

Kloepper, T.H., Kienle, C.N. and Fasshauer, D. (2007) 'An Elaborate Classification of SNARE Proteins Sheds Light on the Conservation of the Eukaryotic Endomembrane System', *Molecular Biology of the Cell*, 18(9), pp. 3463–3471. Available at: https://doi.org/10.1091/mbc.E07-03-0193.

Kubo, K. *et al.* (2015) 'SNAP23/25 and VAMP2 mediate exocytic event of transferrin receptor-containing recycling vesicles', *Biology Open*, 4(7), pp. 910–920. Available at: https://doi.org/10.1242/bio.012146.

Kweon, D.-H., Kim, C.S. and Shin, Y.-K. (2003) 'Regulation of neuronal SNARE assembly by the membrane', *Nature Structural & Molecular Biology*, 10(6), pp. 440–447. Available at: https://doi.org/10.1038/nsb928.

Kweon, Y. *et al.* (2003) 'Ykt6p Is a Multifunctional Yeast R-SNARE That Is Required for Multiple Membrane Transport Pathways to the Vacuole', *Molecular Biology of the Cell*, 14(5), pp. 1868–1881. Available at: https://doi.org/10.1091/mbc.e02-10-0687.

McNew, J.A. *et al.* (1997) 'Ykt6p, a Prenylated SNARE Essential for Endoplasmic Reticulum-Golgi Transport *', *Journal of Biological Chemistry*, 272(28), pp. 17776–17783. Available at: https://doi.org/10.1074/jbc.272.28.17776.

Meiringer, C.T.A. *et al.* (2008) 'Depalmitoylation of Ykt6 Prevents its Entry into the Multivesicular Body Pathway', *Traffic*, 9(9), pp. 1510–1521. Available at: https://doi.org/10.1111/j.1600-0854.2008.00778.x.

Miller, S.E. *et al.* (2011) 'The Molecular Basis for the Endocytosis of Small R-SNAREs by the Clathrin Adaptor CALM', *Cell*, 147(5), pp. 1118–1131. Available at: https://doi.org/10.1016/j.cell.2011.10.038.

Pellizzari, R. *et al.* (1996) 'Structural Determinants of the Specificity for Synaptic Vesicle-associated Membrane Protein/Synaptobrevin of Tetanus and Botulinum Type B and G Neurotoxins *', *Journal of Biological Chemistry*, 271(34), pp. 20353–20358. Available at: https://doi.org/10.1074/jbc.271.34.20353.

Peng, L. *et al.* (2013) 'Cytotoxicity of botulinum neurotoxins reveals a direct role of syntaxin 1 and SNAP-25 in neuron survival', *Nature Communications*, 4(1), p. 1472. Available at: https://doi.org/10.1038/ncomms2462.

Pirazzini, M. *et al.* (2017) 'Botulinum Neurotoxins: Biology, Pharmacology, and Toxicology', *Pharmacological Reviews*, 69(2), pp. 200–235. Available at: https://doi.org/10.1124/pr.116.012658.

Randhawa, V.K. *et al.* (2000) 'VAMP2, but Not VAMP3/Cellubrevin, Mediates Insulin-dependent Incorporation of GLUT4 into the Plasma Membrane of L6 Myoblasts', *Molecular Biology of the Cell*, 11(7), pp. 2403–2417.

Regazzi, R. *et al.* (1995) 'VAMP-2 and cellubrevin are expressed in pancreatic beta-cells and are essential for Ca(2+)-but not for GTP gamma S-induced insulin secretion', *The EMBO journal*, 14(12), pp. 2723–2730. Available at: https://doi.org/10.1002/j.1460-2075.1995.tb07273.x.

Regazzi, R. *et al.* (1996) 'Mutational analysis of VAMP domains implicated in Ca2+-induced insulin exocytosis.', *The EMBO Journal*, 15(24), pp. 6951–6959.

Salpietro, V. *et al.* (2019) 'Mutations in the Neuronal Vesicular SNARE VAMP2 Affect Synaptic Membrane Fusion and Impair Human Neurodevelopment', *American Journal of Human Genetics*, 104(4), pp. 721–730. Available at: https://doi.org/10.1016/j.ajhg.2019.02.016.

Sato, M. *et al.* (2011) 'The Role of VAMP7/TI-VAMP in Cell Polarity and Lysosomal Exocytosis in vivo', *Traffic*, 12(10), pp. 1383–1393. Available at: https://doi.org/10.1111/j.1600-0854.2011.01247.x.

Scales, S.J., Yoo, B.Y. and Scheller, R.H. (2001) 'The ionic layer is required for efficient dissociation of the SNARE complex by α-SNAP and NSF', *Proceedings of the National Academy of Sciences of the United States of America*, 98(25), pp. 14262–14267. Available at: https://doi.org/10.1073/pnas.251547598.

Schiavo, G.G. *et al.* (1992) 'Tetanus and botulinum-B neurotoxins block neurotransmitter release by proteolytic cleavage of synaptobrevin', *Nature*, 359(6398), pp. 832–835. Available at: https://doi.org/10.1038/359832a0.

Schoch, S. *et al.* (2001) 'SNARE Function Analyzed in Synaptobrevin/VAMP Knockout Mice', *Science*, 294(5544), pp. 1117–1122.

van der Sluijs, P. *et al.* (1992) 'The small GTP-binding protein rab4 controls an early sorting event on the endocytic pathway', *Cell*, 70(5), pp. 729–740. Available at: https://doi.org/10.1016/0092-8674(92)90307-X.

Söllner, T. *et al.* (1993) 'A protein assembly-disassembly pathway in vitro that may correspond to sequential steps of synaptic vesicle docking, activation, and fusion', *Cell*, 75(3), pp. 409–418. Available at: https://doi.org/10.1016/0092-8674(93)90376-2.

Steegmaier, M. *et al.* (1999) 'Vesicle-associated Membrane Protein 4 is Implicated in Trans-Golgi Network Vesicle Trafficking', *Molecular Biology of the Cell*, 10(6), pp. 1957–1972.

Steinhardt, R.A., Bi, G. and Alderton, J.M. (1994) 'Cell Membrane Resealing by a Vesicular Mechanism Similar to Neurotransmitter Release', *Science*, 263(5145), pp. 390–393.

Sutton, R.B. *et al.* (1998) 'Crystal structure of a SNARE complex involved in synaptic exocytosis at 2.4 Å resolution', *Nature*, 395(6700), pp. 347–353. Available at: https://doi.org/10.1038/26412.

Takáts, S. *et al.* (2018) 'Non-canonical role of the SNARE protein Ykt6 in autophagosome-lysosome fusion', *PLOS Genetics*, 14(4), p. e1007359. Available at: https://doi.org/10.1371/journal.pgen.1007359.

Ullrich, O. *et al.* (1996) 'Rab11 regulates recycling through the pericentriolar recycling endosome', *The Journal of Cell Biology*, 135(4), pp. 913–924. Available at: https://doi.org/10.1083/jcb.135.4.913.

Watanabe, H. *et al.* (2024) 'Ykt6 functionally overlaps with vacuolar and exocytic R-SNAREs in the yeast Saccharomyces cerevisiae', *Journal of Biological Chemistry*, 300(5). Available at: https://doi.org/10.1016/j.jbc.2024.107274.

Wong, S.H. *et al.* (1998) 'Endobrevin, a Novel Synaptobrevin/VAMP-Like Protein Preferentially Associated with the Early Endosome', *Molecular Biology of the Cell*, 9(6), pp. 1549–1563. Available at: https://doi.org/10.1091/mbc.9.6.1549.

Xu, Y. *et al.* (2002) 'GS15 forms a SNARE complex with syntaxin 5, GS28, and Ykt6 and is implicated in traffic in the early cisternae of the Golgi apparatus', *Molecular Biology of the Cell*, 13(10), pp. 3493–3507. Available at: https://doi.org/10.1091/mbc.e02-01-0004.

Yamasaki, S. *et al.* (1994) 'Cleavage of members of the synaptobrevin/VAMP family by types D and F botulinal neurotoxins and tetanus toxin.', *Journal of Biological Chemistry*, 269(17), pp. 12764–12772. Available at: https://doi.org/10.1016/S0021-9258(18)99941-2.

Yang, C. *et al.* (2001) 'VAMP3 Null Mice Display Normal Constitutive, Insulin- and Exercise-Regulated Vesicle Trafficking', *Molecular and Cellular Biology*, 21(5), pp. 1573–1580. Available at: https://doi.org/10.1128/MCB.21.5.1573-1580.2001.

Zhang, S. *et al.* (2017) 'Identification and characterization of a novel botulinum neurotoxin', *Nature Communications*, 8(1), p. 14130. Available at: https://doi.org/10.1038/ncomms14130.

Chapter 3

3. The recombinant light chain of BoNT/X is cytotoxic to cells by inducing apoptosis

Declaration

This chapter has been submitted for examination in the format of a journal manuscript in accordance with the University of Sheffield's thesis format guidelines.

The manuscript was written by Pollyanna A Rouse and Andrew A Peden.

The following data is my own work:

Figure 3 - All data.

Figure 4 - All data.

Figure 5 - All data.

Figure 6 - All data.

The following data is not my own work:

Figure 7 - THP-1 microscopy data, this was conducted by Daniel M Williams.

Figure 8 - The experiments and data were generated by employees at Ipsen Bioinnovation Ltd. I reformatted and plotted the data myself.

The recombinant light chain of BoNT/X is cytotoxic to cells by inducing apoptosis

Authors: Pollyanna A. Rouse, Sarah Donald, Mark Elliott, Andrew A. Peden

Abstract

Botulinum neurotoxins are used therapeutically for a number of conditions such as blepharospasm and in aesthetics. They are generally well tolerated, causing muscle paralysis and show limited cytotoxicity in cell culture. BoNT/X is a novel serotype which cleaves a broader range of R-SNARE than traditional toxins. Expression of the light chain in tissue cultures models leads to pleiotropic defects in intracellular trafficking and causes alterations in the levels of cell surface receptors. To determine if these dramatic alterations in trafficking impact cell viability we have developed several cell lines which express the light chain of BoNT/X under the control of a Tet inducible promoter and developed approaches to electroporate the recombinant light chain into cells. Using these methods we have observed that 24 hours post intoxication a significant number of cells start dying due to apoptosis triggered by the expression of caspases 3 and 7, and by 40 hours the majority of cells are dead. The intoxication triggered cell death can be rescued by the overexpression of cleavage resistant R-SNAREs (VAMP3 and Ykt6) suggesting that this process is SNARE dependent. In parallel to these studies, we have investigated the impact of intoxication on the cell cycle. We have observed increased DNA content in intoxicated cells suggesting that intoxicated cells accumulate in G2 which may be triggering apoptosis.

Introduction

Strains of Clostridium botulinum produce botulinum neurotoxins which can be used therapeutically for a number of conditions ranging from blepharospasm to aesthetics (Pellizzari *et al.*, 1999; Fonfria *et al.*, 2018). Botulinum toxins cause flaccid paralysis by blocking the release of neurotransmitters through the cleavage of SNARE proteins which are present on synaptic vesicles (Montecucco and Schiavo, 1994). Presently, there are 7 main serotypes (BoNT/A-G) that can be further divided into subtypes (e.g. BoNT/A5). Other BoNT and BoNT-like molecules have been identified, including mosaic toxins and chimeric toxins (Moriishi *et al.*, 1996; Nakamura *et al.*, 2010; Maslanka *et al.*, 2016). In 2017 a new stereotype named BoNT/X was identified which has only ~30% similarity with the other serotypes and is closely related to the BoNT-like molecule BoNT/En (Zhang *et al.*, 2017, 2018). BoNT/X cleaves a broader range of SNAREs than other BoNTs, VAMPs 1-5 and Ykt6. By targeting these different substrates, the toxin may be able to target different cell trafficking pathways that other serotypes are not able to. Previous studies have shown that BoNT/X is able to cleave VAMP2 10 times more efficiently than BoNT/B, and it induces paralysis in mice, however, it didn't cause lethality at a dose that typically causes death in other BoNT serotypes (Zhang *et al.*, 2017; Gregg *et al.*, 2024).

Whilst BoNTs are one of the most toxic substances known to humans, BoNTs show limited cytotoxicity in neurons. Many studies have shown that the loss of SNAP-25, Syntaxin 1 or VAMPs 1-3 do not cause cell death in neurons and knockout studies in mice have shown that the brain develops relatively normally in these animals (Schoch *et al.*, 2001). It is known that generally most BoNTs are well tolerated by cells in terms of cell survival, with therapeutic levels causing paralysis (Burgen, Dickens and Zatman, 1949). Cell cytotoxicity has however been observed in some serotypes of BoNT and within specific cell types. A study in 2013 (Peng *et al.*, 2013) showed that neuronal survival was linked to SNAP-25 and Syntaxin 1, which are targeted by BoNT/C and BoNT/E. The cell death was able to be rescued by other SNAREs not targeted by the toxins (Syntaxin 2/3/4 and SNAP-23), demonstrating a level of redundancy in SNAREs involved in cell survival. Interestingly, the block of cell membrane recycling processes was the cause of the cell death rather than the block in synaptic vesicle exocytosis. Further evidence of the cytotoxic effects of BoNT/C due to the cleavage of SNARE proteins has been shown (Arsenault *et al.*, 2014), with the action of cytotoxicity and

apoptosis depending on whether the cells are undifferentiated or differentiated (Rust *et al.*, 2016). This sensitivity when differentiated can be attributed to the loss of SNAP-23 expression in differentiated cells, as SNAP-23 is able to compensate for the loss of SNAP-25 and prevent neuronal cell death. SNAP-25 is typically expressed in neuronal and neuroendocrine cells, whereas SNAP-23 is ubiquitously expressed. Mouse embryos with SNAP-25 K/O are viable (Washbourne *et al.*, 2002). There appears to be a level of genetic redundancy in SNAREs, for example SNAP-23 K/O mice are non-viable (Suh *et al.*, 2011) however, in some cells that contain both SNAP-23 and SNAP-25, such as pancreatic islet cells, SNAP-23 is redundant in the presence of SNAP-25 (Liang *et al.*, 2020).

SNAREs are essential for maintaining normal intracellular trafficking by facilitating membrane fusion, and disruption of these pathways can impact cell survival (Bhattacharya *et al.*, 2002; Kaul *et al.*, 2015). Ykt6 is an R-SNARE that contains a longin domain and is unusual in that it has an inactive form where it is localised in the cytosol, and an active form when it is membrane bound (Fukasawa *et al.*, 2004). The biology of Ykt6 function and modification is widely debated, as it undergoes various modifications, e.g. geranylgeranylation, farnesylation, palmitoylation (Fukasawa *et al.*, 2004; Pylypenko *et al.*, 2008; Shirakawa *et al.*, 2020; McGrath *et al.*, 2021; Sakata *et al.*, 2021). When Ykt6 is phosphorylated at a conserved site, a conformational change occurs allowing the structure to open or close (therefore membrane-bound or cytosolic) (McGrath *et al.*, 2021). Due to its ability to cycle on and off membranes, Ykt6 plays a role in various intracellular trafficking pathways, such as ER-Golgi trafficking (McNew *et al.*, 1997). It has also been demonstrated to be involved in exosome secretion, which is a key driver for cell-cell signalling in cancer, with increased YKT6 expression being linked to reduced survival in non-small cell lung cancer (Ruiz-Martinez *et al.*, 2016). VAMP3 (also known as cellubrevin) is an R-SNARE that is involved in endosomal recycling and endocytosis in cells (McMahon *et al.*, 1993). Studies have shown the inhibition of VAMP3 results in reduced trafficking of β1 integrin to the cell surface, without the reduction of total levels, suggesting there is a block in the trafficking to the membrane, rather than ER-Golgi (Luftman *et al.*, 2009). Integrin is involved in cell adhesion and migration and facilitates cell morphological changes during the cell cycle (mitosis and interphase). Interestingly, a reduction of VAMP3 resulted in reduced cell adhesion suggesting it could play a role in cell survival/cell cycle, however cell

proliferation was not impacted (Luftman *et al.*, 2009). Whilst a loss of VAMP3 has been reported to not impact cell survival, in neuroblastoma studies it was shown that a reduction of VAMP3 resulted in worse neuroblastoma outcomes for the patient, as increased VAMP3 levels reduced cell proliferation and increased apoptosis (Zhang *et al.*, 2023). VAMP3 may have a potential role in Bax induced apoptosis and possess anti-apoptotic properties (Akintade and Chaudhuri, 2021). Despite the potential role of VAMP3 in key cellular processes such as transferrin recycling, the loss of VAMP3 in mice knockout studies does not have an impact on viability (Yang *et al.*, 2001). This leads to the question of the role of R-SNAREs and compensatory mechanisms that may be in place to compensate for the loss of R-SNAREs, and redundancy amongst SNARE proteins.

Apoptosis is a form of programmed cell death and has two key pathways in cells: the intrinsic and extrinsic pathway (Igney and Krammer, 2002; Elmore, 2007). Both pathways involve the action of a family of protease enzymes called caspases. Caspases are cell death/apoptosis mediators that when activated result in DNA fragmentation, Golgi fragmentation, cell shrinkage and blebbing (Cotter *et al.*, 1992; Coleman *et al.*, 2001; Lane *et al.*, 2002). Pyroptosis is a form of programmed cell death that occurs in a similar way to apoptosis, though is an inflammatory response pathway (Cookson and Brennan, 2001; Yu *et al.*, 2021). Like apoptosis, it causes DNA damage and chromatin condensation and is caspase dependent, however in pyroptosis the cells swell prior to rupturing (Fink and Cookson, 2006). The mechanism of pyroptosis causes pores to form in the plasma membrane and the cytoplasm to flatten, resulting in plasma membrane leakage (Chen *et al.*, 2016). In apoptosis, cells retain membrane integrity until late apoptosis/necrosis.

Autophagy is a crucial cellular process that is implicated in cell survival as well as cell death. A key step of autophagy is autophagosome-lysosome fusion, which is known to be facilitated by Syntaxin 17, SNAP-29 and VAMP7/8 (Itakura, Kishi-Itakura and Mizushima, 2012; Guo *et al.*, 2014). However, interestingly it has been shown that Ykt6 is also required in this process as Ykt6 localises to lysosomes and autolysosomes, and forms a SNARE complex with Syntaxin 17 and SNAP-29 (Takáts *et al.*, 2018). VAMP7 can outcompete Ykt6 from this complex, however in this pathway Ykt6 acts as non-conventional regulatory SNARE. It has been shown that Ykt6 and Sec22B function redundantly, as when both are depleted there is a block in secretion and cargo

is trapped in the ER (Gordon *et al.*, 2017). The R-SNARE Sec22B is a crucial SNARE for plasma cells, where it has a non-redundant role. A loss of Sec22B in plasma cells increased apoptosis and cell cycle defects, with more cells in G0 than G1, demonstrating the role of R-SNAREs in cell survival and cell cycle progression (Bonaud *et al.*, 2023).

Preliminary studies conducted in our lab have suggested that the light chain of BoNT/X may be impacting cell proliferation and cell survival, therefore we wanted to elucidate the mechanisms which underpin these observations. To investigate this, we have developed several cell lines which express the light chain of BoNT/X under the control of a Tet inducible promoter and developed approaches to electroporate the recombinant light chain into cells. Using these methods we have observed that cell death occurs in intoxicated cells due to caspase 3 and 7 mediated apoptosis, and this cell death can be rescued by the overexpression of cleavage resistant R-SNAREs (VAMP3 and Ykt6). We have also investigated the impact of intoxication on the cell cycle and have observed increased DNA content in intoxicated cells suggesting that intoxicated cells accumulate in G2 which may be triggering apoptosis.

Materials

Antibodies and ligands

The following antibodies were used in this study: rabbit polyclonal Anti-Ykt6 antibody (ab241276), mouse anti-Ykt6 (ab77150), mouse anti-gamma adaptin (MAB100.3, prepared in-house), Anti-tubulin (Protein-tech, 66240-1-1g), Rabbit anti-VAMP3 as previously described (Gordon *et al.*, 2010). Secondary HRP-conjugated antibodies for immunoblotting used were HRP conjugated goat anti-mouse (Jackson ImmunoResearch 115-035-008), HRP conjugated goat anti-rabbit (Jackson ImmunoResearch 111-035-144), and HRP Conjugated Goat anti-Rabbit IgG (Sigma A6154). The following ligand was used: Transferrin AlexaFluor™ 594 Conjugate (Invitrogen, T13343).

Plasmids

Table 1. Plasmid constructs

Construct	Vector	Notes
GFP-BoNT/X LC active	pEGFP-C3 (Clontech/Takara)	The light chain of BoNT/X (1-439aa) was codon optimised, synthesised and cloned into the vector using XhoI and EcoRI.
GFP-BoNT/X LC active	pLVX-TetOne-Puro (Clontech/Takara)	The GFP-BoNT/X active LC construct was PCR amplified and cloned into the vector using EcoRI/BamHI.
StrepII tag-BoNT/X LC active	pEGFP-C3 (Clontech/Takara)	The construct was made by swapping eGFP with StrepII tag (AgeI/XhoI).
StrepII tag-BoNT/X LC active	pLVX-TetOne-Puro (Clontech/Takara)	StrepII tagged BoNT/X active LC was PCR amplified and cloned into the vector using EcoRI/BamHI.
HA-VAMP3 (VT mutant)	pIRES-Neo2 (Clontech/Takara)	Human VAMP3 (Refseq NM_004781.4) was synthesised with an N-terminal HA tag, R49V/A50T substitutions and cloned into the expression plasmid using EcoRI and NotI.
HA-VAMP3 (VT mutant)	pLXIN-Mod	HA-VAMP3 (VT mutant) was cloned into the vector using EcoRI and NotI.
HA-Ykt6 (VT mutant)	pIRES-Neo2 (Clontech/Takara)	Human Ykt6 (Refseq NM_006555.4, 1-198aa) was synthesised with an N-terminal HA tag, K173V/S174T substitutions and cloned into the expression plasmid using NheI and NotI.
HA-Ykt6 (VT mutant)	pLXIN-Mod (Clontech/Takara)	HA-Ykt6 (VT mutant) was cloned using XhoI/NotI.

Methods

Cell culture and maintenance

HeLa-M and HEK-293T cells were cultured and maintained in high glucose DMEM media supplemented with 10% fetal bovine serum (FBS), 100 IU/mL penicillin, 100 µg/mL streptomycin and 2 mM glutamine at 37℃ in a 5% CO_2 humidified incubator.

T98G cells were maintained in MEM supplemented with 2 mM Glutamine, 1% Non Essential Amino acids, 1% Sodium Pyruvate and 10% FBS. THP1 cells were maintained in RPMI supplemented with 10% FBS and 100 IU/mL penicillin, 100 µg/mL streptomycin and 2 mM glutamine.

Stable cell line generation using a tet-inducible system

The light chain of BoNT/X (1-439aa) was synthesised either with an N-terminal GFP or StrepII tag by Genscript and cloned into the Tet inducible lentiviral expression vector pLVX-TetOne-Puro. HEK-293T cells were transfected with the 5 µg pLVX-TetOne-Puro-LC/X construct, 5 µg psPAX2 (Addgene:12260) and 1 µg pCMV VSV-G (Addgene:8454) using 33 µg PEI. The viral containing media was collected 48 hours post transfection, polybrene added (final concentration 5 µg/mL) and filtered using a 0.45 µm syringe filter (Sartorius). HeLa-M or THP-1 cells were infected with the virus particles and centrifuged at 2000 x g for 75 minutes at room temperature, prior to incubation at 37℃. Cells expressing the constructs were selected using 1 µg/mL puromycin for 1 week (**Figure 1**).

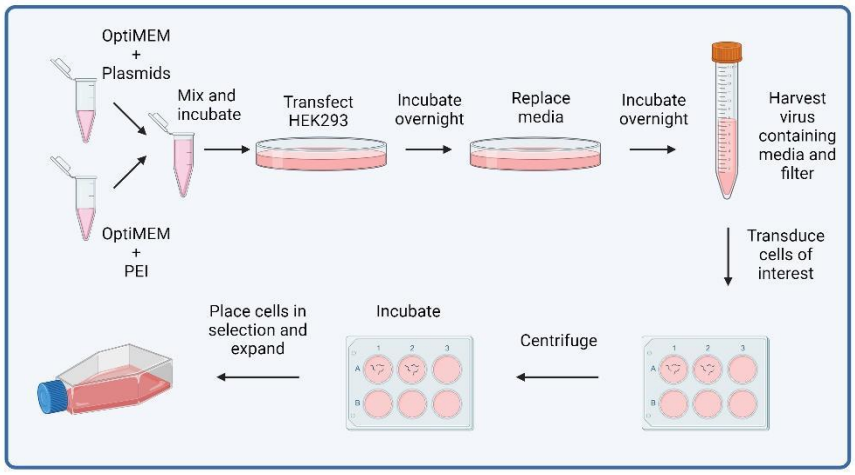

Figure 1. Method for the creation of stable cells expressing a tet-inducible LC/X Created with BioRender.com.

HeLa-M cells were auto-cloned into a 96-well plate using a FACSMelody cell sorter (BD Biosciences). Clonal cell lines were screened for expression of the light chain constructs by inducing the cells with doxycycline and assessing either GFP expression

or StrepII signal by staining with Strep-Tactin XT DY-488 (IBA Lifesciences, 2-1562-050) (**Figure 2**).

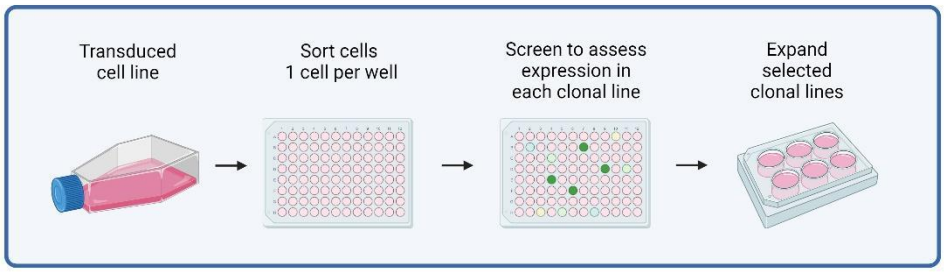

Figure 2. Method for the creation of clonal cell lines
Created with BioRender.com.

Stable cell line generation for tet-inducible rescue constructs

HA-tagged Ykt6^{VT} (K173V/S174T) and HA-tagged VAMP3^{VT} (R49V/A50T) were synthesised by Genscript and cloned into the retrovirus expression vector pLXIN (Clontech). HEK-293T cells were transfected with the 5 µg pLXIN construct, 5 µg puMVC (Addgene: 8449) and 1 µg pCMV VSV-G (Addgene: 8454) using 33 µg PEI. The viral containing media was collected 48 hours post transfection, polybrene added (final concentration 5 µg/mL) and filtered using a 0.45 µm syringe filter (Sartorius). The stably expressed Tet-inducible GFP-LC/X and Strep-LC/X cells were infected with the virus particles and centrifuged at 2000 x g for 75 minutes at room temperature, prior to incubation at 37℃. Cells were selected for 1 week using 1 mg/mL G418 (Roche).

Recombinant production of active and inactive LC/X in bacteria

The following proteins were generated and purified: active LC/X protein (10HT-LC/X (aa 1-438) (C423A)) and inactive LC/X protein: (10HT-LC/X (E228Q/H231Y) (aa 1-438) (C423A)). The C423A mutation prevents dimerisation via the disulphide bridge. To clone the inactive mutation, the Q5 Site-directed Mutagenesis Kit (NEB E0554) was used according to the manufacturer's instructions.

Proteins were expressed in NEB 5-alpha competent E. coli, grown and bacteria was harvested by centrifugation at 4℃. Cells were lysed using a homogeniser (Constant Systems) at 20 kpa and centrifuged for clarification. Proteins were purified using an AKTA Pure FPLC system (Cytiva) using a HisTrap HP column (GE #17524802), and

eluted using increasing concentrations of imidazole: 16%, 25%, 50% and 100% of 50 mM Tris pH 8, 200 mM NaCl, 500 mM Imidazole into fractions. Elution fractions were pooled and desalted using a HiPrep 26/10 desalting column (GE #17508701) into PBS pH 7.2 (Gibco).

Protein electroporation

A Neon transfection system (Invitrogen) was used to electroporate cells. T98G cells were harvested, washed with PBS, and resuspended in Resuspension buffer R to a final density of $2x10^7$ cells/mL. An electroporation tube with 3 mL electrolyte buffer E was placed in the pipette station and the pulse conditions were set. LC/X protein was transferred at the desired concentration to a 0.5 mL tube. Cells were added to the tube and mixed. The cell/protein mixture was drawn up into a tip and the Neon™ device started. Once complete, 400 µL of media was added to the cells and the cells were transferred to cell culture plates (100 µL to 96 well, 50 µL to half area 96 well).

Microscopy

T98G cells in 96 well plates were grown in the Incucyte (Sartorius) for 72 hours post-electroporation and representative images were captured. THP-1 cells were induced with 1 µg/mL doxycycline (Sigma) and 1 µg/mL PI (Merck 81845) in wells prior to live imaging using a Nikon widefield live-cell microscope with a 20x Plan Apo objective lens. Images were captured every 10 minutes for 15 hours. Frames were analysed using FIJI ImageJ (Schindelin ***et al.***, 2012).

Western blotting

Clonal tet-inducible cells were lysed in SDS-PAGE sample buffer (Bio-Rad) supplemented with 5% (v/v) mercaptoethanol and boiled at 95℃, prior to separation using SDS-PAGE gel electrophoresis. Proteins were then transferred overnight onto PVDF membranes using wet transfer methods. The membranes were blocked using 5% milk in one times PBS-Tween20. The membranes were probed with antibodies against VAMP3 and YKT6, and gamma adaptin and beta tubulin were used as loading controls. The primary antibodies were detected by using secondary antibodies conjugated to HRP and developed using ECL substrate. Membranes were imaged

using LI-COR C-DiGit® blot scanner (LI-COR Biosciences) and Image Studio Lite Software (LI-COR Biosciences).

T98G cells were lysed in 25% NuPAGE sample buffer (Fisher Scientific) supplemented with 10 mM DTT and 250 units/µL Benzonase (Sigma), prior to separation using SDS-PAGE gel electrophoresis. Proteins were transferred to nitrocellulose membranes. The membrane was probed with an antibody against Ykt6. The primary antibody was detected by using a secondary antibody conjugated to HRP and developed using ECL substrate (Fisher Scientific). The membrane was imaged and analysed using a Syngene GeneGnome (Syngene Bioimaging).

Cell viability assay

Cells were seeded at 1200 cells/ well in 96 well half-area plates. Cells were treated with 1 µg/mL doxycycline (Sigma) for 16 or 48 hours. Cell viability was assayed using the CellTitre Glo luminescence cell viability assay kit (Promega). Reagents were used according to manufacturer's instructions (50 µL reagent:50 µL media). Luminescence acquired using a Perkin Elmer Envision 2104 Multilabel Plate Reader.

Caspase 3/7 activation assay

Cells were seeded at 1200 cells/ well in 96 well half-area plates. Cells were treated with different concentrations of doxycycline (0.1-2 µg) (Sigma) and incubated for 24 hours at 37℃. The Caspase-Glo 3/7 Assay (Promega) was used according to manufacturer's instructions, incubating for 60 minutes prior to acquisition using a Envision 2104 Multilabel Plate Reader (Perkin Elmer).

GFP-LC/X expression

Tet-inducible cells were seeded in 12 well plates prior to induction with 1 µg/mL doxycycline (Sigma). 8-, 16- and 24-hours post-induction, cells were trypsinised and centrifuged. Fresh media was used to resuspend cells prior to GFP signal measurement using an Attune NXT flow cytometer (Invitrogen).

Transferrin uptake

Tet-inducible cells were seeded in 12 well plates prior to induction with 1 µg/mL doxycycline (Sigma). 16 hours post-induction, cells were trypsinised and centrifuged.

Cell pellets were resuspended in Transferrin Alexa Fluor™ 594 (Invitrogen) diluted in fresh media (25 µg/mL) and incubated for 10 minutes at 37℃. Cells were washed twice with fresh chilled media and resuspended in 1% PFA. Mean fluorescence intensity was measured using an Attune NXT flow cytometer (Invitrogen).

Apoptosis assay

Cells were seeded at 60,000 cells per well and light chain expression induced with 1 µg/mL doxycycline and cells collected 40 h, 24 h and 16 h post induction. Cells were dissociated from the plate using TrypLE (Gibco), then diluted with media prior to centrifugation to remove the TrypLE. The amount of apoptosis was determined by measuring fluorescence of PI and Annexin V staining. Using an Annexin V detection kit (88-8007-72, Invitrogen), cells were incubated for 10 minutes with Annexin V-647, washed, then incubated with PI. Fluorescence was measured using a Cytek Aurora 3 laser cytometer. Data was acquired using SpectroFlo software (Cytek).

Cell cycle analysis

Cells were seeded at 80,000 cells per well. Cells were incubated for 16 hours with 1 µg doxycycline (Sigma) and 9 µM RO-3306 (Santa Cruz, sc-359700). After 16 hours, cells were washed, and media added before returning cells to the incubator for 3 hours. Cells were fixed using 70% EtOH and placed at -20℃. After fixation, cells were washed with 1X PBS then permeabilised using saponin/BSA, prior to staining with Strep-Tactin XT Dy-488 (IBA Lifesciences, 2-1562-050) for 45 minutes. Cells were washed and placed in 1X PBS containing PI (Merck, 81845) and 0.5 mg/mL RNase A (Thermo Scientific, R1253). Cells were incubated at 37℃ for 30 minutes prior to acquisition. Fluorescence was measured using an Attune NXT flow cytometer.

Data analysis

All flow cytometry experiments were analysed using FlowJo™ v10.8 Software (BD Life Sciences. Graphs for figures were made using GraphPad Prism version 9.0. For statistical analyses, One-way ANOVA followed by Dunnett's multiple comparisons test was performed using GraphPad Prism version 9.0 (GraphPad Software, USA).

Results

A lentiviral tet inducible system can be used to regulate LC/X expression

The light chain of BoNT/X can cleave recombinant R-SNAREs VAMPs 1-5 and Ykt6 (Zhang *et al.*, 2017), and severely perturbs endomembrane trafficking when expressed in HeLa-M cells (Asnawi, 2021; Chapter 2). In addition, we also have observed a reduction in cell number and changes in cell morphology in intoxicated cells suggesting that the construct may be cytotoxic (Asnawi, 2021; Chapter 2). To explore these phenotypes more systematically, we have used a tet-inducible lentiviral system to generate transduced cell populations expressing either GFP or StrepII tagged LC/X. Having the ability to tightly regulate the expression of these constructs should make it easier to study the impact of intoxication on cell viability without having to deal with confounding factors caused by transient transfection (Kim and Eberwine, 2010). To determine the optimal time required for light chain expression, a time course experiment was conducted where the cells were treated with doxycycline (**Figure 3A**). We observed that the GFP-LC/X can be detected 8 hours post-induction, with the levels increasing at 16 and 24 hours.

We have previously observed that the light chain of BoNT/X can significantly block transferrin uptake in intoxicated cells 16 h post transfection due to loss of the receptor from the cell surface (Asnawi, 2021; Chapter 2). To determine if the tet-inducible system perturbs transferrin trafficking in a similar way to transient LC/X expression, cells were incubated with Dox for increasing amounts of time and transferrin uptake measured via flow cytometry (**Figure 3B**). In cells expressing the light chain (GFP positive), the uptake of transferrin is significantly perturbed after 8 hours, showing that the tet-inducible promoter can efficiently drive expression of the construct. During these pilot experiments it became clear that not all of the cells in the population were doxycycline responsive so a round of clonal selection was performed to identify clones which showed more uniform expression of the light chain (data not shown). These clonal cell lines were used for all further experiments.

To determine if the transferrin phenotype is specific to the cleavage of SNAREs, a clonal tet-inducible cell line was transduced with versions of Ykt6 and VAMP3 which had been engineered to be resistant to LC/X (as described in Chapter 2) (**Figure 3C**

and D). The stable cells lines were then incubated with dox for 16 h and transferrin uptake measured. As a positive control for GFP expression, non-induced cells were transfected with a GFP plasmid. As previously observed (Chapter 2), overexpression of VAMP3^{VT} and Ykt6^{VT} rescues transferrin uptake. Surprisingly, overexpression of Ykt6^{VT} in intoxicated cells appears to enhance transferrin uptake compared to non-intoxicated cells.

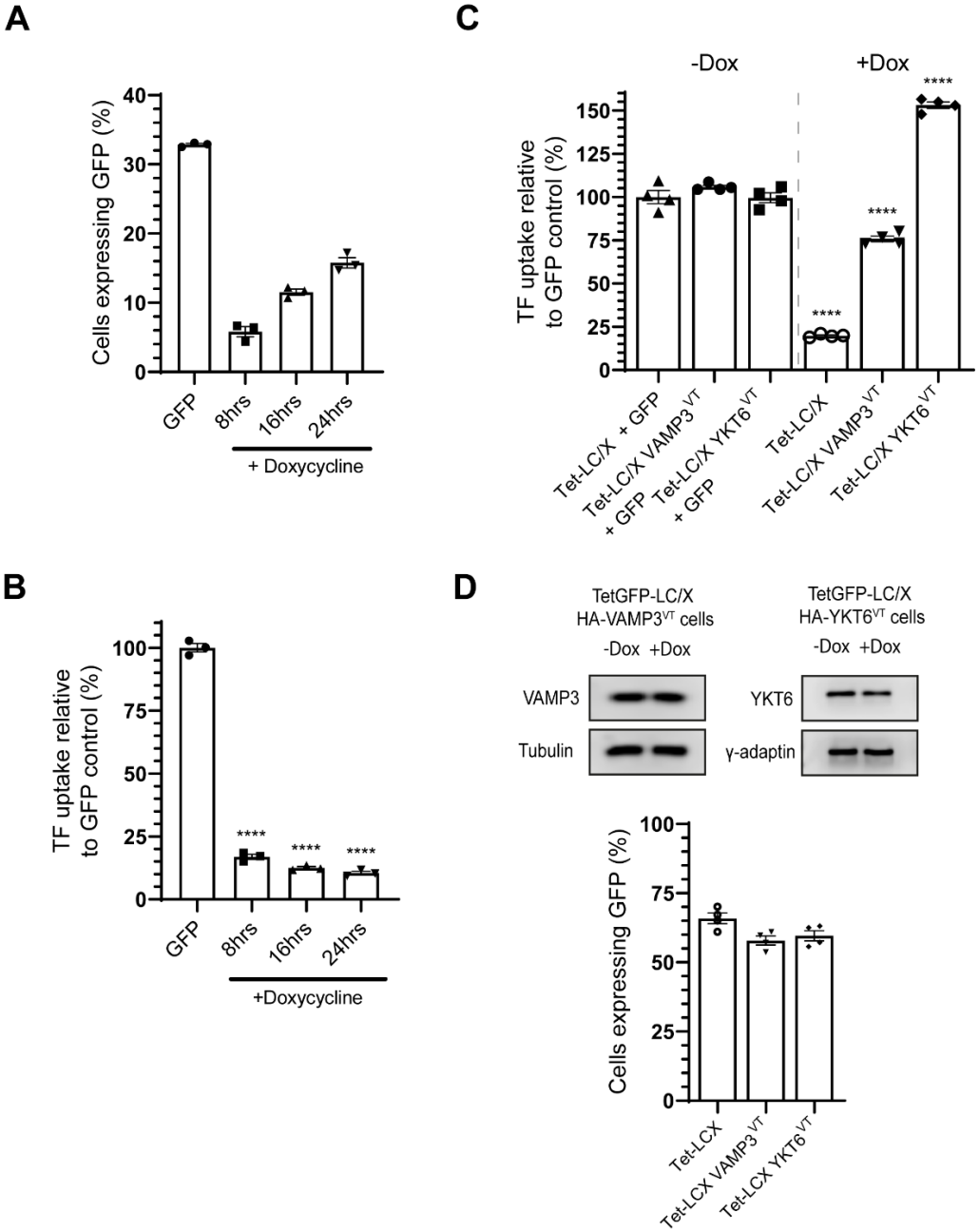

Figure 3. Characterisation of tet-inducible cell lines for studying LC/X intoxication

(**A**) To assess how quickly the GFP-LC/X is expressed in response to doxycycline a stable population of transduced cells was treated for 8-24 hours and the levels of GFP-

LC/X determined by flow cytometry. As a positive control a GFP plasmid was transiently transfected into non-induced cells. Error bars represent the SEM. (**B**) To determine the impact of GFP-LC/X expression on transferrin uptake the cells were incubated with dox for 8, 16 and 24 hours. The cells were then trypsinised and incubated with Transferrin Alexa Fluor™ 594 for 10 minutes at 37℃. The amount of fluorescent transferrin taken up by the GFP/LC-X positive cells was measured using flow cytometry and normalised to the non-induced cells expressing that had been transfected with GFP as control. Error bars represent the SEM. One-way ANOVA with Dunnett's multiple comparison was performed for analysis, **** P<0.0001. (**C**) To determine if the transferrin phenotype is specific to SNARE cleavage the indicated cell lines were incubated with dox for 16 hours. The cells were trypsinised and incubated with Transferrin Alexa Fluor™ 594 for 10 minutes at 37℃. The mean intensity of the transferrin fluorescence was measured using flow cytometry in the GFP/LC-X positive cells and normalised to the non-induced cells which had been transfected with GFP (-Dox). Error bars represent the SEM. One-way ANOVA with Dunnett's multiple comparison was performed for analysis, **** P<0.0001. (**D**) To assess the expression of GFP-LC/X from these cell lines, the percentage of cells expressing GFP was also calculated from the transferrin uptake data. Error bars represent the SEM. To confirm the expression of the R-SNARE constructs (HA-VAMP3^{VT} and HA-Ykt6^{VT}) in the tet inducible cell lines, lysates were prepared and separated by SDS-PAGE. Membranes were probed using antibodies for VAMP3, Ykt6 and GFP. Tubulin and gamma adaptin were used as loading controls.

LC/X Intoxication causes a dramatic loss of cell viability and the activation of caspase 3 and 7

To determine how LC/X expression impacts cell viability the tet-inducible cells were incubated with doxycycline for 16 and 48 hours, and the levels of ATP measured using the CellTitre Glo luminescence reagent (**Figure 4A**). After 16 hours of induction, there is only a slight decrease in viability as previously observed (Asnawi, 2021). However, by 48 hours post treatment the viability drops significantly and only ~2% of cells are viable. Almost identical results were observed for the GFP and StrepII tagged light chain constructs indicating that the tags are not impacting the activity of the recombinant light chains.

To determine if the intoxicated cells were dying via apoptosis, a luminescence-based caspase 3/7 assay was performed on cells after 24 h of induction (**Figure 4B**). The Caspase-Glo 3/7 assay reagent contains a proluminescent aminoluciferin substrate that is cleaved by caspases, allowing for the free aminoluciferin to be consumed by luciferase. This produces a luminescent signal proportional to caspase 3/7 activity. Significant levels of caspase 3/7 activity were observed even with the lowest concentrations of doxycycline suggesting that the light chain expression induces apoptosis in intoxicated cells.

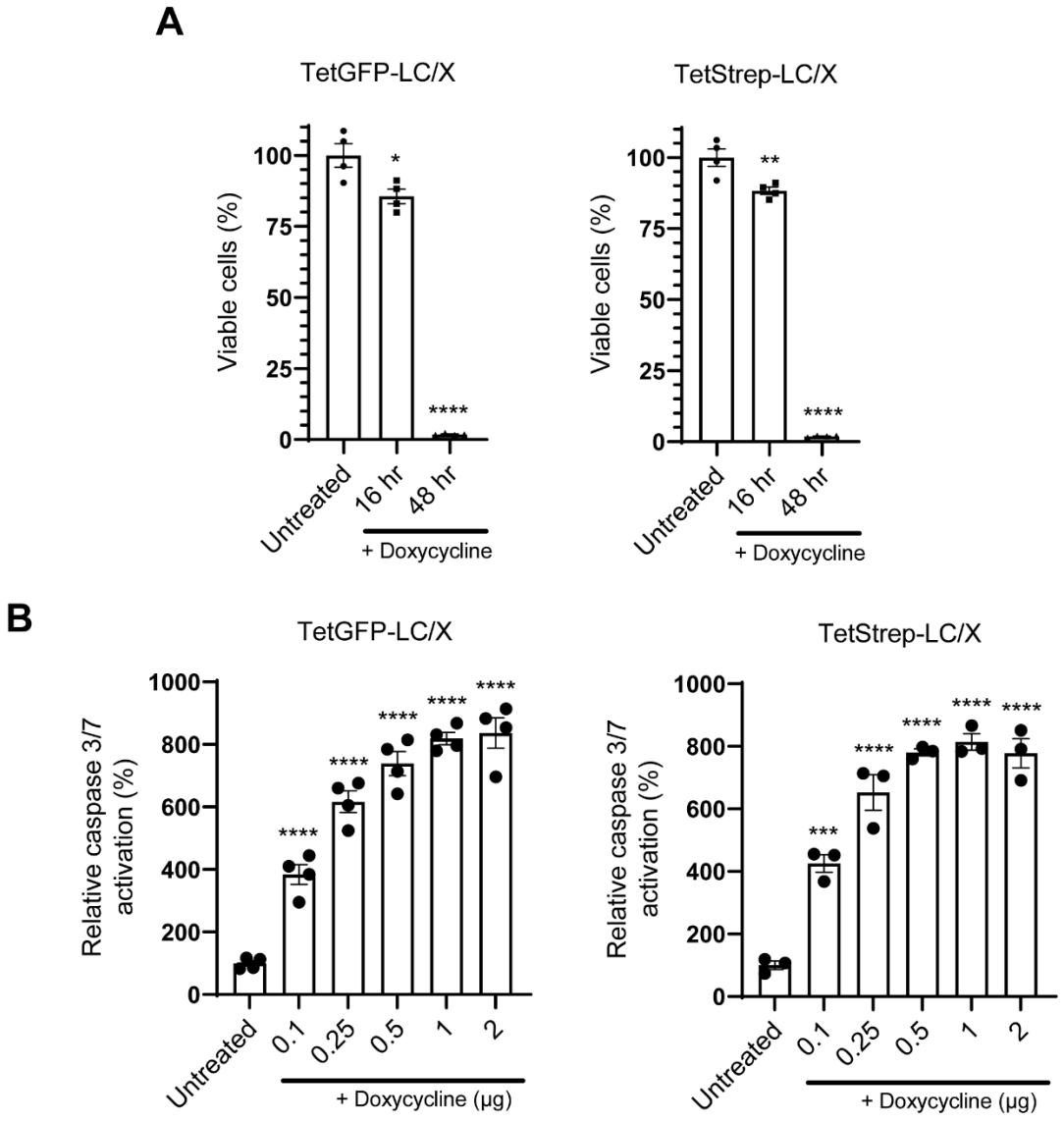

Figure 4. LC/X intoxication results in loss of cell viability and causes caspase 3/7 activation

(**A**) Tet-GFP-LC/X and Tet-Strep-LC/X cells were incubated with 1 µg/mL of doxycycline for 16 or 48 hours, and cell viability measured using the CellTitre Glo

assay (Promega). Error bars represent the SEM. One-way ANOVA with Dunnett's multiple comparison was performed for analysis, * P=0.0100, ** P=0.0040, **** P<0.0001. (**B**) To determine if BoNT/X intoxication induces apoptosis through the activation of Caspases 3/7, Tet-GFP-LC/X and Tet-Strep-LC/X cells were induced for 24 h using either 0.1, 0.25, 0.5, 1 or 2 µg/mL of dox. The Caspase 3/7 Glo reagent was added to the cells and luminescence measured. Caspase activation shown as a percentage compared to the untreated control. Error bars represent the SEM. One-way ANOVA with Dunnett's multiple comparison was performed for analysis, *** P=0.0001, **** P=<0.0001.

Cleavage resistant R-SNAREs can rescue LC/X induced apoptosis

To further explore how the intoxicated cells were dying a time course experiment was performed and the levels of Annexin V and PI staining assessed using flow cytometry (**Figure 5**). Annexin V stains apoptotic cells as phosphatidylserine translocates from the inner surface of the plasma membrane to the external surface in early apoptosis. Cells that are still viable will not stain for PI whereas late apoptotic cells/necrotic cells will stain positively for PI and Annexin V as the cell membrane is no longer intact. At the earlier time points very few cells were PI and Annexin V positive indicating that they are still viable in support of our previous observations (Asnawi, 2021; Chapter 2). However, at the 40 h time point most of the cells are positive for Annexin V and PI indicating that they are in late apoptosis or have already died.

To assess if cleavage of Ykt6 and/or VAMP3 are responsible for cell death we intoxicated cells overexpressing cleavage resistant versions of these proteins and repeated the Annexin V experiment. Approximately 85% of Ykt6^{VT} cells and 70% of VAMP3^{VT} cells were still viable at 40 h suggesting that the loss of these SNAREs is likely the trigger for cell death.

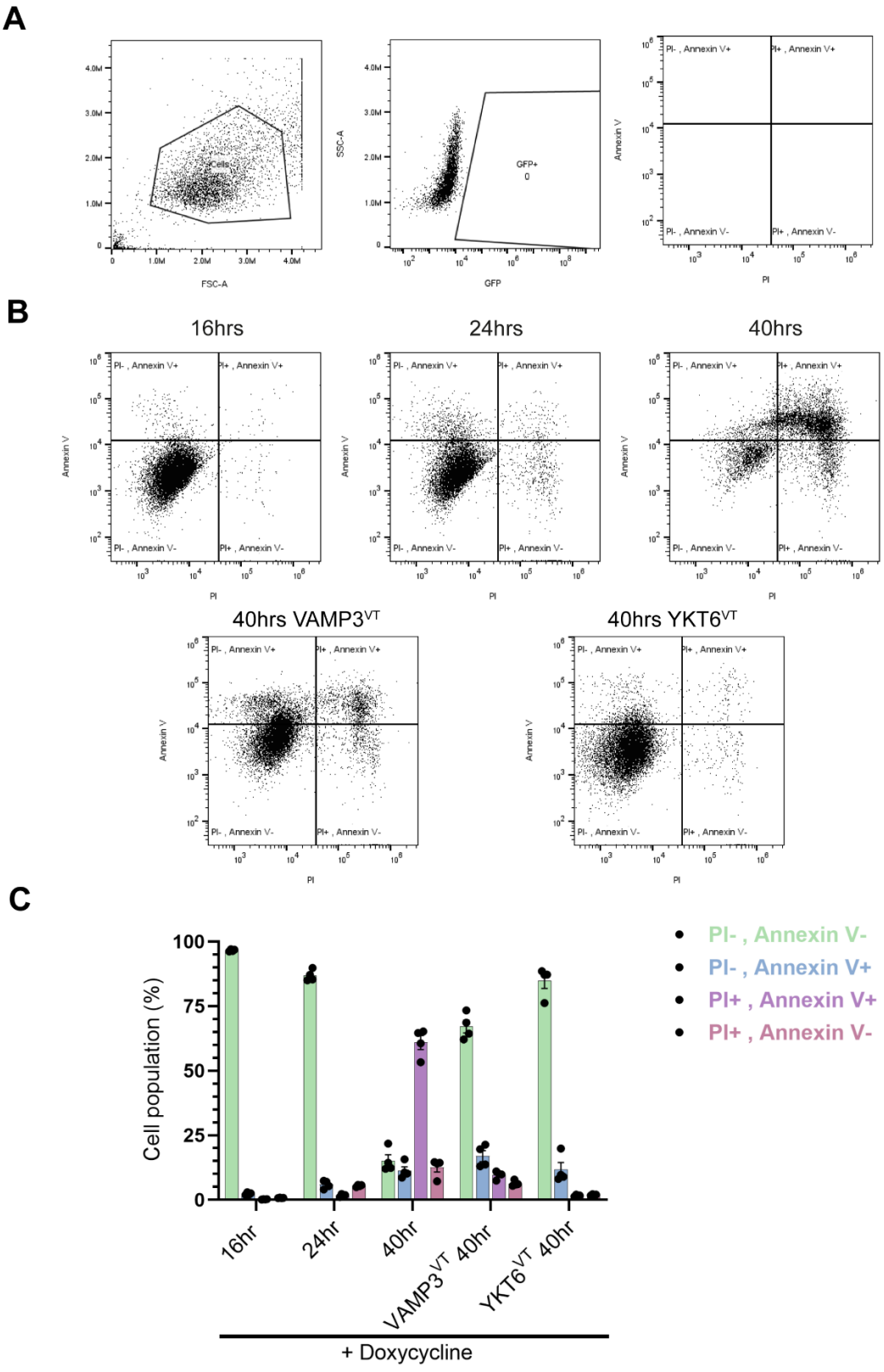

Figure 5. LC/X induced apoptosis can be rescued using cleavage resistant R-SNARE

HeLa-M cells stably expressing Tet-inducible GFP-LC/X were incubated with 1 µg doxycycline for 16, 24 and 40 h. Cells expressing Tet-inducible GFP-LC/X with either

HA-VAMP3^{VT} or HA-Ykt6^{VT} were also induced for 40 h. The cells were then collected and stained with Annexin V and PI. (**A**) Representative examples of gating methods utilised to assess viable/apoptotic/necrotic/dead cell populations. (**B**) Dot plots of the induced cells stained with Annexin V and PI. Using spectral flow cytometry, cells were gated for GFP-LC/X positive cells and the fluorescence of Annexin V APC and PI were measured. (**C**) Percentages of cell populations that are viable, apoptotic, or dead. Error bars show the SEM.

LC/X intoxication perturbs the cell cycle

We have previously observed that transiently intoxicated HeLa cells appear not to proliferate as quickly as mock transfected cells (unpublished observation, Peden lab) suggesting that blocking intracellular trafficking is impacting cell division. To assess if the LC/X is impacting the cells' ability to progress normally through the cell cycle and undergo mitosis, StrepII-LC/X cells were induced for 16 h and cell cycle analysis performed (**Figure 6**). In the non-intoxicated cells, the cells have a normal distribution with 66% of cells in G1, 9% in S phase, and 25% in G2 which is comparable with previous cell cycle studies on HeLa cells (Trinkle-Mulcahy *et al.*, 2003). However, in the intoxicated cells there was a dramatic shift in the distribution of the cells so that almost twice as many were in G2 (50%). To further investigate these observations the cells were synchronised at the G2/M phase using RO-3306 drug (Vassilev *et al.*, 2006) and the block released for 3 hours and cell cycle analysis repeated as before. In the non-intoxicated cells approximately 49% of the cells were in G1, 8% in S-phase, and 42% in G2 indicating that the cells were able to progress through the cell cycle after drug wash out. However, in the intoxicated cells most of the cells remained in the S/G2 phase (87%) and failed to progress to G1 (12%) suggesting that there is a serious defect in cell cycle progression. In the intoxicated cells there is a dramatic reduction in the percentage of cells in G1 (12%) and most of the cells have accumulated in S/G2 phase (87%) suggesting that intoxicated cells are unable to exit the S/G2 phase.

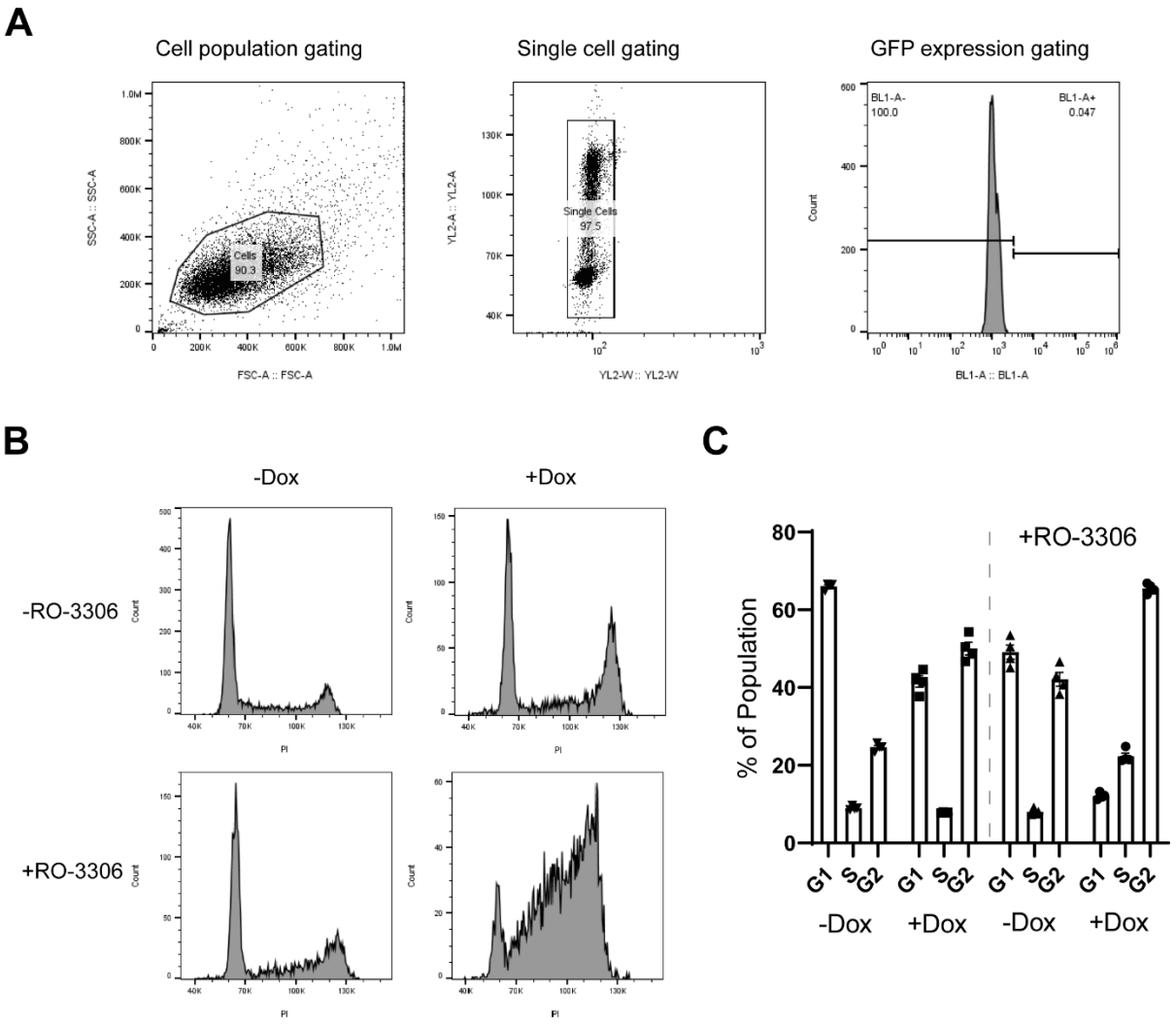

Figure 6. The cell cycle in HeLa-M cells is altered by StrepII-LC/X intoxication

To determine if BoNT/X intoxication reduces cell proliferation due to a block in cell cycle progression, we measured the DNA content in cells expressing the LC/X. (**A**) Gating strategy used. (**B**) Plots to show the DNA content of cells with and without RO-3306 and doxycycline. Cells were incubated with doxycycline and RO-3306 for 16 h, to synchronise and arrest the cells at G2/M. After 16 hours of induction, the cells were released from the synchronisation for 3 hours. The cells were fixed using ethanol, stained with Strep-tactin 488, then treated with RNase A and stained for PI. Cells were gated for single cell population, and for doxycycline treated cells the GFP positive population. The DNA content was measured using an Attune NXT flow cytometer and analysed using FlowJo. (**C**) The percentages of each stage of the cell cycle, calculated using the cell cycle analysis tool (Watson pragmatic) on FlowJo™ Software. One-way ANOVA with Dunnett's multiple comparison was performed for analysis, P=<0.0001.

To investigate the impact of LC/X on another cell type, we transduced THP-1 cells with Tet-StrepII-LC/X. THP-1 cells are monocytes derived from blood from an acute monocytic leukaemia patient (Tsuchiya *et al.*, 1980). They are useful for measuring inflammatory responses in cells and are used to study programmed cell death via pyroptosis (Miglio, Veglia and Fantozzi, 2015; Eudy and da Silva, 2021). To assess the impact of intoxication on THP-1 viability the cells were incubated with propidium iodide (PI) and imaged over 15 hours by live cell microscopy (**Figure 7**). PI is a DNA stain which is excluded from viable cells which have an intact plasma membrane thus cells which become PI positive are dead. In the cells treated with doxycycline there was a dramatic increase in PI positive cells compared to the control indicating that intoxication is killing them. PI positive cells started appearing 3 hours into the incubation which is significantly faster than what we have observed in HeLa-M cells suggesting that these cells are either more sensitive to the toxin and/or are dying via a different mechanism. Interestingly, many of the PI positive cells appear to have two nuclei suggesting that they are undergoing cell division when they die.

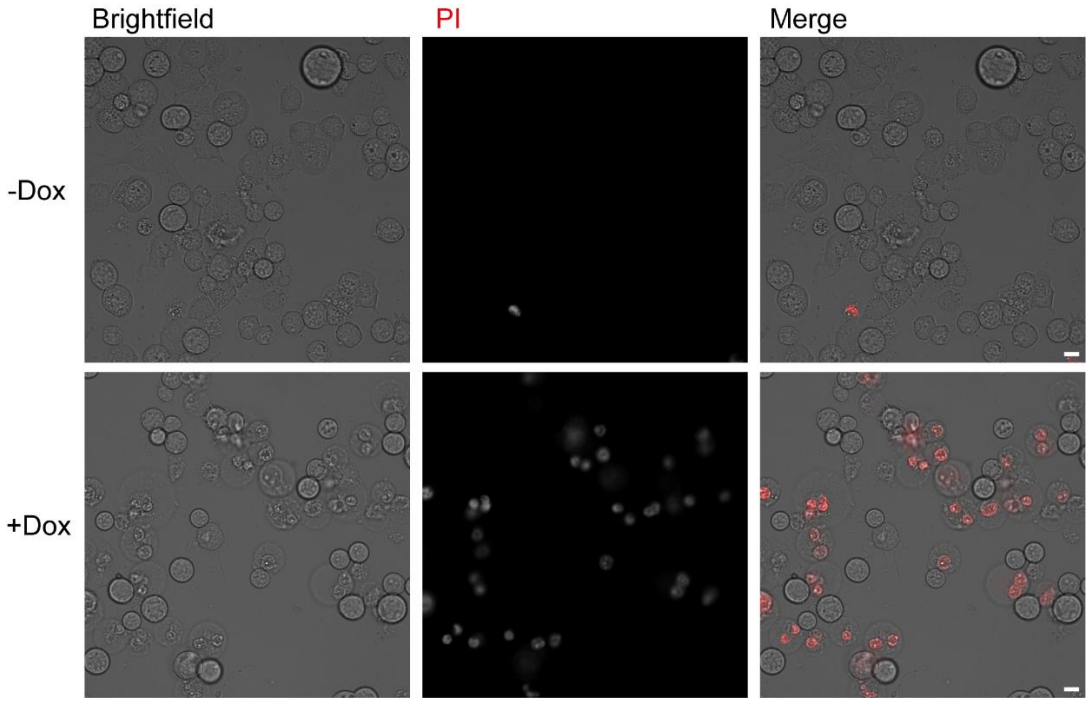

Figure 7. LC/X intoxication results in loss of cell viability in THP-1 cells

THP-1 cells stably expressing Tet-Strep-LC/X were incubated with 1 µg/mL of dox and 1 µg/mL PI and imaged using a Nikon Widefield Live-cell microscope. Images were captured every 10 minutes for 15 hours. The representative images displayed are from 9 hours (T54) post-induction. Scale bar = 20 µm.

Electroporation of LC/X protein into cells drastically reduces cell viability

To establish whether the phenotypes observed in HeLa-M cells are applicable to other tissue culture cell lines and determine if altering the way the light chain is delivered to cells impacts intoxication, we developed a method for delivering His-tagged LC/X into cells via electroporation (**Figure 8**). T98G cells were electroporated with the indicated concentrations of active and inactive His-tagged LC/X and cell viability measured at 24, 48 and 72 h post transfection (**Figure 8A**). LC/X intoxication drastically reduces cell viability in a dose dependent manner unlike the catalytically inactive version of the protein. In support of these observations, intoxicated cells showed a dramatic reduction in cell number and gross changes in cell morphology 72 h post transfection (**Figure 8B**). In parallel to the cell viability studies, samples were prepared in duplicate for immunoblotting to determine whether the changes in viability correlated with Ykt6 cleavage (**Figure 8C**). No Ykt6 cleavage was observed from the samples electroporated with the inactive light chain (5 µM). In the samples treated with active LC/X a dose dependent increase in Ykt6 cleavage was observed by the appearance of a lower molecular weight species on the blots. Due to the limited number of cells present in the 5 µM sample no signal for Ykt6 was detected.

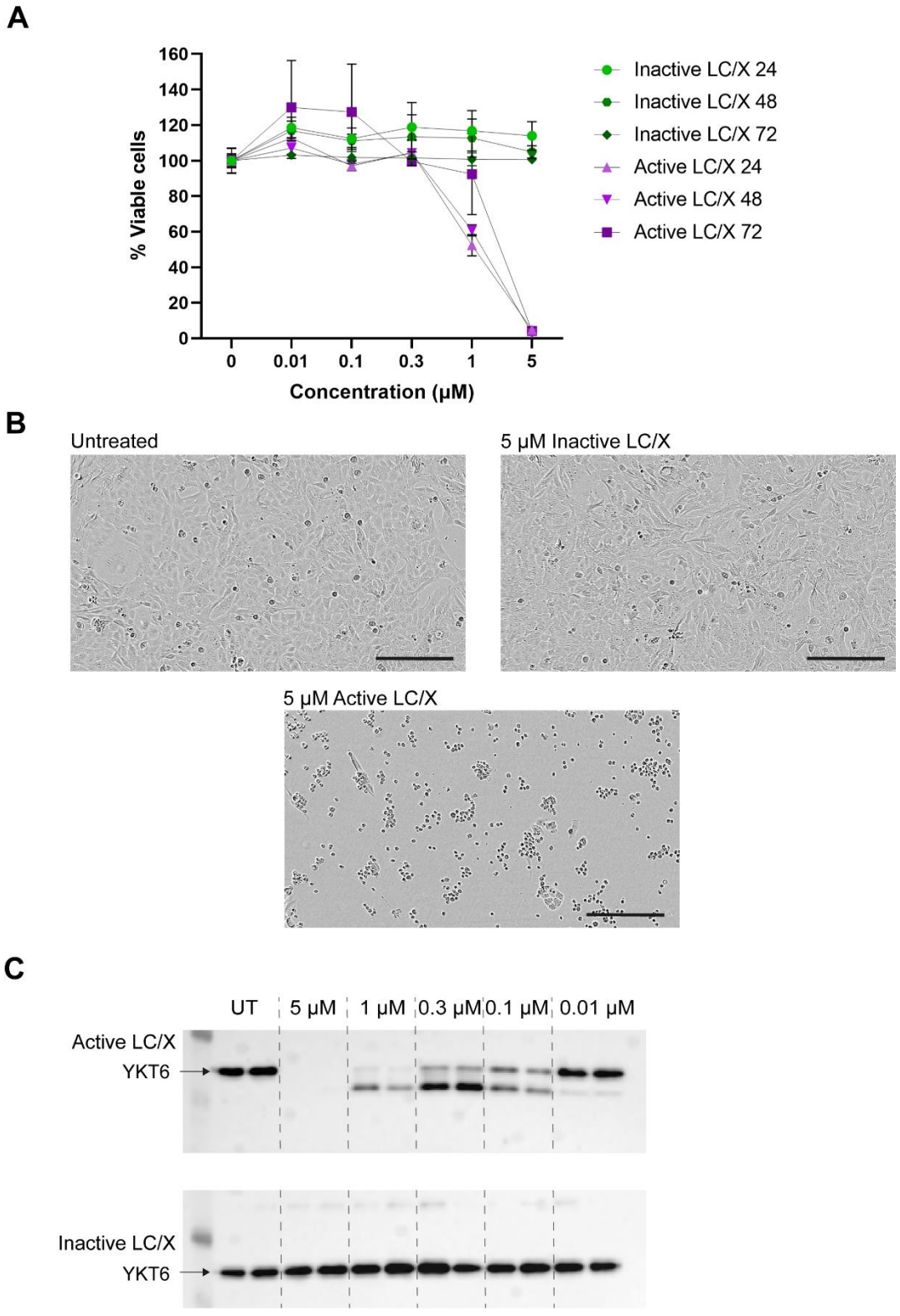

Figure 8. Electroporated LC/X protein reduces cell viability in T98G cells

(**A**) T98G cells were electroporated with the indicated concentrations of LC/X and their viability measured at 24, 48 and 72 h using the CellTitre Glo viability assay. Error bars represent the SEM. (**B**) T98G cells were electroporated with either 5 μM active LC/X or inactive LC/X and imaged using an Incucyte (representative image shown for 72 h

time point). Scale bar = 300 µm. (**C**) T98G cells were electroporated with the indicated concentrations of active LC/X and inactive LC/X and samples collected at 72 h and lysed. Proteins were separated using an SDS-PAGE gel and transferred to a nitrocellulose membrane. Membrane was probed for Ykt6 to assess SNARE cleavage.

Discussion

In this study we aimed to understand the impact of BoNT/X intoxication on cell viability and progression through the cell cycle. We have generated cell lines expressing either a GFP or StrepII tagged LC/X using a tet-inducible promoter, and a clonal tet-inducible cell line that expressed cleavage resistant versions of Ykt6 and VAMP3. In LC/X intoxicated cells, cell viability remains high at 16 hours, however 48 hours post treatment the cells are largely non-viable. We determined that LC/X expression activates caspase 3/7 suggesting the cells are dying due to apoptosis. This was further supported by an Annexin V/PI assay, which indicates that the majority of intoxicated cells were either in late apoptosis or dead 40 h after induction. Overexpression of cleavage resistant forms of VAMP3 and Ykt6 rescue these phenotypes indicating that these phenotypes are caused by SNARE proteolysis. Intoxicated cells accumulate in G2/M of the cell cycle, and in THP-1 cells many of the cells appear to have two nuclei when they die, suggesting that defects in cell division may be triggering apoptosis.

Is BoNT/X causing cell death due to the specific proteolysis of SNAREs?

It has been previously observed that cells intoxicated with BoNT/X show good viability after 16 h of intoxication. However, there was a significant reduction in the number of transfected cells suggesting that BoNT/X may be interfering with cell proliferation. To investigate this further, we developed a tet inducible LC/X cell line and measured cell viability at 24 and 48 hours after induction. LC/X expression leads to significant levels of cell death 48 h after intoxication. To investigate the potential mechanism of cell death we looked at the levels of Caspase 3/7, which are known to be activated during apoptosis. We have demonstrated that intoxication with LC/X induces the expression of Caspase 3/7 and leads to Annexin V positive cells which can partially be rescued by overexpression of VAMP3 and Ykt6. However, it is unclear why loss of these SNAREs is triggering this pathway. The intrinsic pathway of apoptosis can be activated by different processes, either a negative signal where there is a lack of apoptotic

suppression or positive signals that activate apoptosis. There are several mediators of apoptosis activation in cells, such as the Bcl-2 family of proteins. These proteins can be either pro-apoptotic or anti-apoptotic and have been linked to the ER stress response in cells. Another regulator of apoptosis is the BH3 family of proteins, of which BNIP1 is a member. BNIP1 is found in the nuclear envelope and the ER (Boyd *et al.*, 1994) and has been shown to interact with syntaxin 18 to form a SNARE complex (Nakajima *et al.*, 2004). The BNIP1-Syntaxin 18 SNARE complex facilitates retrograde transport from the Golgi to the ER, and the blockage of complex disassembly induces apoptosis (Nishiwaki *et al.*, 2013). This could result in an accumulation of proteins in the ER and therefore cause ER stress. A typical cause of ER stress is also due to misfolded or unfolded proteins accumulating in the ER, also known as the unfolded protein response (UPR). If this ER stress is unresolved, apoptosis pathways will be activated. We know that a reduction in ER-Golgi trafficking, such as by treatment with Brefeldin A (Lippincott-Schwartz *et al.*, 1989), can also cause ER stress, as there is an overload of proteins trapped at the ER (Preston *et al.*, 2009). It has been previously established that several SNAREs are required for secretion of newly synthesised proteins from the ER-Golgi and post-Golgi trafficking to the plasma membrane, such as Syntaxin 5, Syntaxin 18, SNAP-29, Sec22B, and Ykt6 (Gordon *et al.*, 2010). Cleavage of Syntaxin 5 by caspases has been shown to cause an apoptosis phenotype due to the resulting block in ER-Golgi transport (Lowe *et al.*, 2004). As the light chain of BoNT/X severely perturbs trafficking of cargo out of the ER, this accumulation of cargo could be activating an ER stress response, which in turn could initiate the caspase cascade. In addition to ER stress, other organelles are susceptible to stress sensing and signalling, for example prolonged Golgi stress has been shown to induce caspase-3 mediated apoptosis (Suga *et al.*, 2022). Another possible explanation for the induction of apoptosis in intoxicated cells is there could be a block in autophagy, which is required for normal cell homeostasis. The R-SNARE Ykt6 has been shown to be involved in autophagosome-lysosome fusion (Takáts *et al.*, 2018), along with a possible role in mitophagy, where a lack of functional Ykt6 caused reduced cell viability possibly due to inability for mitochondria to be degraded (Sánchez-Martín *et al.*, 2023). As LC/X targets multiple R-SNAREs, there is a possibility that typical autophagic processes are being disrupted. Due to reduced delivery of proteins to the cell surface by LC/X intoxication (Asnawi, 2021; Chapter 2), it is possible that surface receptors essential for mitogenic signalling are perturbed.

How is disruption to R-SNARE function causing defects in cell division?

It has been proposed that SNARE proteins may have a role in processes associated with the cell cycle. For example, after mitosis the nuclear envelope reforms, a process which requires membrane fusion. A study suggested that this may be mediated by SNAREs rather than by other fusion pathways (Baur *et al.*, 2007). During mitosis Golgi stacks also require homotypic fusion to reform into a single Golgi apparatus (Lucocq, Berger and Warren, 1989; Rothman and Warren, 1994). In cell division, the cell-membrane is able to form in the absence of a complete Golgi apparatus, suggesting that the transport of newly synthesised membrane proteins and lipids is not required for cell-membrane formation and instead must involve recycling processes (Boucrot and Kirchhausen, 2007), which could account for the rescue seen by VAMP3^{VT}. It is known that to facilitate mitosis, a block in vesicular transport occurs to prepare the cell for the fragmentation and division of organelles prior to reassembly (Berlin and Oliver, 1980; Warren *et al.*, 1983; Lucocq and Warren, 1987; Jongsma, Berlin and Neefjes, 2015). As LC/X causes a block of vesicular trafficking in cells, the toxin could be inducing a similar effect. In cytokinesis, the cytokinetic bridge connecting the two daughter cells must be broken to allow for successful mitosis to occur. The SNARE VAMP8 (endobrevin) has been implicated in this process, and inhibition of VAMP8 function prevents the successful breakage of the cytokinetic bridge, and thus leading to bi-nucleated cells (Low *et al.*, 2003; Mukai *et al.*, 2008). The SNARE proteins SNAP-25 and VAMP2 have also been shown to be recruited to the cleavage furrow during cytokinesis, as the cellular membrane must be expanded for successful cytokinesis creation (Ming Li *et al.*, 2006). The intoxication of sea urchin embryos by BoNT/C caused an inhibition in cell division due to cleavage of syntaxin (Conner and Wessel, 1999). It is possible that intoxication with BoNT/X may be impacting successful completion of cytokinesis or nuclear envelope formation, and that is why we observe bi-nucleated cells that are unable to progress through mitosis. For successful cell division, replicated chromosomes must segregate for each daughter cell. To segregate the chromosomes, they attach to microtubules which then attach to kinetochores. It has been shown that the Q-SNARE SNAP-29 promotes kinetochore assembly in mitosis, further demonstrating the role of SNARE proteins in successful cell division (Boucrot and Kirchhausen, 2007; Morelli *et al.*, 2016). Ykt6 appears to have a role in cell cycle progression and DNA synthesis, previously it has been shown that

overexpressed Ykt6 resulted in increased DNA synthesis, however this appears to not be due to its function as an R-SNARE (Thayanidhi *et al.*, 2012). Observing the phenotypic changes caused by LC/X intoxication using live microscopy could reveal chromosomal segregation, nuclear envelope reassembly and DNA content over time, potentially identifying the role of R-SNAREs in these pathways.

Could cell rounding be contributing to apoptosis?

BoNT/X intoxicated become more rounded suggesting that their ability to adhere to the extracellular matrix may be perturbed. Existing literature has shown that intoxication with BoNT/C resulted in neuroblastoma cell rounding (Rust *et al.*, 2016). It is known that VAMP3 is involved in cell adhesion (Luftman *et al.*, 2009), with defects in trafficking of β1 integrin to the cell surface in VAMP3 silenced cells. In CHO cells the loss of VAMP3 by tetanus neurotoxin intoxication caused reduced integrin-mediated cell spreading (Skalski and Coppolino, 2005). The role of Ykt6 in cell adhesion has been investigated by (Naydenov *et al.*, 2018), where a loss of Ykt6 was linked to increased cell motility. Could the loss of integrins from the cell surface be contributing to the apoptosis seen in intoxicated cells? Anoikis is an integrin-mediated form of apoptosis (Frisch and Francis, 1994). If LC/X is disrupting typical integrin trafficking and therefore cell adhesion, this could be inducing cell death.

Overexpression of cleavage resistant Ykt6 increases TF uptake in the absence of other R-SNAREs

VAMP3^{VT} and Ykt6^{VT} can rescue transferrin uptake in BoNT/X intoxicated cells suggesting that these SNAREs are involved in the trafficking of the TF-R. Surprisingly, Ykt6^{VT} overexpression in the intoxicated cells appears to enhance transferrin uptake compared to that of the non-intoxicated cells. It is possible that Ykt6^{VT} overexpression drives the delivery of the TF-R to the cell surface in the intoxicated cells. VAMP3^{VT} is also able to rescue transferrin uptake. However, this phenotype can only be observed when Ykt6 has also been disrupted suggesting that Ykt6 can compensate for the loss of VAMP3. In the future it will be interesting to study these phenomena by making endogenous R-SNAREs resistant to the action of the toxin using CRISPR/Cas9 based approaches so overexpression artefacts can potentially be avoided.

In conclusion, we have demonstrated that the prolonged expression of BoNT/X LC triggers apoptosis possibly caused by defects in the cell cycle. In the future it will be important to determine how loss of SNAREs is triggering this process as it will shed new insight into how membrane fusion is linked to cellular homeostasis.

References

Akintade, D.D. and Chaudhuri, B. (2021) 'Human VAMP3 Suppresses or Negatively Regulates Bax Induced Apoptosis in Yeast', *Biomedicines*, 9(1), p. 95. Available at: https://doi.org/10.3390/biomedicines9010095.

Arsenault, J. *et al.* (2014) 'Botulinum protease-cleaved SNARE fragments induce cytotoxicity in neuroblastoma cells', *Journal of Neurochemistry*, 129(5), pp. 781–791. Available at: https://doi.org/10.1111/jnc.12645.

Asnawi, A.W.B.A. (2021) *Botulinum Neurotoxin X: A New Tool to Study Intracellular Transport and Membrane Trafficking*. phd. University of Sheffield. Available at: https://etheses.whiterose.ac.uk/28686/ (Accessed: 27 August 2024).

Baur, T. *et al.* (2007) 'NSF- and SNARE-mediated membrane fusion is required for nuclear envelope formation and completion of nuclear pore complex assembly in Xenopus laevis egg extracts', *Journal of Cell Science*, 120(16), pp. 2895–2903. Available at: https://doi.org/10.1242/jcs.010181.

Berlin, R.D. and Oliver, J.M. (1980) 'Surface functions during mitosis. II. Quantitation of pinocytosis and kinetic characterization of the mitotic cycle with a new fluorescence technique', *The Journal of Cell Biology*, 85(3), pp. 660–671. Available at: https://doi.org/10.1083/jcb.85.3.660.

Bhattacharya, S. *et al.* (2002) 'Members of the synaptobrevin/vesicle-associated membrane protein (VAMP) family in Drosophila are functionally interchangeable in vivo for neurotransmitter release and cell viability', *Proceedings of the National Academy of Sciences of the United States of America*, 99(21), pp. 13867–13872. Available at: https://doi.org/10.1073/pnas.202335999.

Bonaud, A. *et al.* (2023) 'Sec22b is a critical and nonredundant regulator of plasma cell maintenance', *Proceedings of the National Academy of Sciences of the United States of America*, 120(2), p. e2213056120. Available at: https://doi.org/10.1073/pnas.2213056120.

Boucrot, E. and Kirchhausen, T. (2007) 'Endosomal recycling controls plasma membrane area during mitosis', *Proceedings of the National Academy of Sciences of the United States of America*, 104(19), pp. 7939–7944. Available at: https://doi.org/10.1073/pnas.0702511104.

Boyd, J.M. *et al.* (1994) 'Adenovirus E1B 19 kDa and Bcl-2 proteins interact with a common set of cellular proteins', *Cell*, 79(2), pp. 341–351. Available at: https://doi.org/10.1016/0092-8674(94)90202-X.

Burgen, A.S.V., Dickens, F. and Zatman, L.J. (1949) 'The action of botulinum toxin on the neuro-muscular junction', *The Journal of Physiology*, 109(1–2), pp. 10–24.

Chen, X. *et al.* (2016) 'Pyroptosis is driven by non-selective gasdermin-D pore and its morphology is different from MLKL channel-mediated necroptosis', *Cell Research*, 26(9), pp. 1007–1020. Available at: https://doi.org/10.1038/cr.2016.100.

Coleman, M.L. *et al.* (2001) 'Membrane blebbing during apoptosis results from caspase-mediated activation of ROCK I', *Nature Cell Biology*, 3(4), pp. 339–345. Available at: https://doi.org/10.1038/35070009.

Conner, S.D. and Wessel, G.M. (1999) 'Syntaxin Is Required for Cell Division', *Molecular Biology of the Cell*, 10(8), pp. 2735–2743. Available at: https://doi.org/10.1091/mbc.10.8.2735.

Cookson, B.T. and Brennan, M.A. (2001) 'Pro-inflammatory programmed cell death', *Trends in Microbiology*, 9(3), pp. 113–114. Available at: https://doi.org/10.1016/S0966-842X(00)01936-3.

Cotter, T.G. *et al.* (1992) 'Microfilament-disrupting agents prevent the formation of apoptotic bodies in tumor cells undergoing apoptosis', *Cancer Research*, 52(4), pp. 997–1005.

Elmore, S. (2007) 'Apoptosis: A Review of Programmed Cell Death', *Toxicologic pathology*, 35(4), pp. 495–516. Available at: https://doi.org/10.1080/01926230701320337.

Eudy, B.J. and da Silva, R.P. (2021) 'Systematic deletion of adenosine receptors reveals novel roles in inflammation and pyroptosis in THP-1 macrophages', *Molecular Immunology*, 132, pp. 1–7. Available at: https://doi.org/10.1016/j.molimm.2021.01.018.

Fink, S.L. and Cookson, B.T. (2006) 'Caspase-1-dependent pore formation during pyroptosis leads to osmotic lysis of infected host macrophages', *Cellular Microbiology*, 8(11), pp. 1812–1825. Available at: https://doi.org/10.1111/j.1462-5822.2006.00751.x.

Fonfria, E. *et al.* (2018) 'The Expanding Therapeutic Utility of Botulinum Neurotoxins', *Toxins*, 10(5). Available at: https://doi.org/10.3390/toxins10050208.

Frisch, S.M. and Francis, H. (1994) 'Disruption of epithelial cell-matrix interactions induces apoptosis', *The Journal of Cell Biology*, 124(4), pp. 619–626. Available at: https://doi.org/10.1083/jcb.124.4.619.

Fukasawa, M. *et al.* (2004) 'Localization and activity of the SNARE Ykt6 determined by its regulatory domain and palmitoylation', *Proceedings of the National Academy of Sciences*, 101(14), pp. 4815–4820. Available at: https://doi.org/10.1073/pnas.0401183101.

Gordon, D.E. *et al.* (2010) 'A targeted siRNA screen to identify SNAREs required for constitutive secretion in mammalian cells', *Traffic (Copenhagen, Denmark)*, 11(9), pp. 1191–1204. Available at: https://doi.org/10.1111/j.1600-0854.2010.01087.x.

Gordon, D.E. *et al.* (2017) 'VAMP3/Syb and YKT6 are required for the fusion of constitutive secretory carriers with the plasma membrane', *PLOS Genetics*, 13(4), p. e1006698. Available at: https://doi.org/10.1371/journal.pgen.1006698.

Gregg, B.M. *et al.* (2024) 'Botulinum neurotoxin X lacks potency in mice and in human neurons', *mBio*, 15(3), p. e0310623. Available at: https://doi.org/10.1128/mbio.03106-23.

Guo, B. *et al.* (2014) 'O-GlcNAc-modification of SNAP-29 regulates autophagosome maturation', *Nature Cell Biology*, 16(12), pp. 1215–1226. Available at: https://doi.org/10.1038/ncb3066.

Igney, F.H. and Krammer, P.H. (2002) 'Death and anti-death: tumour resistance to apoptosis', *Nature Reviews Cancer*, 2(4), pp. 277–288. Available at: https://doi.org/10.1038/nrc776.

Itakura, E., Kishi-Itakura, C. and Mizushima, N. (2012) 'The Hairpin-type Tail-Anchored SNARE Syntaxin 17 Targets to Autophagosomes for Fusion with Endosomes/Lysosomes', *Cell*, 151(6), pp. 1256–1269. Available at: https://doi.org/10.1016/j.cell.2012.11.001.

Jongsma, M.L.M., Berlin, I. and Neefjes, J. (2015) 'On the move: organelle dynamics during mitosis', *Trends in Cell Biology*, 25(3), pp. 112–124. Available at: https://doi.org/10.1016/j.tcb.2014.10.005.

Kaul, S. *et al.* (2015) 'Expression of the SNARE Protein SNAP-23 Is Essential for Cell Survival', *PLOS ONE*, 10(2), p. e0118311. Available at: https://doi.org/10.1371/journal.pone.0118311.

Kim, T.K. and Eberwine, J.H. (2010) 'Mammalian cell transfection: the present and the future', *Analytical and Bioanalytical Chemistry*, 397(8), pp. 3173–3178. Available at: https://doi.org/10.1007/s00216-010-3821-6.

Lane, J.D. *et al.* (2002) 'Caspase-mediated cleavage of the stacking protein GRASP65 is required for Golgi fragmentation during apoptosis', *The Journal of Cell Biology*, 156(3), pp. 495–509. Available at: https://doi.org/10.1083/jcb.200110007.

Liang, T. *et al.* (2020) 'SNAP23 depletion enables more SNAP25/calcium channel excitosome formation to increase insulin exocytosis in type 2 diabetes', *JCI insight*, 5(3), pp. e129694, 129694. Available at: https://doi.org/10.1172/jci.insight.129694.

Lippincott-Schwartz, J. *et al.* (1989) 'Rapid redistribution of Golgi proteins into the ER in cells treated with brefeldin A: evidence for membrane cycling from Golgi to ER', *Cell*, 56(5), pp. 801–813. Available at: https://doi.org/10.1016/0092-8674(89)90685-5.

Low, S.H. *et al.* (2003) 'Syntaxin 2 and Endobrevin Are Required for the Terminal Step of Cytokinesis in Mammalian Cells', *Developmental Cell*, 4(5), pp. 753–759. Available at: https://doi.org/10.1016/S1534-5807(03)00122-9.

Lowe, M. *et al.* (2004) 'Caspase-mediated cleavage of syntaxin 5 and giantin accompanies inhibition of secretory traffic during apoptosis', *Journal of Cell Science*, 117(7), pp. 1139–1150. Available at: https://doi.org/10.1242/jcs.00950.

Lucocq, J.M., Berger, E.G. and Warren, G. (1989) 'Mitotic Golgi fragments in HeLa cells and their role in the reassembly pathway', *The Journal of Cell Biology*, 109(2), pp. 463–474. Available at: https://doi.org/10.1083/jcb.109.2.463.

Lucocq, J.M. and Warren, G. (1987) 'Fragmentation and partitioning of the Golgi apparatus during mitosis in HeLa cells', *The EMBO Journal*, 6(11), p. 3239. Available at: https://doi.org/10.1002/j.1460-2075.1987.tb02641.x.

Luftman, K. *et al.* (2009) 'Silencing of VAMP3 inhibits cell migration and integrin-mediated adhesion', *Biochemical and Biophysical Research Communications*, 380(1), pp. 65–70. Available at: https://doi.org/10.1016/j.bbrc.2009.01.036.

Maslanka, S.E. *et al.* (2016) 'A Novel Botulinum Neurotoxin, Previously Reported as Serotype H, Has a Hybrid-Like Structure With Regions of Similarity to the Structures of Serotypes A and F and Is Neutralized With Serotype A Antitoxin', *The Journal of Infectious Diseases*, 213(3), pp. 379–385. Available at: https://doi.org/10.1093/infdis/jiv327.

McGrath, K. *et al.* (2021) 'A conformational switch driven by phosphorylation regulates the activity of the evolutionarily conserved SNARE Ykt6', *Proceedings of the National Academy of Sciences*, 118(12), p. e2016730118. Available at: https://doi.org/10.1073/pnas.2016730118.

McMahon, H.T. *et al.* (1993) 'Cellubrevin is a ubiquitous tetanus-toxin substrate homologous to a putative synaptic vesicle fusion protein', *Nature*, 364(6435), pp. 346–349. Available at: https://doi.org/10.1038/364346a0.

McNew, J.A. *et al.* (1997) 'Ykt6p, a Prenylated SNARE Essential for Endoplasmic Reticulum-Golgi Transport *', *Journal of Biological Chemistry*, 272(28), pp. 17776–17783. Available at: https://doi.org/10.1074/jbc.272.28.17776.

Miglio, G., Veglia, E. and Fantozzi, R. (2015) 'Fumaric acid esters prevent the NLRP3 inflammasome-mediated and ATP-triggered pyroptosis of differentiated THP-1 cells', *International Immunopharmacology*, 28(1), pp. 215–219. Available at: https://doi.org/10.1016/j.intimp.2015.06.011.

Ming Li, W. *et al.* (2006) 'Recruitment and SNARE-mediated fusion of vesicles in furrow membrane remodeling during cytokinesis in zebrafish embryos', *Experimental Cell Research*, 312(17), pp. 3260–3275. Available at: https://doi.org/10.1016/j.yexcr.2006.06.028.

Montecucco, C. and Schiavo, G. (1994) 'Mechanism of action of tetanus and botulinum neurotoxins', *Molecular Microbiology*, 13(1), pp. 1–8. Available at: https://doi.org/10.1111/j.1365-2958.1994.tb00396.x.

Morelli, E. *et al.* (2016) 'An essential step of kinetochore formation controlled by the SNARE protein Snap29', *The EMBO Journal*, 35(20), pp. 2223–2237. Available at: https://doi.org/10.15252/embj.201693991.

Moriishi, K. *et al.* (1996) 'Mosaic structures of neurotoxins produced from Clostridium botulinum types C and D organisms', *Biochimica et Biophysica Acta (BBA) - Gene Structure and Expression*, 1307(2), pp. 123–126. Available at: https://doi.org/10.1016/0167-4781(96)00006-1.

Mukai, A. *et al.* (2008) 'Dynamic regulation of ubiquitylation and deubiquitylation at the central spindle during cytokinesis', *Journal of Cell Science*, 121(8), pp. 1325–1333. Available at: https://doi.org/10.1242/jcs.027417.

Nakajima, K. *et al.* (2004) 'Involvement of BNIP1 in apoptosis and endoplasmic reticulum membrane fusion', *The EMBO Journal*, 23(16), pp. 3216–3226. Available at: https://doi.org/10.1038/sj.emboj.7600333.

Nakamura, K. *et al.* (2010) 'Characterization of the D/C mosaic neurotoxin produced by Clostridium botulinum associated with bovine botulism in Japan', *Veterinary Microbiology*, 140(1), pp. 147–154. Available at: https://doi.org/10.1016/j.vetmic.2009.07.023.

Naydenov, N.G. *et al.* (2018) 'A membrane fusion protein, Ykt6, regulates epithelial cell migration via microRNA-mediated suppression of Junctional Adhesion Molecule A', *Cell Cycle*, 17(14), pp. 1812–1831. Available at: https://doi.org/10.1080/15384101.2018.1496755.

Nishiwaki, Y. *et al.* (2013) 'The BH3-Only SNARE BNip1 Mediates Photoreceptor Apoptosis in Response to Vesicular Fusion Defects', *Developmental Cell*, 25(4), pp. 374–387. Available at: https://doi.org/10.1016/j.devcel.2013.04.015.

Pellizzari, R. *et al.* (1999) 'Tetanus and botulinum neurotoxins: mechanism of action and therapeutic uses.', *Philosophical Transactions of the Royal Society B: Biological Sciences*, 354(1381), pp. 259–268.

Peng, L. *et al.* (2013) 'Cytotoxicity of botulinum neurotoxins reveals a direct role of syntaxin 1 and SNAP-25 in neuron survival', *Nature Communications*, 4(1), p. 1472. Available at: https://doi.org/10.1038/ncomms2462.

Preston, A.M. *et al.* (2009) 'Reduced endoplasmic reticulum (ER)-to-Golgi protein trafficking contributes to ER stress in lipotoxic mouse beta cells by promoting protein overload',

Diabetologia, 52(11), pp. 2369–2373. Available at: https://doi.org/10.1007/s00125-009-1506-5.

Pylypenko, O. *et al.* (2008) 'Farnesylation of the SNARE protein Ykt6 increases its stability and helical folding', *Journal of Molecular Biology*, 377(5), pp. 1334–1345. Available at: https://doi.org/10.1016/j.jmb.2008.01.099.

Rothman, J.E. and Warren, G. (1994) 'Implications of the SNARE hypothesis for intracellular membrane topology and dynamics', *Current Biology*, 4(3), pp. 220–233. Available at: https://doi.org/10.1016/S0960-9822(00)00051-8.

Ruiz-Martinez, M. *et al.* (2016) 'YKT6 expression, exosome release, and survival in non-small cell lung cancer', *Oncotarget*, 7(32), pp. 51515–51524. Available at: https://doi.org/10.18632/oncotarget.9862.

Rust, A. *et al.* (2016) 'Botulinum neurotoxin type C protease induces apoptosis in differentiated human neuroblastoma cells', *Oncotarget*, 7(22), pp. 33220–33228. Available at: https://doi.org/10.18632/oncotarget.8903.

Sakata, N. *et al.* (2021) 'Double prenylation of SNARE protein Ykt6 is required for lysosomal hydrolase trafficking', *The Journal of Biochemistry*, 169(3), pp. 363–370. Available at: https://doi.org/10.1093/jb/mvaa111.

Sánchez-Martín, P. *et al.* (2023) 'ULK1-mediated phosphorylation regulates the conserved role of YKT6 in autophagy', *Journal of Cell Science*, 136(3), p. jcs260546. Available at: https://doi.org/10.1242/jcs.260546.

Schindelin, J. *et al.* (2012) 'Fiji: an open-source platform for biological-image analysis', *Nature Methods*, 9(7), pp. 676–682. Available at: https://doi.org/10.1038/nmeth.2019.

Schoch, S. *et al.* (2001) 'SNARE Function Analyzed in Synaptobrevin/VAMP Knockout Mice', *Science*, 294(5544), pp. 1117–1122.

Shirakawa, R. *et al.* (2020) 'A SNARE geranylgeranyltransferase essential for the organization of the Golgi apparatus', *The EMBO journal*, 39(8), p. e104120. Available at: https://doi.org/10.15252/embj.2019104120.

Skalski, M. and Coppolino, M.G. (2005) 'SNARE-mediated trafficking of α5β1 integrin is required for spreading in CHO cells', *Biochemical and Biophysical Research Communications*, 335(4), pp. 1199–1210. Available at: https://doi.org/10.1016/j.bbrc.2005.07.195.

Suga, K. *et al.* (2022) 'Golgi stress induces upregulation of the ER-Golgi SNARE Syntaxin-5, altered βAPP processing, and Caspase-3-dependent apoptosis in NG108-15 cells', *Molecular and Cellular Neuroscience*, 121, p. 103754. Available at: https://doi.org/10.1016/j.mcn.2022.103754.

Suh, Y.H. *et al.* (2011) 'Deletion of SNAP-23 Results in Pre-Implantation Embryonic Lethality in Mice', *PLoS ONE*, 6(3), p. e18444. Available at: https://doi.org/10.1371/journal.pone.0018444.

Takáts, S. *et al.* (2018) 'Non-canonical role of the SNARE protein Ykt6 in autophagosome-lysosome fusion', *PLOS Genetics*, 14(4), p. e1007359. Available at: https://doi.org/10.1371/journal.pgen.1007359.

Thayanidhi, N. *et al.* (2012) 'R-SNARE ykt6 resides in membrane-associated protease-resistant protein particles and modulates cell cycle progression when over-expressed', *Biology of the Cell*, 104(7), pp. 397–417. Available at: https://doi.org/10.1111/boc.201100048.

Trinkle-Mulcahy, L. *et al.* (2003) 'Time-lapse Imaging Reveals Dynamic Relocalization of PP1γ throughout the Mammalian Cell Cycle', *Molecular Biology of the Cell*, 14(1), pp. 107–117. Available at: https://doi.org/10.1091/mbc.E02-07-0376.

Tsuchiya, S. *et al.* (1980) 'Establishment and characterization of a human acute monocytic leukemia cell line (THP-1)', *International Journal of Cancer*, 26(2), pp. 171–176. Available at: https://doi.org/10.1002/ijc.2910260208.

Vassilev, L.T. *et al.* (2006) 'Selective small-molecule inhibitor reveals critical mitotic functions of human CDK1', *Proceedings of the National Academy of Sciences of the United States of America*, 103(28), pp. 10660–10665. Available at: https://doi.org/10.1073/pnas.0600447103.

Warren, G. *et al.* (1983) 'Newly synthesized G protein of vesicular stomatitis virus is not transported to the cell surface during mitosis', *The Journal of Cell Biology*, 97(5 Pt 1), pp. 1623–1628. Available at: https://doi.org/10.1083/jcb.97.5.1623.

Washbourne, P. *et al.* (2002) 'Genetic ablation of the t-SNARE SNAP-25 distinguishes mechanisms of neuroexocytosis', *Nature Neuroscience*, 5(1), pp. 19–26. Available at: https://doi.org/10.1038/nn783.

Yang, C. *et al.* (2001) 'VAMP3 Null Mice Display Normal Constitutive, Insulin- and Exercise-Regulated Vesicle Trafficking', *Molecular and Cellular Biology*, 21(5), pp. 1573–1580. Available at: https://doi.org/10.1128/MCB.21.5.1573-1580.2001.

Yu, P. *et al.* (2021) 'Pyroptosis: mechanisms and diseases', *Signal Transduction and Targeted Therapy*, 6(1), pp. 1–21. Available at: https://doi.org/10.1038/s41392-021-00507-5.

Zhang, S. *et al.* (2017) 'Identification and characterization of a novel botulinum neurotoxin', *Nature Communications*, 8(1), p. 14130. Available at: https://doi.org/10.1038/ncomms14130.

Zhang, S. *et al.* (2018) 'Identification of a botulinum neurotoxin-like toxin in a commensal strain of Enterococcus faecium', *Cell host & microbe*, 23(2), pp. 169-176.e6. Available at: https://doi.org/10.1016/j.chom.2017.12.018.

Zhang, X. *et al.* (2023) 'miR-124 and VAMP3 Act Antagonistically in Human Neuroblastoma', *International Journal of Molecular Sciences*, 24(19), p. 14877. Available at: https://doi.org/10.3390/ijms241914877.

Chapter 4

4. Discussion

We know that BoNT/X is a serotype of BoNT that is the least similar to any known serotype and cleaves SNAREs not currently targeted by other BoNTs (VAMPs 1-5 and Ykt6) (Zhang *et al.*, 2017; Asnawi, 2021). Despite its broad specificity, it is unable to cleave VAMP7, VAMP8 and Sec22B which demonstrates that it does have a limited action (Zhang *et al.*, 2017; Asnawi, 2021). We have demonstrated that BoNT/X cleaves VAMPs 1-4 and Ykt6 in vivo, and causes severe defects in intracellular trafficking. Intoxicated cells cause significant reductions in transferrin uptake due to a loss of surface transferrin receptor levels. Additionally, the delivery of newly synthesised proteins to the plasma membrane is perturbed, as there is a loss of soluble cargo and secretory cargo (CD8 and CD63) on the plasma membrane. We generated R-SNAREs that resist cleavage by BoNT/X to establish if these phenotypes are specific to R-SNARE cleavage. VAMP3 was able to partially rescue these phenotypes, along with some rescue in other post-Golgi SNAREs VAMP2 and VAMP8. Surprisingly Ykt6 was able to rescue despite not previously having an established role in these pathways. We established that these assays can be used to investigate disease-causing mutations in VAMP3, as well as structural mutations. These resulted in partial rescues or loss of function, which provides insight into important residues required for SNARE function.

In addition to gross abnormalities in intracellular trafficking, we wanted to establish if these defects would impact cell viability. We know that intoxicated cells appear to reduce in number and round up, however they remain viable at 16 hrs. We developed cell lines expressing the LC/X via a tet-inducible promoter to observe cell viability over a longer period of time. We observed using these cell lines and by electroporation of recombinant LC/X protein that at 24 hours post-intoxication there are significant populations of dead cells due to apoptosis, and by 40 h most cells are dead. This can however be rescued by overexpression of the cleavage resistant VAMP3 and Ykt6, suggesting that it is due to SNAREs. As cell numbers in intoxicated samples were reduced, we investigated the impact of intoxication on the cell cycle. Intoxicated HeLa cells appear to accumulate in G2 and are unable to progress through mitosis. In THP-

1 cells intoxication results in bi-nucleated cells that then proceed to die prior to cell division.

4.1 Mitochondrially targeted SNAREs as new reporters of LC activity

As studies have shown, BoNT/X targets SNAREs not currently targeted by other BoNTs. To assess LC activity, we successfully created an assay where we tagged SNAREs with GFP and a MAO to tether the construct to mitochondria. When the SNARE is cleaved the GFP is released from the mitochondria anchor and becomes cytoplasmic. We have used this assay to easily assess cleavage of SNAREs by microscopy or western blotting, demonstrating the substrate specificity of LC/X. We have also used this assay to help develop cleavage resistant SNAREs, demonstrating its utility. There are several methods currently utilised to assess toxin activity (Rasetti-Escargueil and Popoff, 2022). For example, immunosensors, where the substrate (SNAP-25/VAMP2) is immobilised on a sensor and the BoNT flows across it. It is a very sensitive method that does not require large quantities of material and has a comparable sensitivity to the mouse bioassay (Patel *et al.*, 2017), however they are more suited to measuring activity rather than substrate specificity. There are also FRET-based assays, which are effective at assessing cleavage however are known to have photobleaching/bleedthrough effects and are not as good to use in fixed cells, which may limit their application (Berney and Danuser, 2003). Mass spectrometry is an excellent tool to detect serotypes and any subtypes, however it relies upon the existence of an antibody against that serotype, which works well for well-characterised and studied serotypes such as BoNT/A (Barr *et al.*, 2005). To measure LC activity, Endopeptidase-MS assays have been developed, and can detect the cleaved peptide and cleavage site based on the fragment sizes (Barr *et al.*, 2005; Boyer *et al.*, 2005). The endopeptidase-ELISA is highly effective at monitoring cleavage of SNAP-25 and VAMP2, however it relies on the availability of suitable antibodies (Michalik *et al.*, 1986). Current cell-based assays are time consuming and technically challenging, and whilst they are sensitive and can accurately measure BoNT activity, they are not designed as tools to quickly screen substrate cleavage for novel serotypes/subtypes that may target non-conventional substrates. The main advantage of our assay over other existing assays such as immunoassays and FRET-based assays is that it is fast, cheap, and simple to perform. One major challenge when looking at the cleavage of VAMPs, is that they get degraded after cleavage. By adding the GFP tag we can

protect the cleavage product from degradation, making it easier to monitor (Rust *et al.*, 2017). There are some limitations of this approach; for example, we have not developed approaches to quantify the assay, and have only utilised the assay to monitor activity of the light chain rather than the full-length toxin.

It has previously been shown that SNAREs can be mutated to resist cleavage by other BoNTs (Pellizzari *et al.*, 1996; Regazzi *et al.*, 1996; Peng *et al.*, 2013). To establish if we can make R-SNAREs resistant to cleavage by LC/X, VT mutations were introduced to the cleavage site of the R-SNAREs. We have shown that by mutating the cleavage site of the R-SNAREs they are able to resist cleavage, however these mutations are specific to these residues as other mutations were tested that either offered partial resistance or caused the R-SNARE to mis-localise (unpublished, Peden Lab). Interestingly, we discovered that whilst the R-SNAREs were resistant to cleavage by LC/X, the VAMP4^{VT} appeared to cleave when exposed to higher levels of intoxication. This partial cleavage could be explained if there is an alternative cleavage site or conformational change that makes the protein more sensitive to cleavage. Further analysis such as by mass-spectrometry to determine the cleavage fragments/residues could be interesting, as reengineered toxins have been made to display more specific cleavage (Blum *et al.*, 2021), therefore understanding the residues and interactions involved could help for future studies.

4.2 BoNT/X can be used to explore the function of SNAREs in intracellular trafficking

LC/X intoxication causes dramatic defects transferrin receptor trafficking and blocks the transport of cargo from the Golgi to the plasma membrane. Cleavage resistant SNAREs are able to rescue the phenotypes caused by LC intoxication and Ykt6 is most effective at this. However, it is unclear whether Ykt6 normally acts on these pathways. It should be noted that cells reconstituted with Ykt6 take up significantly more transferrin compared to that of the non-intoxicated cells and the total levels of the TF-R are not fully restored by Ykt6 expression suggesting that the transferrin receptor trafficking is not normal in the rescued cells. Thus, in the future it will be important to carefully measure TF-R endocytosis and/or recycling kinetics.

LC/X intoxication disrupts CD63 trafficking and significantly reduces its cell surface levels. CD63 is a key molecule involved in exosome secretion (Escola *et al.*, 1998) so it will be interesting to determine whether LC/X intoxication blocks exosome secretion.

If this is the case it may have interesting implications to cancer signalling (Ruiz-Martinez *et al.*, 2016).

Surprisingly, VAMPs 2-3 and 8 failed to rescue the secretion of our soluble secretory reporter in LC/X intoxicated cells. However, we only observed a partial rescue for Ykt6 in this assay suggesting that there may have been technical issues with these experiments.

4.3 Why does LC/X intoxication cause cytotoxicity and impact cell survival?

We have shown that LC/X intoxication causes caspase 3 and 7 activation, and apoptosis in immortal cell lines. Intoxicated cells remain viable at 16 h post-induction, however by 40 h almost all cells are dead. These phenotypes can be partially rescued by re-expression of Ykt6 and VAMP3 suggesting that these SNAREs play an important role in this process. At present it is unclear why loss of these SNAREs is causing caspase 3/7 activation and cell death. It could be because their loss leads to defects in:

1. The ability of cells to respond to mitogenic signals as receptor trafficking is perturbed.
2. The adherence of cells caused by changes in integrin trafficking.
3. Biosynthetic transport which causes acute ER stress.
4. Nuclear envelope and/or endomembrane reassembly after cell division.

However, it is also possible that these SNAREs have additional non-fusogenic roles which are separate from their role in membrane trafficking.

When we look at cytotoxicity of BoNTs, not many cause cytotoxicity and are generally well tolerated, hence their use therapeutically. However, despite this, BoNT/C and BoNT/E have shown cytotoxicity and neurodegeneration in hippocampal and motor neurons (Peng *et al.*, 2013). As BoNT/X acts on numerous SNAREs, we hypothesised that it may impact cell survival. This reduction in cell viability appears to be at least partially rescued by Ykt6 and VAMP3 that have been mutated to resist cleavage by the LC. This suggests that these R-SNAREs may be involved in cell survival. It is not yet known the long-term impact of these rescues, or the impact of combinatory resistant SNAREs, as different SNAREs may be involved in multiple stages of membrane fusion that is essential for cell survival. We do not yet know the exact cause

of apoptosis induction in BoNT/X intoxicated cells. The loss of R-SNAREs could be causing ER stress due to the block in ER-Golgi trafficking and therefore accumulation of proteins in the ER, as this is seen when cells are treated with Brefeldin A and when SNAREs involved in ER-Golgi trafficking such as Syntaxin 5 are cleaved (Lippincott-Schwartz *et al.*, 1989; Lowe *et al.*, 2004). There may also be an impairment in cell division, accounting for the bi-nucleated cells we observed as R-SNAREs such as VAMP8 have been implicated in cytokinesis (Low *et al.*, 2003; Mukai *et al.*, 2008). Another possible cause of apoptosis could be defects in typical cell autophagy, as Ykt6 is involved in autophagosome-lysosome fusion (Takáts *et al.*, 2018), which may be perturbed in intoxicated cells. The phenotypes observed may also not be directly a result of their fusogenic properties as SNAREs, and so could be caused by another mechanism.

4.4 Can we use LC/X as a tool to dissect SNARE function and structure?

Studying the function of R-SNAREs has been challenging because their disruption in cells and/or whole organisms often does not yield the anticipated results. For example, loss of VAMP3 causes no gross abnormalities in mice (Yang, Mora, *et al.*, 2001), where mice remain viable, similar observations have been seen with VAMP7 and VAMP4 (Sato *et al.*, 2011; Ivanova *et al.*, 2021). In addition, disruption of some SNAREs such as Ykt6 leads to embryonic lethality (*International Mouse Phenotyping Consortium*, no date) which also makes them challenging to study.

The genetic reconstitution assay we have developed is relatively simple and should be less impacted by issues of compensation often seen with RNAi or CRISPR based approaches (Pereira *et al.*, 2023). Using this approach we have shown that cleavage resistant SNAREs can rescue a range of LC/X induced phenotypes.

In addition to studying the function of SNAREs, using this approach we have shown that Ykt6 needs to be lipidated to function, which is in agreement with the current literature indicating that Ykt6 must cycle on and off membranes to function (Fukasawa *et al.*, 2004). By mutating residues within the structure of Ykt6 we can begin to uncover residues that are functionally important. Recently a disease-causing Ykt6 mutant was discovered, demonstrating that understanding mutations in SNAREs could be of benefit for understanding how they contribute to function and disease (Ma *et al.*, 2024).

We mutated VAMP3^{VT} to include disease-causing mutations and structure/function indicated mutations: V30A/M33A, S58P, R39Q, W71A/W72A and a C-terminally tagged VAMP3 (Sutton *et al.*, 1998; Katz and Brennwald, 2000; Graham *et al.*, 2001; Scales, Yoo and Scheller, 2001; Harel *et al.*, 2008; Gordon *et al.*, 2009; Miller *et al.*, 2011; Salpietro *et al.*, 2019). Surprisingly, we observed that R39Q, V30A/M33A and W71A/W72A were able to partially rescue transferrin uptake suggesting that these residues are not essential for VAMP3 to function, however, we did not carefully look at TF-R trafficking kinetics. The S58P and the C-terminally tagged VAMP3 mutants failed to rescue transferrin uptake, suggesting that the disease-causing mutation in VAMP2 (S75P) when applied to VAMP3 blocks the ability of VAMP3 to drive membrane fusion providing novel insight into the role of this mutation in the neurodevelopmental disorder (Salpietro *et al.*, 2019). The C-terminally tagged VAMP3 construct has a normal steady state localisation and has been extremely useful in elucidating how VAMP3 is trafficked (Gordon *et al.*, 2009; Miller *et al.*, 2011). However, it is clearly non-functional so care must be taken when using these types of constructs to study R-SNARE biology (Miller *et al.*, 2011; Verboogen *et al.*, 2017). The C-terminally tagged R-SNARE constructs are still capable of forming SNARE complexes (Gordon *et al.*, 2009; Verboogen *et al.*, 2017). However, they must not be fusogenic.

4.5 Does making R-SNAREs resistant to BoNT/X impact their function?

It has recently been shown that the phosphorylation of serine residue (S174) in the SNARE domain of Ykt6 regulates its activity (Karuna M *et al.*, 2020). To create a BoNT/X cleavage resistant version of Ykt6, we mutated the cleavage site at K173V/S174T. As this is localised at residues possibly essential for function, we questioned if this could be forcing the molecule into a permanently active conformation? We know that Ykt6 cycles on and off membranes to function (Fukasawa *et al.*, 2004). The steady-state localisation of the VT construct suggests that the mutation does not appear to have grossly impacted this feature as the protein remains largely cytosolic, contrasting to an FtoE mutation (F42E) (Fukasawa *et al.*, 2004) which drives the protein to membranes (data not shown). Whilst this does not impact our studies into the action of the LC/X, mutations in Ykt6 should be studied to further dissect the function and modifications made to the protein for further functional studies.

4.6 Future work

To further enhance this work, the VAMP-MAO assay can be developed in neuronal cell lines and used to test the cleavage of SNAREs using full length purified proteins. Using neuronal cell and primary cell models for the rescue and functional experiments will allow us to assess the impact of LC/X intoxication on a more relevant cell model.

To further understand the effect of BoNT/X intoxication on cell viability, studies that look at the impact of rescue experiments over a longer time course would provide useful information to determine if these pathways are essential for survival. To monitor in real-time the impact of intoxication in cell cycle progression and cell survival, live imaging could be used to establish membrane integrity and nuclear content, as well as observing nuclear envelope formation. To confirm the cell cycle arrest seen, and establish if it is reversible, the experiments should be repeated with known cell cycle inhibitor drugs, and different cell synchronisation methods.

It will be useful to conduct assays using the full length BoNT/X protein, or chimeric versions using the binding domain of BoNT/A or BoNT/B as BoNT/X is not known to bind, to study the impact of the binding and translocation domains on the activity of the light chain. The light chain in isolation could behave differently, where there may be upstream effects of the rest of the protein that affect the activity or availability for the light chain to function.

Our rescue experiments in this study involve using N-terminally tagged R-SNAREs. Previous studies have utilised a VAMP3 that is C-terminally tagged, and demonstrate the ability for the VAMP to traffic and localise as expected (Gordon ***et al.***, 2009; Miller ***et al.***, 2011). Interestingly, in our study the C-terminally tagged VAMP3^{VT} was unable to rescue, however it expresses as expected which could indicate that the placement of the tag can change its interactions in forming SNARE complexes and function within cells. Whilst some of these mutations restore function in this assay, further work should be carried out to establish SNARE complex formation and fusion with these mutants.

4.7 Summary

In conclusion, we have shown that LC/X intoxication causes pleiotropic defects in intracellular trafficking and eventually triggers caspase mediated apoptosis. These phenotypes can be rescued using cleavage resistant SNAREs indicating that these phenotypes are specific to SNARE proteolysis. Combining cleavage resistant SNAREs with LC/X intoxication has allowed the development of a simple and robust genetic reconstitution assay which have made it possible to explore the role of R-SNAREs in post-Golgi trafficking. Using this approach we have uncovered an unexpected role for Ykt6 in transferrin receptor trafficking and identified key residues in VAMP3 important for its function. At present it is unclear why the loss of these R-SNAREs leads to caspase mediated cell death. However, it is clear that the light chain of BoNT/X will be a novel and exciting tool to explore the role of SNAREs in this process. In the longer term this information will be key to determining whether BoNT/X has the potential to be a novel therapeutic.

References

5. References

Advani, R.J. *et al.* (1998) 'Seven Novel Mammalian SNARE Proteins Localize to Distinct Membrane Compartments', *Journal of Biological Chemistry*, 273(17), pp. 10317–10324. Available at: https://doi.org/10.1074/jbc.273.17.10317.

Akintade, D.D. and Chaudhuri, B. (2021) 'Human VAMP3 Suppresses or Negatively Regulates Bax Induced Apoptosis in Yeast', *Biomedicines*, 9(1), p. 95. Available at: https://doi.org/10.3390/biomedicines9010095.

Ampah, K.K. *et al.* (2018) 'S-acylation regulates the trafficking and stability of the unconventional Q-SNARE STX19', *Journal of Cell Science*, 131(20), p. jcs212498. Available at: https://doi.org/10.1242/jcs.212498.

Antonin, W. *et al.* (2000) 'The R-SNARE Endobrevin/VAMP-8 Mediates Homotypic Fusion of Early Endosomes and Late Endosomes', *Molecular Biology of the Cell*, 11(10), pp. 3289–3298.

Arnon, S.S. *et al.* (2001) 'Botulinum Toxin as a Biological WeaponMedical and Public Health Management', *JAMA*, 285(8), pp. 1059–1070. Available at: https://doi.org/10.1001/jama.285.8.1059.

Arrazola Sastre, A. *et al.* (2021) 'Small GTPases of the Rab and Arf Families: Key Regulators of Intracellular Trafficking in Neurodegeneration', *International Journal of Molecular Sciences*, 22(9), p. 4425. Available at: https://doi.org/10.3390/ijms22094425.

Arsenault, J. *et al.* (2014) 'Botulinum protease-cleaved SNARE fragments induce cytotoxicity in neuroblastoma cells', *Journal of Neurochemistry*, 129(5), pp. 781–791. Available at: https://doi.org/10.1111/jnc.12645.

Asnawi, A.W.B.A. (2021) *Botulinum Neurotoxin X: A New Tool to Study Intracellular Transport and Membrane Trafficking*. phd. University of Sheffield. Available at: https://etheses.whiterose.ac.uk/28686/ (Accessed: 27 August 2024).

Azarnia Tehran, D. *et al.* (2017) 'Hsp90 is involved in the entry of clostridial neurotoxins into the cytosol of nerve terminals', *Cellular Microbiology*, 19(2). Available at: https://doi.org/10.1111/cmi.12647.

Bajno, L. *et al.* (2000) 'Focal Exocytosis of Vamp3-Containing Vesicles at Sites of Phagosome Formation', *The Journal of Cell Biology*, 149(3), pp. 697–706.

Barash, J.R. and Arnon, S.S. (2014) 'A Novel Strain of Clostridium botulinum That Produces Type B and Type H Botulinum Toxins', *The Journal of Infectious Diseases*, 209(2), pp. 183–191. Available at: https://doi.org/10.1093/infdis/jit449.

Barouch, W. *et al.* (1994) 'ATPase activity associated with the uncoating of clathrin baskets by Hsp70.', *Journal of Biological Chemistry*, 269(46), pp. 28563–28568. Available at: https://doi.org/10.1016/S0021-9258(19)61942-3.

Barr, C.L. *et al.* (2000) 'Identification of DNA variants in the SNAP-25 gene and linkage study of these polymorphisms and attention-deficit hyperactivity disorder', *Molecular Psychiatry*, 5(4), pp. 405–409. Available at: https://doi.org/10.1038/sj.mp.4000733.

Barr, F.A. and Gruneberg, U. (2007) 'Cytokinesis: Placing and Making the Final Cut', *Cell*, 131(5), pp. 847–860. Available at: https://doi.org/10.1016/j.cell.2007.11.011.

Barr, J.R. *et al.* (2005) 'Botulinum Neurotoxin Detection and Differentiation by Mass Spectrometry', *Emerging Infectious Diseases*, 11(10), pp. 1578–1583. Available at: https://doi.org/10.3201/eid1110.041279.

Baumert, M. *et al.* (1989) 'Synaptobrevin: an integral membrane protein of 18,000 daltons present in small synaptic vesicles of rat brain', *The EMBO Journal*, 8(2), p. 379. Available at: https://doi.org/10.1002/j.1460-2075.1989.tb03388.x.

Baur, T. *et al.* (2007) 'NSF- and SNARE-mediated membrane fusion is required for nuclear envelope formation and completion of nuclear pore complex assembly in Xenopus laevis egg extracts', *Journal of Cell Science*, 120(16), pp. 2895–2903. Available at: https://doi.org/10.1242/jcs.010181.

Bennett, M.K. *et al.* (1993) 'The syntaxin family of vesicular transport receptors', *Cell*, 74(5), pp. 863–873. Available at: https://doi.org/10.1016/0092-8674(93)90466-4.

Berney, C. and Danuser, G. (2003) 'FRET or No FRET: A Quantitative Comparison', *Biophysical Journal*, 84(6), pp. 3992–4010.

Berntsson, R.P.-A. *et al.* (2013) 'Structure of dual receptor binding to botulinum neurotoxin B', *Nature Communications*, 4(1), p. 2058. Available at: https://doi.org/10.1038/ncomms3058.

Bizzini, B. (1979) 'Tetanus toxin', *Microbiological Reviews*, 43(2), pp. 224–240. Available at: https://doi.org/10.1128/mr.43.2.224-240.1979.

Blum, T.R. *et al.* (2021) 'Phage-assisted evolution of botulinum neurotoxin proteases with reprogrammed specificity', *Science*, 371(6531), pp. 803–810. Available at: https://doi.org/10.1126/science.abf5972.

Bogdanovic, A. *et al.* (2002) 'Syntaxin 7, syntaxin 8, Vti1 and VAMP7 (vesicle-associated membrane protein 7) form an active SNARE complex for early macropinocytic compartment fusion in Dictyostelium discoideum', *The Biochemical Journal*, 368(Pt 1), pp. 29–39. Available at: https://doi.org/10.1042/BJ20020845.

Bonaud, A. *et al.* (2023) 'Sec22b is a critical and nonredundant regulator of plasma cell maintenance', *Proceedings of the National Academy of Sciences of the United States of America*, 120(2), p. e2213056120. Available at: https://doi.org/10.1073/pnas.2213056120.

Boucrot, E. and Kirchhausen, T. (2007) 'Endosomal recycling controls plasma membrane area during mitosis', *Proceedings of the National Academy of Sciences of the United States of America*, 104(19), pp. 7939–7944. Available at: https://doi.org/10.1073/pnas.0702511104.

Bourassa, C.V. *et al.* (2012) 'VAMP1 Mutation Causes Dominant Hereditary Spastic Ataxia in Newfoundland Families', *American Journal of Human Genetics*, 91(3), pp. 548–552. Available at: https://doi.org/10.1016/j.ajhg.2012.07.018.

Boyer, A.E. *et al.* (2005) 'From the Mouse to the Mass Spectrometer: Detection and Differentiation of the Endoproteinase Activities of Botulinum Neurotoxins A−G by Mass Spectrometry', *Analytical Chemistry*, 77(13), pp. 3916–3924. Available at: https://doi.org/10.1021/ac050485f.

Brandhorst, D. *et al.* (2006) 'Homotypic fusion of early endosomes: SNAREs do not determine fusion specificity', *Proceedings of the National Academy of Sciences*, 103(8), pp. 2701–2706. Available at: https://doi.org/10.1073/pnas.0511138103.

Brophy, K. *et al.* (2002) 'Synaptosomal-associated protein 25 (SNAP-25) and attention deficit hyperactivity disorder (ADHD): evidence of linkage and association in the Irish population', *Molecular Psychiatry*, 7(8), pp. 913–917. Available at: https://doi.org/10.1038/sj.mp.4001092.

Brunger, A.T. and Rummel, A. (2009) 'Receptor and substrate interactions of clostridial neurotoxins', *Toxicon*, 54(5), pp. 550–560. Available at: https://doi.org/10.1016/j.toxicon.2008.12.027.

Bushara, K.O. and Park, D.M. (1994) 'Botulinum toxin and sweating.', *Journal of Neurology, Neurosurgery, and Psychiatry*, 57(11), pp. 1437–1438.

Buss, F. *et al.* (2001) 'Myosin VI isoform localized to clathrin-coated vesicles with a role in clathrin-mediated endocytosis', *The EMBO Journal*, 20(14), pp. 3676–3684. Available at: https://doi.org/10.1093/emboj/20.14.3676.

Chen, Y.A. *et al.* (1999) 'SNARE Complex Formation Is Triggered by Ca2+ and Drives Membrane Fusion', *Cell*, 97(2), pp. 165–174. Available at: https://doi.org/10.1016/S0092-8674(00)80727-8.

Choi, U.B. *et al.* (2018) 'NSF-mediated disassembly of on- and off-pathway SNARE complexes and inhibition by complexin', *eLife*. Edited by V. Malhotra, 7, p. e36497. Available at: https://doi.org/10.7554/eLife.36497.

Clary, D.O., Griff, I.C. and Rothman, J.E. (1990) 'SNAPs, a family of NSF attachment proteins involved in intracellular membrane fusion in animals and yeast', *Cell*, 61(4), pp. 709–721. Available at: https://doi.org/10.1016/0092-8674(90)90482-T.

Contreras, E. *et al.* (2019) 'A neurotoxin that specifically targets Anopheles mosquitoes', *Nature Communications*, 10(1), p. 2869. Available at: https://doi.org/10.1038/s41467-019-10732-w.

Crowther, R.A. and Pearse, B.M. (1981) 'Assembly and packing of clathrin into coats', *The Journal of Cell Biology*, 91(3 Pt 1), pp. 790–797. Available at: https://doi.org/10.1083/jcb.91.3.790.

Cuddy, L.K. *et al.* (2019) 'Stress-induced cellular clearance is mediated by SNARE protein ykt6 and disrupted by a-synuclein', *Neuron*, 104(5), pp. 869-884.e11. Available at: https://doi.org/10.1016/j.neuron.2019.09.001.

Daro, E. *et al.* (1996) 'Rab4 and cellubrevin define different early endosome populations on the pathway of transferrin receptor recycling.', *Proceedings of the National Academy of Sciences of the United States of America*, 93(18), pp. 9559–9564.

Dascher, C., Matteson, J. and Balch, W.E. (1994) 'Syntaxin 5 regulates endoplasmic reticulum to Golgi transport.', *Journal of Biological Chemistry*, 269(47), pp. 29363–29366. Available at: https://doi.org/10.1016/S0021-9258(18)43884-7.

Dautry-Varsat, A., Ciechanover, A. and Lodish, H.F. (1983) 'pH and the recycling of transferrin during receptor-mediated endocytosis.', *Proceedings of the National Academy of Sciences of the United States of America*, 80(8), pp. 2258–2262.

Deák, F. *et al.* (2006) 'Structural Determinants of Synaptobrevin 2 Function in Synaptic Vesicle Fusion', *Journal of Neuroscience*, 26(25), pp. 6668–6676. Available at: https://doi.org/10.1523/JNEUROSCI.5272-05.2006.

Dickson, E.C. (1918) 'Botulism', *Canadian Medical Association Journal*, 8(10), pp. 903–909.

Donaldson, J.G., Johnson ,Debra L. and and Dutta, D. (2016) 'Rab and Arf G proteins in endosomal trafficking and cell surface homeostasis', *Small GTPases*, 7(4), pp. 247–251. Available at: https://doi.org/10.1080/21541248.2016.1212687.

Dong, M. *et al.* (2003) 'Synaptotagmins I and II mediate entry of botulinum neurotoxin B into cells', *Journal of Cell Biology*, 162(7), pp. 1293–1303. Available at: https://doi.org/10.1083/jcb.200305098.

Dong, M. *et al.* (2006) 'SV2 Is the Protein Receptor for Botulinum Neurotoxin A', *Science*, 312(5773), pp. 592–596. Available at: https://doi.org/10.1126/science.1123654.

Dong, M. *et al.* (2007) 'Mechanism of botulinum neurotoxin B and G entry into hippocampal neurons', *Journal of Cell Biology*, 179(7), pp. 1511–1522. Available at: https://doi.org/10.1083/jcb.200707184.

Dulubova, I. *et al.* (1999) 'A conformational switch in syntaxin during exocytosis: role of munc18', *The EMBO Journal*, 18(16), pp. 4372–4382. Available at: https://doi.org/10.1093/emboj/18.16.4372.

Dulubova, I. *et al.* (2007) 'Munc18-1 binds directly to the neuronal SNARE complex', *Proceedings of the National Academy of Sciences*, 104(8), pp. 2697–2702. Available at: https://doi.org/10.1073/pnas.0611318104.

Eleopra, R. *et al.* (2004) 'Different types of botulinum toxin in humans', *Movement Disorders*, 19(S8), pp. S53–S59. Available at: https://doi.org/10.1002/mds.20010.

Escola, J.-M. *et al.* (1998) 'Selective Enrichment of Tetraspan Proteins on the Internal Vesicles of Multivesicular Endosomes and on Exosomes Secreted by Human B-lymphocytes *', *Journal of Biological Chemistry*, 273(32), pp. 20121–20127. Available at: https://doi.org/10.1074/jbc.273.32.20121.

Etain, B. *et al.* (2010) 'A SNAP25 promoter variant is associated with early-onset bipolar disorder and a high expression level in brain', *Molecular Psychiatry*, 15(7), pp. 748–755. Available at: https://doi.org/10.1038/mp.2008.148.

Fader, C.M. *et al.* (2009) 'TI-VAMP/VAMP7 and VAMP3/cellubrevin: two v-SNARE proteins involved in specific steps of the autophagy/multivesicular body pathways', *Biochimica et Biophysica Acta (BBA) - Molecular Cell Research*, 1793(12), pp. 1901–1916. Available at: https://doi.org/10.1016/j.bbamcr.2009.09.011.

Fasshauer, D. *et al.* (1998) 'Conserved structural features of the synaptic fusion complex: SNARE proteins reclassified as Q- and R-SNAREs', *Proceedings of the National Academy of Sciences*, 95(26), pp. 15781–15786. Available at: https://doi.org/10.1073/pnas.95.26.15781.

Filippini, F. *et al.* (2001) 'Longins: a new evolutionary conserved VAMP family sharing a novel SNARE domain', *Trends in Biochemical Sciences*, 26(7), pp. 407–409. Available at: https://doi.org/10.1016/S0968-0004(01)01861-8.

Fischer, A. and Montal, M. (2007) 'Crucial Role of the Disulfide Bridge between Botulinum Neurotoxin Light and Heavy Chains in Protease Translocation across Membranes*', *Journal of Biological Chemistry*, 282(40), pp. 29604–29611. Available at: https://doi.org/10.1074/jbc.M703619200.

Fonfria, E. *et al.* (2018) 'The Expanding Therapeutic Utility of Botulinum Neurotoxins', *Toxins*, 10(5). Available at: https://doi.org/10.3390/toxins10050208.

Franciosa, G., Ferreira, J.L. and Hatheway, C.L. (1994) 'Detection of type A, B, and E botulism neurotoxin genes in Clostridium botulinum and other Clostridium species by PCR: evidence of unexpressed type B toxin genes in type A toxigenic organisms', *Journal of Clinical Microbiology*, 32(8), pp. 1911–1917. Available at: https://doi.org/10.1128/jcm.32.8.1911-1917.1994.

Fu, Z. *et al.* (2009) 'Glycosylated SV2 and Gangliosides as Dual Receptors for Botulinum Neurotoxin Serotype F', *Biochemistry*, 48(24), pp. 5631–5641. Available at: https://doi.org/10.1021/bi9002138.

Fukasawa, M. *et al.* (2004) 'Localization and activity of the SNARE Ykt6 determined by its regulatory domain and palmitoylation', *Proceedings of the National Academy of Sciences*, 101(14), pp. 4815–4820. Available at: https://doi.org/10.1073/pnas.0401183101.

Gaisano, H.Y. *et al.* (1994) 'Tetanus toxin light chain cleaves a vesicle-associated membrane protein (VAMP) isoform 2 in rat pancreatic zymogen granules and inhibits enzyme secretion.', *Journal of Biological Chemistry*, 269(25), pp. 17062–17066. Available at: https://doi.org/10.1016/S0021-9258(17)32520-6.

Galli, T. *et al.* (1994) 'Tetanus toxin-mediated cleavage of cellubrevin impairs exocytosis of transferrin receptor-containing vesicles in CHO cells.', *Journal of Cell Biology*, 125(5), pp. 1015–1024. Available at: https://doi.org/10.1083/jcb.125.5.1015.

Galli, T. *et al.* (1998) 'A Novel Tetanus Neurotoxin-insensitive Vesicle-associated Membrane Protein in SNARE Complexes of the Apical Plasma Membrane of Epithelial Cells', *Molecular Biology of the Cell*, 9(6), pp. 1437–1448. Available at: https://doi.org/10.1091/mbc.9.6.1437.

Galloux, M. *et al.* (2008) 'Membrane Interaction of botulinum neurotoxin A translocation (T) domain. The belt region is a regulatory loop for membrane interaction', *The Journal of Biological Chemistry*, 283(41), pp. 27668–27676. Available at: https://doi.org/10.1074/jbc.M802557200.

Godlee, C. and Kaksonen, M. (2013) 'From uncertain beginnings: Initiation mechanisms of clathrin-mediated endocytosis', *The Journal of Cell Biology*, 203(5), pp. 717–725. Available at: https://doi.org/10.1083/jcb.201307100.

Gordon, D.E. *et al.* (2009) 'Coiled-coil interactions are required for post-Golgi R-SNARE trafficking', *EMBO reports*, 10(8), pp. 851–856. Available at: https://doi.org/10.1038/embor.2009.96.

Gordon, D.E. *et al.* (2010) 'A targeted siRNA screen to identify SNAREs required for constitutive secretion in mammalian cells', *Traffic (Copenhagen, Denmark)*, 11(9), pp. 1191–1204. Available at: https://doi.org/10.1111/j.1600-0854.2010.01087.x.

Gordon, D.E. *et al.* (2017) 'VAMP3/Syb and YKT6 are required for the fusion of constitutive secretory carriers with the plasma membrane', *PLOS Genetics*, 13(4), p. e1006698. Available at: https://doi.org/10.1371/journal.pgen.1006698.

Graham, M.E. *et al.* (2001) 'SNAP-25 with mutations in the zero layer supports normal membrane fusion kinetics', *Journal of Cell Science*, 114(24), pp. 4397–4405. Available at: https://doi.org/10.1242/jcs.114.24.4397.

Grant, B.D. and Donaldson, J.G. (2009) 'Pathways and mechanisms of endocytic recycling', *Nature Reviews Molecular Cell Biology*, 10(9), pp. 597–608. Available at: https://doi.org/10.1038/nrm2755.

Greener, T. *et al.* (2000) 'Role of Cyclin G-associated Kinase in Uncoating Clathrin-coated Vesicles from Non-neuronal Cells *', *Journal of Biological Chemistry*, 275(2), pp. 1365–1370. Available at: https://doi.org/10.1074/jbc.275.2.1365.

Gregg, B.M. *et al.* (2024) 'Botulinum neurotoxin X lacks potency in mice and in human neurons', *mBio*, 15(3), p. e0310623. Available at: https://doi.org/10.1128/mbio.03106-23.

Gromley, A. *et al.* (2005) 'Centriolin anchoring of exocyst and SNARE complexes at the midbody is required for secretory-vesicle-mediated abscission', *Cell*, 123(1), pp. 75–87. Available at: https://doi.org/10.1016/j.cell.2005.07.027.

Guo, B. *et al.* (2014) 'O-GlcNAc-modification of SNAP-29 regulates autophagosome maturation', *Nature Cell Biology*, 16(12), pp. 1215–1226. Available at: https://doi.org/10.1038/ncb3066.

Han, G.A. *et al.* (2011) 'Munc18-1 domain-1 controls vesicle docking and secretion by interacting with syntaxin-1 and chaperoning it to the plasma membrane', *Molecular Biology of the Cell*, 22(21), pp. 4134–4149. Available at: https://doi.org/10.1091/mbc.e11-02-0135.

Hanson, P.I. *et al.* (1997) 'Structure and conformational changes in NSF and its membrane receptor complexes visualized by quick-freeze/deep-etch electron microscopy', *Cell*, 90(3), pp. 523–535. Available at: https://doi.org/10.1016/s0092-8674(00)80512-7.

Harel, A. *et al.* (2008) 'Evidence for CALM in Directing VAMP2 Trafficking', *Traffic*, 9(3), pp. 417–429. Available at: https://doi.org/10.1111/j.1600-0854.2007.00694.x.

Hasegawa, H. *et al.* (2003) 'Mammalian Ykt6 Is a Neuronal SNARE Targeted to a Specialized Compartment by its Profilin-like Amino Terminal Domain', *Molecular Biology of the Cell*, 14(2), pp. 698–720. Available at: https://doi.org/10.1091/mbc.E02-09-0556.

Hata, Y., Slaughter, C.A. and Südhof, T.C. (1993) 'Synaptic vesicle fusion complex contains unc-18 homologue bound to syntaxin', *Nature*, 366(6453), pp. 347–351. Available at: https://doi.org/10.1038/366347a0.

Hatheway, C.L. (1990) 'Toxigenic clostridia.', *Clinical Microbiology Reviews*, 3(1), pp. 66–98.

Hayashi, T. *et al.* (1994) 'Synaptic vesicle membrane fusion complex: action of clostridial neurotoxins on assembly.', *The EMBO Journal*, 13(21), pp. 5051–5061.

Hazzard, J., Südhof, T.C. and Rizo, J. (1999) 'NMR analysis of the structure of synaptobrevin and of its interaction with syntaxin', *Journal of Biomolecular NMR*, 14(3), pp. 203–207. Available at: https://doi.org/10.1023/A:1008382027065.

Hess, D. *et al.* (1992) 'The 25 kDa synaptosomal-associated protein SNAP-25 is the major methionine-rich polypeptide in rapid axonal transport and a major substrate for palmitoylation in adult CNS', *The Journal of neuroscience : the official journal of the Society for Neuroscience*, 12(12). Available at: https://doi.org/10.1523/JNEUROSCI.12-12-04634.1992.

Holt, M. *et al.* (2006) 'Identification of SNAP-47, a novel Qbc-SNARE with ubiquitous expression', *The Journal of Biological Chemistry*, 281(25), pp. 17076–17083. Available at: https://doi.org/10.1074/jbc.M513838200.

Humeau, Y. *et al.* (2000) 'How botulinum and tetanus neurotoxins block neurotransmitter release**This paper is dedicated to the memory of Heiner Niemann.', *Biochimie*, 82(5), pp. 427–446. Available at: https://doi.org/10.1016/S0300-9084(00)00216-9.

Hyytiä, E., Hielm, S. and Korkeala, H. (1998) 'Prevalence of Clostridium botulinum type E in Finnish fish and fishery products', *Epidemiology & Infection*, 120(3), pp. 245–250. Available at: https://doi.org/10.1017/S0950268898008693.

Ikezawa, M. *et al.* (2018) 'Loss of VAMP5 in mice results in duplication of the ureter and insufficient expansion of the lung', *Developmental Dynamics*, 247(5), pp. 754–762. Available at: https://doi.org/10.1002/dvdy.24618.

Itakura, E., Kishi-Itakura, C. and Mizushima, N. (2012) 'The Hairpin-type Tail-Anchored SNARE Syntaxin 17 Targets to Autophagosomes for Fusion with Endosomes/Lysosomes', *Cell*, 151(6), pp. 1256–1269. Available at: https://doi.org/10.1016/j.cell.2012.11.001.

Ivanova, D. *et al.* (2021) 'Control of synaptic vesicle release probability via VAMP4 targeting to endolysosomes', *Science Advances*, 7(18), p. eabf3873. Available at: https://doi.org/10.1126/sciadv.abf3873.

Jahn, R. and Südhof, T.C. (1999) 'Membrane Fusion and Exocytosis', *Annual Review of Biochemistry*, 68(Volume 68, 1999), pp. 863–911. Available at: https://doi.org/10.1146/annurev.biochem.68.1.863.

Jantsch-Plunger, V. and Glotzer, M. (1999) 'Depletion of syntaxins in the early Caenorhabditis elegans embryo reveals a role for membrane fusion events in cytokinesis', *Current Biology*, 9(14), pp. 738–745. Available at: https://doi.org/10.1016/S0960-9822(99)80333-9.

Kakinuma, H. *et al.* (1996) 'The first case of type B infant botulism in Japan', *Acta Paediatrica Japonica: Overseas Edition*, 38(5), pp. 541–543. Available at: https://doi.org/10.1111/j.1442-200x.1996.tb03542.x.

Karuna M, P. *et al.* (2020) 'Phosphorylation of Ykt6 SNARE Domain Regulates Its Membrane Recruitment and Activity', *Biomolecules*, 10(11). Available at: https://doi.org/10.3390/biom10111560.

Katz, L. and Brennwald, P. (2000) 'Testing the 3Q:1R "Rule": Mutational Analysis of the Ionic "Zero" Layer in the Yeast Exocytic SNARE Complex Reveals No Requirement for Arginine', *Molecular Biology of the Cell*, 11(11), pp. 3849–3858.

Keller, J.E., Cai, F. and Neale, E.A. (2004) 'Uptake of Botulinum Neurotoxin into Cultured Neurons', *Biochemistry*, 43(2), pp. 526–532. Available at: https://doi.org/10.1021/bi0356698.

Kelly, R.B. (1985) 'Pathways of Protein Secretion in Eukaryotes', *Science*, 230(4721), pp. 25–32.

Kimura, T. *et al.* (2017) 'Dedicated SNAREs and specialized TRIM cargo receptors mediate secretory autophagy', *The EMBO Journal*, 36(1), pp. 42–60. Available at: https://doi.org/10.15252/embj.201695081.

Klöckner, C. *et al.* (2021) 'De novo variants in SNAP25 cause an early-onset developmental and epileptic encephalopathy', *Genetics in Medicine*, 23(4), pp. 653–660. Available at: https://doi.org/10.1038/s41436-020-01020-w.

Kouranti, I. *et al.* (2006a) 'Rab35 Regulates an Endocytic Recycling Pathway Essential for the Terminal Steps of Cytokinesis', *Current Biology*, 16(17), pp. 1719–1725. Available at: https://doi.org/10.1016/j.cub.2006.07.020.

Kouranti, I. *et al.* (2006b) 'Rab35 Regulates an Endocytic Recycling Pathway Essential for the Terminal Steps of Cytokinesis', *Current Biology*, 16(17), pp. 1719–1725. Available at: https://doi.org/10.1016/j.cub.2006.07.020.

Kovačević, J. *et al.* (2018) 'Protein instability, haploinsufficiency, and cortical hyper-excitability underlie STXBP1 encephalopathy', *Brain*, 141(5), pp. 1350–1374. Available at: https://doi.org/10.1093/brain/awy046.

Krzewski, K. *et al.* (2011) 'VAMP4- and VAMP7-expressing vesicles are both required for cytotoxic granule exocytosis in NK cells', *European journal of immunology*, 41(11), pp. 3323–3329. Available at: https://doi.org/10.1002/eji.201141582.

Kubo, K. *et al.* (2015) 'SNAP23/25 and VAMP2 mediate exocytic event of transferrin receptor-containing recycling vesicles', *Biology Open*, 4(7), pp. 910–920. Available at: https://doi.org/10.1242/bio.012146.

Kukulski, W. *et al.* (2012) 'Plasma Membrane Reshaping during Endocytosis Is Revealed by Time-Resolved Electron Tomography', *Cell*, 150(3), pp. 508–520. Available at: https://doi.org/10.1016/j.cell.2012.05.046.

Kustanovich, V. *et al.* (2003) 'Biased paternal transmission of SNAP-25 risk alleles in attention-deficit hyperactivity disorder', *Molecular Psychiatry*, 8(3), pp. 309–315. Available at: https://doi.org/10.1038/sj.mp.4001247.

Kweon, Y. *et al.* (2003) 'Ykt6p Is a Multifunctional Yeast R-SNARE That Is Required for Multiple Membrane Transport Pathways to the Vacuole', *Molecular Biology of the Cell*, 14(5), pp. 1868–1881. Available at: https://doi.org/10.1091/mbc.e02-10-0687.

Lacy, D.B. *et al.* (1998) 'Crystal structure of botulinum neurotoxin type A and implications for toxicity', *Nature Structural Biology*, 5(10), pp. 898–902. Available at: https://doi.org/10.1038/2338.

Ledda, C. *et al.* (2022) 'Time to onset and duration of botulinum toxin efficacy in movement disorders', *Journal of Neurology*, 269(7), pp. 3706–3712. Available at: https://doi.org/10.1007/s00415-022-10995-2.

Lerman, J.C. *et al.* (2000) 'Structural Analysis of the Neuronal SNARE Protein Syntaxin-1A', *Biochemistry*, 39(29), pp. 8470–8479. Available at: https://doi.org/10.1021/bi0003994.

Liang, T. *et al.* (2020) 'SNAP23 depletion enables more SNAP25/calcium channel excitosome formation to increase insulin exocytosis in type 2 diabetes', *JCI insight*, 5(3), pp. e129694, 129694. Available at: https://doi.org/10.1172/jci.insight.129694.

Lippincott-Schwartz, J. *et al.* (1989) 'Rapid redistribution of Golgi proteins into the ER in cells treated with brefeldin A: evidence for membrane cycling from Golgi to ER', *Cell*, 56(5), pp. 801–813. Available at: https://doi.org/10.1016/0092-8674(89)90685-5.

Liu, Y. and Barlowe, C. (2002) 'Analysis of Sec22p in Endoplasmic Reticulum/Golgi Transport Reveals Cellular Redundancy in SNARE Protein Function', *Molecular Biology of the Cell*, 13(9), pp. 3314–3324. Available at: https://doi.org/10.1091/mbc.E02-04-0204.

Lloyd, C.S. *et al.* (1976) 'Wild bird mortality caused by botulism in Britain, 1975', *Biological Conservation*, 10(2), pp. 119–129. Available at: https://doi.org/10.1016/0006-3207(76)90056-2.

Low, S.H. *et al.* (2003) 'Syntaxin 2 and Endobrevin Are Required for the Terminal Step of Cytokinesis in Mammalian Cells', *Developmental Cell*, 4(5), pp. 753–759. Available at: https://doi.org/10.1016/S1534-5807(03)00122-9.

Lowe, M. *et al.* (2004) 'Caspase-mediated cleavage of syntaxin 5 and giantin accompanies inhibition of secretory traffic during apoptosis', *Journal of Cell Science*, 117(7), pp. 1139–1150. Available at: https://doi.org/10.1242/jcs.00950.

Luftman, K. *et al.* (2009) 'Silencing of VAMP3 inhibits cell migration and integrin-mediated adhesion', *Biochemical and Biophysical Research Communications*, 380(1), pp. 65–70. Available at: https://doi.org/10.1016/j.bbrc.2009.01.036.

Ma, M. *et al.* (2024) 'Homozygous missense variants in *YKT6* result in loss of function and are associated with developmental delay, with or without severe infantile liver disease and risk for hepatocellular carcinoma', *Genetics in Medicine*, 26(7), p. 101125. Available at: https://doi.org/10.1016/j.gim.2024.101125.

Madeira, F. *et al.* (2024) 'The EMBL-EBI Job Dispatcher sequence analysis tools framework in 2024', *Nucleic acids research*, 52(W1), pp. W521–W525. Available at: https://doi.org/10.1093/nar/gkae241.

Malhotra, V. *et al.* (1988) 'Role of an N-ethylmaleimide-sensitive transport component in promoting fusion of transport vesicles with cisternae of the Golgi stack', *Cell*, 54(2), pp. 221–227. Available at: https://doi.org/10.1016/0092-8674(88)90554-5.

Martinez-Arca, S. *et al.* (2000) 'Role of Tetanus Neurotoxin Insensitive Vesicle-Associated Membrane Protein (Ti-Vamp) in Vesicular Transport Mediating Neurite Outgrowth', *The Journal of Cell Biology*, 149(4), pp. 889–900.

Martinez-Arca, S. *et al.* (2001) 'A Common Exocytotic Mechanism Mediates Axonal and Dendritic Outgrowth', *Journal of Neuroscience*, 21(11), pp. 3830–3838. Available at: https://doi.org/10.1523/JNEUROSCI.21-11-03830.2001.

Martínez-Carranza, M. *et al.* (2024) 'Activity of botulinum neurotoxin X and its structure when shielded by a non-toxic non-hemagglutinin protein', *Communications Chemistry*, 7(1), pp. 1–15. Available at: https://doi.org/10.1038/s42004-024-01262-8.

Maslanka, S.E. *et al.* (2016) 'A Novel Botulinum Neurotoxin, Previously Reported as Serotype H, Has a Hybrid-Like Structure With Regions of Similarity to the Structures of Serotypes A and F and Is Neutralized With Serotype A Antitoxin', *The Journal of Infectious Diseases*, 213(3), pp. 379–385. Available at: https://doi.org/10.1093/infdis/jiv327.

Masuyer, G. *et al.* (2018) 'Structural characterisation of the catalytic domain of botulinum neurotoxin X - high activity and unique substrate specificity', *Scientific Reports*, 8(1), p. 4518. Available at: https://doi.org/10.1038/s41598-018-22842-4.

Matsui, T. *et al.* (2018) 'Autophagosomal YKT6 is required for fusion with lysosomes independently of syntaxin 17', *Journal of Cell Biology*, 217(8), pp. 2633–2645. Available at: https://doi.org/10.1083/jcb.201712058.

Matveeva, E. and Whiteheart, S.W. (1998) 'The effects of SNAP/SNARE complexes on the ATPase of NSF', *FEBS Letters*, 435(2), pp. 211–214. Available at: https://doi.org/10.1016/S0014-5793(98)01071-0.

Mayor, S. and Pagano, R.E. (2007) 'Pathways of clathrin-independent endocytosis', *Nature Reviews Molecular Cell Biology*, 8(8), pp. 603–612. Available at: https://doi.org/10.1038/nrm2216.

McGrath, K. *et al.* (2021) 'A conformational switch driven by phosphorylation regulates the activity of the evolutionarily conserved SNARE Ykt6', *Proceedings of the National Academy of Sciences*, 118(12), p. e2016730118. Available at: https://doi.org/10.1073/pnas.2016730118.

McMahon, H.T. *et al.* (1993) 'Cellubrevin is a ubiquitous tetanus-toxin substrate homologous to a putative synaptic vesicle fusion protein', *Nature*, 364(6435), pp. 346–349. Available at: https://doi.org/10.1038/364346a0.

McMahon, H.T. and Boucrot, E. (2011) 'Molecular mechanism and physiological functions of clathrin-mediated endocytosis', *Nature Reviews Molecular Cell Biology*, 12(8), pp. 517–533. Available at: https://doi.org/10.1038/nrm3151.

McNew, J.A. *et al.* (1997) 'Ykt6p, a Prenylated SNARE Essential for Endoplasmic Reticulum-Golgi Transport *', *Journal of Biological Chemistry*, 272(28), pp. 17776–17783. Available at: https://doi.org/10.1074/jbc.272.28.17776.

Merrifield, C.J. *et al.* (2002) 'Imaging actin and dynamin recruitment during invagination of single clathrin-coated pits', *Nature Cell Biology*, 4(9), pp. 691–698. Available at: https://doi.org/10.1038/ncb837.

Michalik, M. *et al.* (1986) 'Enzyme-linked immunosorbent assay (ELISA) for the detection and differentiation of *clostridium botulinum* toxins type A and B', *Journal of Immunological Methods*, 93(2), pp. 225–230. Available at: https://doi.org/10.1016/0022-1759(86)90193-6.

Miller, S.E. *et al.* (2011) 'The Molecular Basis for the Endocytosis of Small R-SNAREs by the Clathrin Adaptor CALM', *Cell*, 147(5), pp. 1118–1131. Available at: https://doi.org/10.1016/j.cell.2011.10.038.

Ming Li, W. *et al.* (2006) 'Recruitment and SNARE-mediated fusion of vesicles in furrow membrane remodeling during cytokinesis in zebrafish embryos', *Experimental Cell Research*, 312(17), pp. 3260–3275. Available at: https://doi.org/10.1016/j.yexcr.2006.06.028.

Misura, K.M.S., Scheller, R.H. and Weis, W.I. (2000) 'Three-dimensional structure of the neuronal-Sec1–syntaxin 1a complex', *Nature*, 404(6776), pp. 355–362. Available at: https://doi.org/10.1038/35006120.

Miyashita, S.-I. *et al.* (2021) 'Delivery of single-domain antibodies into neurons using a chimeric toxin–based platform is therapeutic in mouse models of botulism', *Science Translational Medicine*, 13(575), p. eaaz4197. Available at: https://doi.org/10.1126/scitranslmed.aaz4197.

Montecucco, C. (1986) 'How do tetanus and botulinum toxins bind to neuronal membranes?', *Trends in Biochemical Sciences*, 11(8), pp. 314–317. Available at: https://doi.org/10.1016/0968-0004(86)90282-3.

Montecucco, C. and Schiavo, G. (1994) 'Mechanism of action of tetanus and botulinum neurotoxins', *Molecular Microbiology*, 13(1), pp. 1–8. Available at: https://doi.org/10.1111/j.1365-2958.1994.tb00396.x.

Montecucco, C. and Schiavo, G. (1995) 'Structure and function of tetanus and botulinum neurotoxins', *Quarterly Reviews of Biophysics*, 28(4), pp. 423–472. Available at: https://doi.org/10.1017/S0033583500003292.

Montecucco, C., Schiavo, G. and Pantano, S. (2005) 'SNARE complexes and neuroexocytosis: how many, how close?', *Trends in Biochemical Sciences*, 30(7), pp. 367–372. Available at: https://doi.org/10.1016/j.tibs.2005.05.002.

Morelli, E. *et al.* (2016) 'An essential step of kinetochore formation controlled by the SNARE protein Snap29', *The EMBO Journal*, 35(20), pp. 2223–2237. Available at: https://doi.org/10.15252/embj.201693991.

Morgan, J.R. *et al.* (1999) 'A Role for the Clathrin Assembly Domain of AP180 in Synaptic Vesicle Endocytosis', *Journal of Neuroscience*, 19(23), pp. 10201–10212. Available at: https://doi.org/10.1523/JNEUROSCI.19-23-10201.1999.

Moriishi, K. *et al.* (1996) 'Mosaic structures of neurotoxins produced from Clostridium botulinum types C and D organisms', *Biochimica et Biophysica Acta (BBA) - Gene Structure and Expression*, 1307(2), pp. 123–126. Available at: https://doi.org/10.1016/0167-4781(96)00006-1.

Mukai, A. *et al.* (2008) 'Dynamic regulation of ubiquitylation and deubiquitylation at the central spindle during cytokinesis', *Journal of Cell Science*, 121(8), pp. 1325–1333. Available at: https://doi.org/10.1242/jcs.027417.

Mullock, B.M. *et al.* (2000) 'Syntaxin 7 Is Localized to Late Endosome Compartments, Associates with Vamp 8, and Is Required for Late Endosome–Lysosome Fusion', *Molecular Biology of the Cell*, 11(9), pp. 3137–3153. Available at: https://doi.org/10.1091/mbc.11.9.3137.

Nakamura, K. *et al.* (2010) 'Characterization of the D/C mosaic neurotoxin produced by Clostridium botulinum associated with bovine botulism in Japan', *Veterinary Microbiology*, 140(1), pp. 147–154. Available at: https://doi.org/10.1016/j.vetmic.2009.07.023.

Navaroli, D.M. *et al.* (2012) 'Rabenosyn-5 defines the fate of the transferrin receptor following clathrin-mediated endocytosis', *Proceedings of the National Academy of Sciences*, 109(8), pp. E471–E480. Available at: https://doi.org/10.1073/pnas.1115495109.

Nielsen, E. *et al.* (1999) 'Rab5 regulates motility of early endosomes on microtubules', *Nature Cell Biology*, 1(6), pp. 376–382. Available at: https://doi.org/10.1038/14075.

Nishiki, T. *et al.* (1994) 'Identification of protein receptor for Clostridium botulinum type B neurotoxin in rat brain synaptosomes.', *Journal of Biological Chemistry*, 269(14), pp. 10498–10503.

Nystuen, A.M. *et al.* (2007) 'A null mutation in VAMP1/synaptobrevin is associated with neurological defects and prewean mortality in the lethal-wasting mouse mutant', *Neurogenetics*, 8(1), pp. 1–10. Available at: https://doi.org/10.1007/s10048-006-0068-7.

Ortolani, E.L. *et al.* (1997) 'Botulism outbreak associated with poultry litter consumption in three Brazilian cattle herds', *Veterinary and Human Toxicology*, 39(2), pp. 89–92.

Osen-Sand, A. *et al.* (1996) 'Common and distinct fusion proteins in axonal growth and transmitter release', *Journal of Comparative Neurology*, 367(2), pp. 222–234. Available at: https://doi.org/10.1002/(SICI)1096-9861(19960401)367:2<222::AID-CNE5>3.0.CO;2-7.

Park, M. *et al.* (2023) 'NSF/αSNAP2-mediated cis-SNARE complex disassembly precedes vesicle fusion in Arabidopsis cytokinesis', *Nature Plants*, 9(6), pp. 889–897. Available at: https://doi.org/10.1038/s41477-023-01427-8.

Patel, K. *et al.* (2017) 'A Novel Surface Plasmon Resonance Biosensor for the Rapid Detection of Botulinum Neurotoxins', *Biosensors*, 7(3), p. 32. Available at: https://doi.org/10.3390/bios7030032.

Pearse, B.M. (1976) 'Clathrin: a unique protein associated with intracellular transfer of membrane by coated vesicles.', *Proceedings of the National Academy of Sciences of the United States of America*, 73(4), pp. 1255–1259.

Peden, A.A., Park, G.Y. and Scheller, R.H. (2001) 'The Di-leucine Motif of Vesicle-associated Membrane Protein 4 Is Required for Its Localization and AP-1 Binding*', *Journal of Biological Chemistry*, 276(52), pp. 49183–49187. Available at: https://doi.org/10.1074/jbc.M106646200.

Pellizzari, R. *et al.* (1996) 'Structural Determinants of the Specificity for Synaptic Vesicle-associated Membrane Protein/Synaptobrevin of Tetanus and Botulinum Type B and G Neurotoxins *', *Journal of Biological Chemistry*, 271(34), pp. 20353–20358. Available at: https://doi.org/10.1074/jbc.271.34.20353.

Peng, L. *et al.* (2013) 'Cytotoxicity of botulinum neurotoxins reveals a direct role of syntaxin 1 and SNAP-25 in neuron survival', *Nature Communications*, 4(1), p. 1472. Available at: https://doi.org/10.1038/ncomms2462.

Pereira, C. *et al.* (2023) 'The exocyst complex is an essential component of the mammalian constitutive secretory pathway', *The Journal of Cell Biology*, 222(5), p. e202205137. Available at: https://doi.org/10.1083/jcb.202205137.

Pirazzini, M. *et al.* (2014) 'Thioredoxin and Its Reductase Are Present on Synaptic Vesicles, and Their Inhibition Prevents the Paralysis Induced by Botulinum Neurotoxins', *Cell Reports*, 8(6), pp. 1870–1878. Available at: https://doi.org/10.1016/j.celrep.2014.08.017.

Pirazzini, M. *et al.* (2016) 'On the translocation of botulinum and tetanus neurotoxins across the membrane of acidic intracellular compartments', *Biochimica et Biophysica Acta (BBA) - Biomembranes*, 1858(3), pp. 467–474. Available at: https://doi.org/10.1016/j.bbamem.2015.08.014.

Pirazzini, M. *et al.* (2017) 'Botulinum Neurotoxins: Biology, Pharmacology, and Toxicology', *Pharmacological Reviews*, 69(2), pp. 200–235. Available at: https://doi.org/10.1124/pr.116.012658.

Prekeris, R., Klumperman, J. and Scheller, R.H. (2000) 'Syntaxin 11 is an atypical SNARE abundant in the immune system', *European Journal of Cell Biology*, 79(11), pp. 771–780. Available at: https://doi.org/10.1078/0171-9335-00109.

Pryor, P.R. *et al.* (2004) 'Combinatorial SNARE complexes with VAMP7 or VAMP8 define different late endocytic fusion events', *EMBO reports*, 5(6), pp. 590–595. Available at: https://doi.org/10.1038/sj.embor.7400150.

Rannou, Y. *et al.* (2012) 'MNK1 kinase activity is required for abscission', *Journal of Cell Science*, 125(Pt 12), pp. 2844–2852. Available at: https://doi.org/10.1242/jcs.058081.

Rasetti-Escargueil, C. and Popoff, M.R. (2022) 'Recent Developments in Botulinum Neurotoxins Detection', *Microorganisms*, 10(5), p. 1001. Available at: https://doi.org/10.3390/microorganisms10051001.

Rebane, A.A. *et al.* (2018) 'Two Disease-Causing SNAP-25B Mutations Selectively Impair SNARE C-terminal Assembly', *Journal of molecular biology*, 430(4), pp. 479–490. Available at: https://doi.org/10.1016/j.jmb.2017.10.012.

Regazzi, R. *et al.* (1995) 'VAMP-2 and cellubrevin are expressed in pancreatic beta-cells and are essential for Ca(2+)-but not for GTP gamma S-induced insulin secretion', *The EMBO journal*, 14(12), pp. 2723–2730. Available at: https://doi.org/10.1002/j.1460-2075.1995.tb07273.x.

Regazzi, R. *et al.* (1996) 'Mutational analysis of VAMP domains implicated in Ca2+-induced insulin exocytosis.', *The EMBO Journal*, 15(24), pp. 6951–6959.

Renna, M. *et al.* (2011) 'Autophagic substrate clearance requires activity of the syntaxin-5 SNARE complex', *Journal of Cell Science*, 124(3), pp. 469–482. Available at: https://doi.org/10.1242/jcs.076489.

Robinson, P.J. *et al.* (1994) 'Phosphorylation of dynamin I and synaptic-vesicle recycling', *Trends in Neurosciences*, 17(8), pp. 348–353. Available at: https://doi.org/10.1016/0166-2236(94)90179-1.

Rose, A.J. *et al.* (2009) 'Effects of contraction on localization of GLUT4 and v-SNARE isoforms in rat skeletal muscle', *American Journal of Physiology-Regulatory, Integrative and Comparative Physiology*, 297(5), pp. R1228–R1237. Available at: https://doi.org/10.1152/ajpregu.00258.2009.

Rothman, J.E. (1994) 'Mechanisms of intracellular protein transport', *Nature*, 372(6501), pp. 55–63. Available at: https://doi.org/10.1038/372055a0.

Rowe, J. *et al.* (2001) 'Syntaxin 1A is delivered to the apical and basolateral domains of epithelial cells: the role of munc-18 proteins', *Journal of Cell Science*, 114(18), pp. 3323–3332. Available at: https://doi.org/10.1242/jcs.114.18.3323.

Ruiz-Martinez, M. *et al.* (2016) 'YKT6 expression, exosome release, and survival in non-small cell lung cancer', *Oncotarget*, 7(32), pp. 51515–51524. Available at: https://doi.org/10.18632/oncotarget.9862.

Rummel, A., Karnath, T., *et al.* (2004) 'Synaptotagmins I and II Act as Nerve Cell Receptors for Botulinum Neurotoxin G', *Journal of Biological Chemistry*, 279(29), pp. 30865–30870. Available at: https://doi.org/10.1074/jbc.M403945200.

Rummel, A., Mahrhold, S., *et al.* (2004) 'The HCC-domain of botulinum neurotoxins A and B exhibits a singular ganglioside binding site displaying serotype specific carbohydrate interaction', *Molecular Microbiology*, 51(3), pp. 631–643. Available at: https://doi.org/10.1046/j.1365-2958.2003.03872.x.

Rummel, A. *et al.* (2009) 'Botulinum neurotoxins C, E and F bind gangliosides via a conserved binding site prior to stimulation-dependent uptake with botulinum neurotoxin F utilising the three isoforms of SV2 as second receptor', *Journal of Neurochemistry*, 110(6), pp. 1942–1954. Available at: https://doi.org/10.1111/j.1471-4159.2009.06298.x.

Rust, A. *et al.* (2016) 'Botulinum neurotoxin type C protease induces apoptosis in differentiated human neuroblastoma cells', *Oncotarget*, 7(22), pp. 33220–33228. Available at: https://doi.org/10.18632/oncotarget.8903.

Rust, A. *et al.* (2017) 'A Cell Line for Detection of Botulinum Neurotoxin Type B', *Frontiers in Pharmacology*, 8, p. 796. Available at: https://doi.org/10.3389/fphar.2017.00796.

Ryu, J.-K. *et al.* (2015) 'Spring-loaded unraveling of a single SNARE complex by NSF in one round of ATP turnover', *Science*, 347(6229), pp. 1485–1489. Available at: https://doi.org/10.1126/science.aaa5267.

Sakamoto, M. *et al.* (2024) 'VAMP7 knockdown in secretory granules impairs CCL2 secretion in mast cells', *Biochemical and Biophysical Research Communications*, 691, p. 149258. Available at: https://doi.org/10.1016/j.bbrc.2023.149258.

Sakata, N. *et al.* (2021) 'Double prenylation of SNARE protein Ykt6 is required for lysosomal hydrolase trafficking', *The Journal of Biochemistry*, 169(3), pp. 363–370. Available at: https://doi.org/10.1093/jb/mvaa111.

Salpietro, V. *et al.* (2019) 'Mutations in the Neuronal Vesicular SNARE VAMP2 Affect Synaptic Membrane Fusion and Impair Human Neurodevelopment', *American Journal of Human Genetics*, 104(4), pp. 721–730. Available at: https://doi.org/10.1016/j.ajhg.2019.02.016.

Sato, M. *et al.* (2011) 'The Role of VAMP7/TI-VAMP in Cell Polarity and Lysosomal Exocytosis in vivo', *Traffic*, 12(10), pp. 1383–1393. Available at: https://doi.org/10.1111/j.1600-0854.2011.01247.x.

Scales, S.J., Yoo, B.Y. and Scheller, R.H. (2001) 'The ionic layer is required for efficient dissociation of the SNARE complex by α-SNAP and NSF', *Proceedings of the National Academy of Sciences of the United States of America*, 98(25), pp. 14262–14267. Available at: https://doi.org/10.1073/pnas.251547598.

Schiavo, G. *et al.* (1994) 'Tetanus and Botulinum Neurotoxins Are Zinc Proteases Specific for Components of the Neuroexocytosis Apparatusa', *Annals of the New York Academy of Sciences*, 710(1), pp. 65–75. Available at: https://doi.org/10.1111/j.1749-6632.1994.tb26614.x.

Schiavo, G.G. *et al.* (1992) 'Tetanus and botulinum-B neurotoxins block neurotransmitter release by proteolytic cleavage of synaptobrevin', *Nature*, 359(6398), pp. 832–835. Available at: https://doi.org/10.1038/359832a0.

Schiel, J.A. *et al.* (2011) 'Endocytic membrane fusion and buckling-induced microtubule severing mediate cell abscission', *Journal of Cell Science*, 124(9), pp. 1411–1424. Available at: https://doi.org/10.1242/jcs.081448.

Schlierf, B. *et al.* (2000) 'Rab11b Is Essential for Recycling of Transferrin to the Plasma Membrane', *Experimental Cell Research*, 259(1), pp. 257–265. Available at: https://doi.org/10.1006/excr.2000.4947.

Schoch, S. *et al.* (2001) 'SNARE Function Analyzed in Synaptobrevin/VAMP Knockout Mice', *Science*, 294(5544), pp. 1117–1122.

Scott, A.B. (1980) 'Botulinum Toxin Injection into Extraocular Muscles as an Alternative to Strabismus Surgery', *Journal of Pediatric Ophthalmology and Strabismus*, 17(1), pp. 21–25. Available at: https://doi.org/10.3928/0191-3913-19800101-06.

Shah, N. *et al.* (2015) 'Three αSNAP and 10 ATP Molecules Are Used in SNARE Complex Disassembly by N-ethylmaleimide-sensitive Factor (NSF) *', *Journal of Biological Chemistry*, 290(4), pp. 2175–2188. Available at: https://doi.org/10.1074/jbc.M114.620849.

Sharma, D.K. *et al.* (2003) 'Glycosphingolipids Internalized via Caveolar-related Endocytosis Rapidly Merge with the Clathrin Pathway in Early Endosomes and Form Microdomains for Recycling*', *Journal of Biological Chemistry*, 278(9), pp. 7564–7572. Available at: https://doi.org/10.1074/jbc.M210457200.

Shirakawa, R. *et al.* (2020) 'A SNARE geranylgeranyltransferase essential for the organization of the Golgi apparatus', *The EMBO journal*, 39(8), p. e104120. Available at: https://doi.org/10.15252/embj.2019104120.

van der Sluijs, P. *et al.* (1992) 'The small GTP-binding protein rab4 controls an early sorting event on the endocytic pathway', *Cell*, 70(5), pp. 729–740. Available at: https://doi.org/10.1016/0092-8674(92)90307-X.

Söllner, T., Bennett, M.K., *et al.* (1993) 'A protein assembly-disassembly pathway in vitro that may correspond to sequential steps of synaptic vesicle docking, activation, and fusion', *Cell*, 75(3), pp. 409–418. Available at: https://doi.org/10.1016/0092-8674(93)90376-2.

Söllner, T., Whiteheart, S.W., *et al.* (1993) 'SNAP receptors implicated in vesicle targeting and fusion', *Nature*, 362(6418), pp. 318–324. Available at: https://doi.org/10.1038/362318a0.

Song, S.J. *et al.* (2009) 'Aurora B–Mediated Phosphorylation of RASSF1A Maintains Proper Cytokinesis by Recruiting Syntaxin16 to the Midzone and Midbody', *Cancer Research*, 69(22), pp. 8540–8544. Available at: https://doi.org/10.1158/0008-5472.CAN-09-1554.

Steegmaier, M. *et al.* (1998) 'Three Novel Proteins of the Syntaxin/SNAP-25 Family *', *Journal of Biological Chemistry*, 273(51), pp. 34171–34179. Available at: https://doi.org/10.1074/jbc.273.51.34171.

Steegmaier, M. *et al.* (1999) 'Vesicle-associated Membrane Protein 4 is Implicated in Trans-Golgi Network Vesicle Trafficking', *Molecular Biology of the Cell*, 10(6), pp. 1957–1972.

Steinhardt, R.A., Bi, G. and Alderton, J.M. (1994) 'Cell Membrane Resealing by a Vesicular Mechanism Similar to Neurotransmitter Release', *Science*, 263(5145), pp. 390–393.

Stenmark, P. *et al.* (2010) 'Crystal Structure of the Botulinum Neurotoxin Type G Binding Domain: Insight into Cell Surface Binding', *Journal of Molecular Biology*, 397(5), pp. 1287–1297. Available at: https://doi.org/10.1016/j.jmb.2010.02.041.

Stowell, M.H.B. *et al.* (1999) 'Nucleotide-dependent conformational changes in dynamin: evidence for a mechanochemical molecular spring', *Nature Cell Biology*, 1(1), pp. 27–32. Available at: https://doi.org/10.1038/8997.

Suh, Y.H. *et al.* (2011) 'Deletion of SNAP-23 Results in Pre-Implantation Embryonic Lethality in Mice', *PLoS ONE*, 6(3), p. e18444. Available at: https://doi.org/10.1371/journal.pone.0018444.

Sun, S. *et al.* (2012) 'Botulinum neurotoxins B and E translocate at different rates and exhibit divergent responses to GT1b and low pH', *Biochemistry*, 51(28), pp. 5655–5662. Available at: https://doi.org/10.1021/bi3004928.

Sun, W. *et al.* (2020) 'The function of SEC22B and its role in human diseases', *Cytoskeleton*, 77(8), pp. 303–312. Available at: https://doi.org/10.1002/cm.21628.

Sun, Y., Martin, A.C. and Drubin, D.G. (2006) 'Endocytic Internalization in Budding Yeast Requires Coordinated Actin Nucleation and Myosin Motor Activity', *Developmental Cell*, 11(1), pp. 33–46. Available at: https://doi.org/10.1016/j.devcel.2006.05.008.

Sutton, R.B. *et al.* (1998) 'Crystal structure of a SNARE complex involved in synaptic exocytosis at 2.4 Å resolution', *Nature*, 395(6700), pp. 347–353. Available at: https://doi.org/10.1038/26412.

Swaminathan, S. and Eswaramoorthy, S. (2000) 'Structural analysis of the catalytic and binding sites of Clostridium botulinum neurotoxin B', *Nature Structural Biology*, 7(8), pp. 693–699. Available at: https://doi.org/10.1038/78005.

Sweitzer, S.M. and Hinshaw, J.E. (1998) 'Dynamin Undergoes a GTP-Dependent Conformational Change Causing Vesiculation', *Cell*, 93(6), pp. 1021–1029. Available at: https://doi.org/10.1016/S0092-8674(00)81207-6.

Takahashi, M. *et al.* (2013) 'The localization of VAMP5 in skeletal and cardiac muscle', *Histochemistry and Cell Biology*, 139(4), pp. 573–582. Available at: https://doi.org/10.1007/s00418-012-1050-0.

Takáts, S. *et al.* (2018) 'Non-canonical role of the SNARE protein Ykt6 in autophagosome-lysosome fusion', *PLOS Genetics*, 14(4), p. e1007359. Available at: https://doi.org/10.1371/journal.pgen.1007359.

Tang, B.L., Low, D.Y.H., *et al.* (1998) 'Molecular Cloning and Localization of Human Syntaxin 16, a Member of the Syntaxin Family of SNARE Proteins', *Biochemical and Biophysical Research Communications*, 242(3), pp. 673–679. Available at: https://doi.org/10.1006/bbrc.1997.8029.

Tang, B.L., Tan, A.E.H., *et al.* (1998) 'Syntaxin 12, a Member of the Syntaxin Family Localized to the Endosome *', *Journal of Biological Chemistry*, 273(12), pp. 6944–6950. Available at: https://doi.org/10.1074/jbc.273.12.6944.

Teng, F.Y.H., Wang, Y. and Tang, B.L. (2001) 'The syntaxins', *Genome Biology*, 2(11), p. reviews3012.1. Available at: https://doi.org/10.1186/gb-2001-2-11-reviews3012.

Thwaites, C.L. (2017) 'Botulism and tetanus', *Medicine*, 45(12), pp. 739–742. Available at: https://doi.org/10.1016/j.mpmed.2017.09.004.

Toonen, R.F.G. *et al.* (2005) 'Munc18–1 stabilizes syntaxin 1, but is not essential for syntaxin 1 targeting and SNARE complex formation', *Journal of Neurochemistry*, 93(6), pp. 1393–1400. Available at: https://doi.org/10.1111/j.1471-4159.2005.03128.x.

Trimble, W.S., Cowan, D.M. and Scheller, R.H. (1988) 'VAMP-1: a synaptic vesicle-associated integral membrane protein.', *Proceedings of the National Academy of Sciences*, 85(12), pp. 4538–4542. Available at: https://doi.org/10.1073/pnas.85.12.4538.

Turton, K., Chaddock, J.A. and Acharya, K.R. (2002) 'Botulinum and tetanus neurotoxins: structure, function and therapeutic utility', *Trends in Biochemical Sciences*, 27(11), pp. 552–558. Available at: https://doi.org/10.1016/S0968-0004(02)02177-1.

Ulloa, F. *et al.* (2015) 'Blockade of the SNARE Protein Syntaxin 1 Inhibits Glioblastoma Tumor Growth', *PLoS ONE*, 10(3), p. e0119707. Available at: https://doi.org/10.1371/journal.pone.0119707.

Vardar, G. *et al.* (2020) 'Epilepsy-causing STX1B mutations translate altered protein functions into distinct phenotypes in mouse neurons', *Brain*, 143(7), pp. 2119–2138. Available at: https://doi.org/10.1093/brain/awaa151.

Veit, M., Söllner, T.H. and Rothman, J.E. (1996) 'Multiple palmitoylation of synaptotagmin and the t-SNARE SNAP-25', *FEBS Letters*, 385(1), pp. 119–123. Available at: https://doi.org/10.1016/0014-5793(96)00362-6.

Verboogen, D.R.J. *et al.* (2017) 'Fluorescence Lifetime Imaging Microscopy reveals rerouting of SNARE trafficking driving dendritic cell activation', *eLife*, 6, p. e23525. Available at: https://doi.org/10.7554/eLife.23525.

Verderio, C. *et al.* (2012) 'TI-VAMP/VAMP7 is the SNARE of secretory lysosomes contributing to ATP secretion from astrocytes', *Biology of the Cell*, 104(4), pp. 213–228. Available at: https://doi.org/10.1111/boc.201100070.

Verhage, M. and Sørensen, J.B. (2020) 'SNAREopathies: Diversity in Mechanisms and Symptoms', *Neuron*, 107(1), pp. 22–37. Available at: https://doi.org/10.1016/j.neuron.2020.05.036.

Viability Outcome (IMPC_VIA_001_001) chart for Ykt6 | International Mouse Phenotyping Consortium (no date). Available at: https://www.mousephenotype.org/data/charts?accession=MGI:1927550&allele_accession_id=MGI:6360693&zygosity=homozygote&parameter_stable_id=IMPC_VIA_001_001&pipeline_stable_id=JAX_001&procedure_stable_id=IMPC_VIA_001&parameter_stable_id=IMPC_VIA_001_001&phenotyping_center=JAX (Accessed: 17 October 2024).

Vigers, G. P., Crowther, R.A. and Pearse, B.M. (1986) 'Location of the 100 kd-50 kd accessory proteins in clathrin coats', *The EMBO journal*, 5(9), pp. 2079–2085. Available at: https://doi.org/10.1002/j.1460-2075.1986.tb04469.x.

Vigers, G P, Crowther, R.A. and Pearse, B.M. (1986) 'Three-dimensional structure of clathrin cages in ice.', *The EMBO Journal*, 5(3), pp. 529–534.

Wang, C.-C. *et al.* (2004) 'A Role of VAMP8/Endobrevin in Regulated Exocytosis of Pancreatic Acinar Cells', *Developmental Cell*, 7(3), pp. 359–371. Available at: https://doi.org/10.1016/j.devcel.2004.08.002.

Wang, C.-C. *et al.* (2007) 'VAMP8/Endobrevin as a General Vesicular SNARE for Regulated Exocytosis of the Exocrine System', *Molecular Biology of the Cell*, 18(3), pp. 1056–1063. Available at: https://doi.org/10.1091/mbc.E06-10-0974.

Washbourne, P. *et al.* (2002) 'Genetic ablation of the t-SNARE SNAP-25 distinguishes mechanisms of neuroexocytosis', *Nature Neuroscience*, 5(1), pp. 19–26. Available at: https://doi.org/10.1038/nn783.

Weigert, R. *et al.* (2004) 'Rab22a Regulates the Recycling of Membrane Proteins Internalized Independently of Clathrin', *Molecular Biology of the Cell*, 15(8), pp. 3758–3770. Available at: https://doi.org/10.1091/mbc.e04-04-0342.

Weis, W.I. and Scheller, R.H. (1998) 'SNARE the rod, coil the complex', *Nature*, 395(6700), pp. 328–329. Available at: https://doi.org/10.1038/26354.

Williamson, L.C. and Neale, E.A. (1998) 'Syntaxin and 25-kDa synaptosomal-associated protein: Differential effects of botulinum neurotoxins C1 and A on neuronal survival', *Journal of Neuroscience Research*, 52(5), pp. 569–583. Available at: https://doi.org/10.1002/(SICI)1097-4547(19980601)52:5<569::AID-JNR9>3.0.CO;2-A.

Winner, B.M., Bodt, S.M.L. and McNutt, P.M. (2020) 'Special Delivery: Potential Mechanisms of Botulinum Neurotoxin Uptake and Trafficking within Motor Nerve Terminals', *International Journal of Molecular Sciences*, 21(22), p. 8715. Available at: https://doi.org/10.3390/ijms21228715.

Wojnacki, J. *et al.* (2020) 'Role of VAMP7-Dependent Secretion of Reticulon 3 in Neurite Growth', *Cell Reports*, 33(12). Available at: https://doi.org/10.1016/j.celrep.2020.108536.

Wong, S.H. *et al.* (1998) 'Endobrevin, a Novel Synaptobrevin/VAMP-Like Protein Preferentially Associated with the Early Endosome', *Molecular Biology of the Cell*, 9(6), pp. 1549–1563. Available at: https://doi.org/10.1091/mbc.9.6.1549.

Xu, J., Mashimo, T. and Südhof, T.C. (2007) 'Synaptotagmin-1, -2, and -9: Ca2+ Sensors for Fast Release that Specify Distinct Presynaptic Properties in Subsets of Neurons', *Neuron*, 54(4), pp. 567–581. Available at: https://doi.org/10.1016/j.neuron.2007.05.004.

Yang, C., Coker, K.J., *et al.* (2001) 'Syntaxin 4 heterozygous knockout mice develop muscle insulin resistance', *The Journal of Clinical Investigation*, 107(10), pp. 1311–1318. Available at: https://doi.org/10.1172/JCI12274.

Yang, C., Mora, S., *et al.* (2001) 'VAMP3 Null Mice Display Normal Constitutive, Insulin- and Exercise-Regulated Vesicle Trafficking', *Molecular and Cellular Biology*, 21(5), pp. 1573–1580. Available at: https://doi.org/10.1128/MCB.21.5.1573-1580.2001.

Yang, C. *et al.* (2022) 'Actin polymerization promotes invagination of flat clathrin-coated lattices in mammalian cells by pushing at lattice edges', *Nature Communications*, 13(1), p. 6127. Available at: https://doi.org/10.1038/s41467-022-33852-2.

Yeo, J.C. *et al.* (2024) 'Botulinum toxin intoxication requires retrograde transport and membrane translocation at the ER in RenVM neurons', *eLife*, 12. Available at: https://doi.org/10.7554/eLife.92806.2.

Young, C.E. *et al.* (1998) 'SNAP-25 deficit and hippocampal connectivity in schizophrenia.', *Cerebral Cortex*, 8(3), pp. 261–268. Available at: https://doi.org/10.1093/cercor/8.3.261.

Zeng, Q. *et al.* (1998) 'A novel synaptobrevin/VAMP homologous protein (VAMP5) is increased during in vitro myogenesis and present in the plasma membrane', *Molecular Biology of the Cell*, 9(9), pp. 2423–2437. Available at: https://doi.org/10.1091/mbc.9.9.2423.

Zeng, Q. *et al.* (2003) 'The cytoplasmic domain of Vamp4 and Vamp5 is responsible for their correct subcellular targeting: the N-terminal extenSion of VAMP4 contains a dominant autonomous targeting signal for the trans-Golgi network', *The Journal of biological chemistry*, 278(25). Available at: https://doi.org/10.1074/jbc.M303214200.

Zhang, S. *et al.* (2017) 'Identification and characterization of a novel botulinum neurotoxin', *Nature Communications*, 8(1), p. 14130. Available at: https://doi.org/10.1038/ncomms14130.

Zhang, S. *et al.* (2018) 'Identification of a botulinum neurotoxin-like toxin in a commensal strain of Enterococcus faecium', *Cell host & microbe*, 23(2), pp. 169-176.e6. Available at: https://doi.org/10.1016/j.chom.2017.12.018.

Zhang, T. and Hong, W. (2001) 'Ykt6 Forms a SNARE Complex with Syntaxin 5, GS28, and Bet1 and Participates in a Late Stage in Endoplasmic Reticulum-Golgi Transport', *Journal of Biological Chemistry*, 276(29), pp. 27480–27487. Available at: https://doi.org/10.1074/jbc.M102786200.

Zhang, X. *et al.* (2023) 'miR-124 and VAMP3 Act Antagonistically in Human Neuroblastoma', *International Journal of Molecular Sciences*, 24(19), p. 14877. Available at: https://doi.org/10.3390/ijms241914877.

Zhao, M. *et al.* (2015) 'Mechanistic insights into the recycling machine of the SNARE complex', *Nature*, 518(7537), pp. 61–67. Available at: https://doi.org/10.1038/nature14148.

Zhou, Q. *et al.* (2015) 'Architecture of the synaptotagmin–SNARE machinery for neuronal exocytosis', *Nature*, 525(7567), pp. 62–67. Available at: https://doi.org/10.1038/nature14975.

Zornetta, I. *et al.* (2016) 'The first non Clostridial botulinum-like toxin cleaves VAMP within the juxtamembrane domain', *Scientific Reports*, 6(1), p. 30257. Available at: https://doi.org/10.1038/srep30257.